AD NUMBER: AD0848524
LIMITATION CHANGES
TO: Approved for public release; distribution is unlimited.
FROM: Further dissemination only as directed by DoD 1 Dec 1968 or higher DoD authority.
AUTHORITY
DoD/Boeing ltr 23 Jan 1974 f/5 to a/1

BOEING

SEATTLE, WASHINGTON

STATEMENT #5 UNCLASSIFIED

This document may be further distributed by holder only with specific prior approval of Boeing Co. Missile & Info Systems Div. Seattle, Washington

REV LTR

THE BOEING COMPANY

(11) Dec 68

CODE IDENT. NO. 81205

NUMBER (14) D2-125929-1

(12) 936.

(6) TITLE: Particle Erosion Testing in The Boeing Hypersonic Wind Tunnel

ORIGINAL RELEASE DATE _____. FOR THE RELEASE DATE OF SUBSEQUENT REVISIONS, SEE THE REVISIONS SHEET. FOR LIMITATIONS IMPOSED ON THE DISTRIBUTION AND USE OF INFORMATION CONTAINED IN THIS DOCUMENT, SEE THE LIMITATIONS SHEET.

MODEL _____

ISSUE NO. _____

ISSUE TO _____

PREPARED UNDER:

☐ CONTRACT NO.

☒ IR&D

☐ OTHER

PREPARED BY (10) George C. Lorenz

SUPERVISED BY Bruce E. Cl[illegible]gan

APPROVED BY S. I. Gravitz

APPROVED BY _____

This document may be further distributed by holder only with specific prior approval of _____

1473

SHEET 1

U3 4802 1430 REV. 9/68

059 600

elk

PARTICLE EROSION TESTING IN THE BOEING HYPERSONIC WIND TUNNEL

George C. Lorenz
THE BOEING COMPANY

FOREWORD

The experimental research program described in this report was performed under the direction of the Structures Staff as part of The Boeing Company's Independent Research and Development Programs. Funding was provided by the Airborne Vehicle Hardening Program (TRP 321 and TRP 974), and Thermal Protection Systems Program (TRP 970). The tests were conducted in the Boeing Hypersonic Wind Tunnel with the essential assistance of the Flight Technology Staff. Special acknowledgement is extended to Dick Allen, Ross Osburn and L. Webb for direction of Tunnel Operations, Instrumentation, and Shop Support, respectively.

ABSTRACT

Missiles flying in the atmosphere could be subjected to passage through dust clouds formed by surface bursts of nuclear weapons. Such flight would result in the erosion of frontal surfaces, particularly the regions covered with ablative-insulative materials. The technique described in this paper was developed to provide data on the erosive effects of dust on cork, carborazole and silicone rubber (DC-93-072) in the Mach 3 to 6 flight regime.

The Erosion Test technique was developed utilizing the Boeing 12-inch Hypersonic Wind Tunnel. The wind tunnel was modified so that sand and glass beads could be introduced into the tunnel flow anytime during a test run. The material was injected up-stream of the nozzle throat and drag accelerated to high velocities prior to arrival at the test section. Drag computations based upon spherical particle drag, with the drag coefficient a function of Mach Number and Reynolds Number, indicate that the particles attained velocities, dependent upon size, of 2550 to 3250 feet-per-second. The tests were conducted at Mach Numbers of 6.05 and 6.50, P_t = 850, 1000 and 1150 PSI, T_t = 1000°F, with the test section gas velocity remaining constant at approximately 4000 ft/sec.

The conical test specimens introduced into the test stream were subjected to either an ablative or a combined ablative-erosive stream. The debris injection mechanism was capable of varying both the duration and the density of the particulate cloud. The cloud distribution throughout the tunnel test core was calibrated with a specially designed "cloud-sampler".

This sampling technique provided the contamination profile existing within the test section. From this profile the amount of material impinging upon the model position could be readily determined. The surface temperature of the models was increased above the nominal recovery temperature of 850°F by an auxiliary radiant furnace that completely enclosed the tunnel test section. This furnace produced a maximum radiant heat flux of 37.5 BTU/FT^2-SEC resulting in a measured model surface temperature of 2100°F.

The conclusions derived from this experimental program can be summarized as follows:

1. Contamination on the order of 1 LB/FT^2-MIN can increase the weight loss incurred by ablative-insulative materials by a factor of 5 to 10.

2. The erosion loss is highly dependent upon temperature with materials exhibiting threshold levels beyond which the loss is greatly accelerated.

3. Virgin materials are the most resistant to particle erosion with a cold char exhibiting somewhat more resistance than a hot char.

4. The erosion loss increases proportionally with the mass of the impinging material.

5. As the dust cloud particle density increases the erosion loss ratio, mass eroded/mass impinged, decreases approaching some asymptotic value.

6. The analyses of cork and carborazole hemispheres by the Neilson-Gilchrist method indicate that they exhibit the general characteristics of a material like plexiglas. These results also show why the half-angles tested, 9°, 15°, 25°, did not reveal a most vulnerable angle; the loss ratio curves tend to be very flat at impingement angles between 10 and 20 degrees.

7. This test technique is the only one known to the author that can provide the combined effects of erosion and ablation while in an environment closely simulating the important parameters of shear, heat flux and surface temperature.

KEY WORDS

Ablation	Heat Transfer
Ablation-Erosion	Hypersonic Flow
Aerodynamic Heating	Nuclear Cloud Debris
Carborazole	Particle Velocity
Collection Efficiency	Radiant Heating
Contamination	Shear
Cork	Silicone Rubber
Drag Coefficient	Wear
Dust Cloud	Wind Tunnel
Dust Sampler	

TABLE OF CONTENTS

LIST OF FIGURES

USE FOR TYPEWRITTEN MATERIAL ONLY

LIST OF SYMBOLS

A = Particle Area, FT^2

C_d = Particle Drag Coefficient, Dimensionless

D = Drag, Lbs

F = Force, Lbs

g = Gravitational Constant, FT/SEC^2

K = Particle Velocity Component Normal to Surface, FT/SEC

k = Ratio of Specific Heats, Dimensionless

M = Mach Number, Dimensionless

MW = Model or Specimen Weight, Grams

m = Particle Mass Density, $LB\ SEC^2/FT^4$

Re = Reynolds Number, Dimensionless

r = Particle Radius, FT

T = Temperature, ^oF

V = Velocity, FT/SEC

v = Particle Residual Parallel Velocity Component, FT/SEC

W = Dust Weight, Lbs

WR = Wear, Grams

Greek Letters

α = Impingement Angle, Degrees

γ = Particle Specific Weight, LB/FT^3

ε = Resistance Factor For Impact Wear, FT-LB/GM

η = Collection and/or Impingement Ratio, Dimensionless

ρ = Gas Density, $SLUGS/FT^3$

ϕ = Resistance Factor for Cutting Wear, FT-LB/GM

Subscripts

A = After

AB = Ablation

B = Before

C = Collected

Cu = Cutting

D = Impact

d = Dispensed

g = Gas

INC = Incompressible

i = Impinged

o = Initial Conditions

p = Particle

s = Surface

t = Total

1.0 INTRODUCTION

Missile flight through dust clouds induced by nuclear bombs would result in multiple particle impacts on the frontal surfaces of the vehicle. The size of these particles would be dependent upon the time after burst and cloud altitude. The question that arises is: what effect do these impacts, with the possible resultant damage and erosive wear, have on the vehicle's thermal protection and structural requirements?

Techniques for determining the effects of large particle impacts are well developed. These particles (down to 0.030" diameter) can be fired at test specimens from various types of launching devices at velocities up to 50,000 feet/sec. The damage to these specimens is readily discernible and consists primarily of damage to the thermal insulation and substructure, and penetration resulting in damage to internal components. However, the erosive effects of the multiple impacts of micron-sized particles is a different matter. Here the problem becomes one of whether or not excessive structural temperatures occur because of the wear sustained by the heat resistance covering; i.e., does enough of the ablation or ablation-insulation material erode away to cause loss of structural integrity because of excessive structural temperatures?

A considerable amount of research has been done in the field of low velocity erosion similar to the effects of sand-blasting. In this work the velocities are largely subsonic and the specimens are static non-ablative type materials, unheated and unaffected by aerodynamic forces. Some of the theoretical concepts developed from this work have been found to be applicable and have been used to analyze the data derived from the subject program.

A limited amount of research has been done using the hot-shot type tunnel to launch small particles to velocities ranging from 5000 to 20,000 feet/second. This activity has been directed toward ablative materials, particularly cork, where in some cases the material has been pre-charred and even heated prior to impact. However, at best, this testing procedure lacks the capability of simulating the parameters of aerodynamic heating coupled with wind shear and material charring.

The purpose here was to develop an experimental technique that could evaluate the erosive effects while simulating the existing aerodynamic heating, flow forces and simultaneous effects of erosion and ablation. The technique was developed by introducing particles into the flow of a hypersonic wind tunnel, drag accelerating them to velocities up to 3250 feet-per-second and then having them impact upon ablation material specimens. The parameters of specimen surface temperature, particle size, particle impingement angle, condition of the surface char, particle mass weight and particle mass-density were investigated.

The first portion of this study reviews the information on the erosion and wear of multiple impacts. Next, the experimental program is described and the results presented. Finally, the "Appendices" present the details of the NEILSON-GILCHRIST method of analysis and a summary of a range of flow parameters that could be attained in the Boeing Hypersonic Wind Tunnel (used for this work) and other available facilities. The parameters described would be limited to those applicable to the boost phases of ballistic missile flight or the flight of various low-speed missiles that remain in the atmosphere.

2.0 STATUS OF PARTICLE EROSION

Much research, theoretical and experimental, has been done in the field of high velocity, large particle, single impact damage mechanics. Since this work is directed primarily toward penetration, kill probability, and structural damage, it is beyond the scope of this study and report. For those that are interested, a sample of this work may be found in References 1, 2 or 3.

The Structures Technology Staff conducted, in 1967, a limited experimental program directed toward obtaining single impact data on various ablation materials. A light gas gun was used to launch small glass beads at cork over aluminum honeycomb and phenolic silica over aluminum targets. Some penetration threshold data were obtained. The extent of the work performed can be found in References 4 and 5.

2.1 THEORETICAL EROSION STUDIES

The early work in erosion effects was mostly experimental (circa 1930) and was directed mainly toward sand blasting techniques. In 1958, FINNIE [6] presented a theoretical approach by analyzing an idealized case of an abrasive grain striking and removing material from a flat surface. He followed this by a more comprehensive article [7] that included an extensive literature search and introduced aerodynamic flow and surface hardness. In one of the articles, HOLTLEY [8], introduced the concept of attributing the weight loss to two wearing factors: (1) loss by impact wear, and (2) by cutting wear. This weight loss principle was examined thoroughly by BITTER who presented a comprehensive theoretical analysis of both wearing factors in Reference 9. This was followed in 1968 by NEILSON AND GILCHRIST [10] who

expanded Bitter's work with theoretical expressions based upon empirical data. This latter approach has been applied in the analysis of the data obtained in the subject test program with considerable success.

2.2 EXPERIMENTAL BACKGROUND

Early concern about particle erosion was precipitated by the wear of steam turbine blades caused by condensing water droplets. This problem was compounded when powdered coal was considered as the fuel for railroad gas turbine locomotives. As a result an experimental program (Reference 11) was conducted blowing high temperature "fly-ash" on metals representative of turbine blades. At the same time other experiments (Reference 12) were being conducted to derive data with regard to the gas-solid problem in catalytic cracking plants. A related problem, that of sand erosion of hydroelectric water wheel buckets was also being investigated. However, these papers, although of general interest, do not develop useful trends toward the basic problem of erosion with respect to heated ablation materials.

In 1959 a more meaningful experiment was conducted by FINNIE [13]. He developed an abrasion flow apparatus (200 - 600 FT/SEC) and obtained wear data as a function of impingement angle for various metals and glass. The most meaningful test data and empirical expressions appear in the previously mentioned Reference 10 by NEILSON AND GILCHRIST. In this work experimental data are broken down into the impact and cutting wear for various metals, glass, graphite, and plexiglas. From these data they developed methods that are fairly applicable to other types of material. These methods have been applied to charred cork and carborazole and are described in another portion of this report. The authors of Reference 10 have also prepared Reference 14, which deals with the problem of erosion in rocket motor nozzles.

Another erosion test technique where ablation material specimens are used, is one developed by Rhodes and Bloxom. This technique utilizes a hot-shot tunnel to accelerate a few micron-sized particles to velocities in excess of 10,000 feet-per-second. These particles impinge on small test specimens that can either be virgin, pre-charred, or in the process of being heated by a torch. This technique has recently been expanded, along the principles of the Gatling Gun to permit the firing of a series of particle during one run. The details of this test technique and a sample of some of the data can be obtained from Reference 15.

3.0 EXPERIMENTAL PROGRAM

3.1 ANALYTICAL PREPARATION

3.1.1 Particle Velocity Analysis

At the onset of this experimental program some effort was made to measure the actual particle velocity. However, it was soon determined that the usual and ordinary photographic techniques would not suffice in this task. Since it appeared that an accurate and reliable velocity measurement system would be quite costly, it was decided that the particle velocities would be based on the computed values. Later calculations of the sensitivity of computed velocities to uncertainties in the drag coefficients showed that the variation in computed velocities was small for a realistic range of drag coefficient variation.

The particles were injected into the wind tunnel approximately 18 inches upstream of the throat. Since they were injected downstream, and the gas velocity in this region is low, the assumption was made that the particles attained gas velocity at the beginning of the converging section; 50 to 85 feet-per-second. It was also assumed that they were uneffected by gravity.

The force acting upon the particles is drag:

$$F = D = \frac{1}{2} \rho (V_g - V_p)^2 A C_d$$

and the particle is accelerated to a velocity approaching that of the gas:

$$F = m \dot{V}_p \quad \text{OR}$$

$$V_p = \int \frac{F}{m} dt + V_{p_o}$$

$$V_p = \int \frac{\frac{1}{2} \rho (V_g - V_p)^2 A C_d}{m} dt + V_{p_o}$$

$$V_p = \int \frac{3}{8} \frac{\rho (V_g - V_p)^2 C_d}{\gamma r} dt + V_{p_0}$$

$$V_p = \int 12.075 \frac{C_d \rho}{\gamma r} (V_g - V_p)^2 dt + V_{p_0}$$

In the above expression, the particle radius, r, and particle density, γ, are given constants, and the wind tunnel velocity, V_g and stream density, ρ are inputs dependent upon flow conditions within the nozzle. The value of C_d remains as a critical item highly dependent upon Reynolds Number and the relative Mach Number. After an extensive literature search the expression derived by CROWE [16] was used to compute the value of C_d.

$$C_d = \left(C_{d_{INC}} - 2\right) e^{-A} + \frac{h(M)}{R^{0.5} M} e^{-B} + 2$$

where $A = 3.07 R^{0.5} \left(\frac{M}{R_e}\right) g(R_e)$

$$\text{Log}_{10} g(R_e) = 1.35 \left[1 + \text{Tanh}\left(0.77 \text{Log}_{10} R_e - 1.92\right)\right]$$

$$h(M) = \left[2.3 + 1.7 \left(\frac{T_g}{T_p}\right)^{0.5}\right] - 2.3 \text{Tanh}\left(1.17 \text{Log}_{10} M\right)$$

$$B = -\frac{R_e}{2M}$$

The values of C_d computed with this expression compare favorably with the curves developed from the experimental results of SELBERG AND NICHOLLS.[17]

The computed velocities for the dust material used during the subject test are shown in Figure 1.

3.1.2 Model Collection Efficiency

In order to evaluate the data obtained from these tests it was imperative that the mass of material impinging upon the models be known with reasonable accuracy. A cloud sampler was designed (described in detail later in this report) which would determine the ratio of the impinging material to the total amount of material dispensed into the tunnel. However, since the shape of this sampler and the models differed the question arose as to whether the model shock and flow patterns would divert an appreciable number of the particles from their original trajectories. (See Figure 2) Therefore, this analysis was undertaken to determine the magnitude of this correction factor.

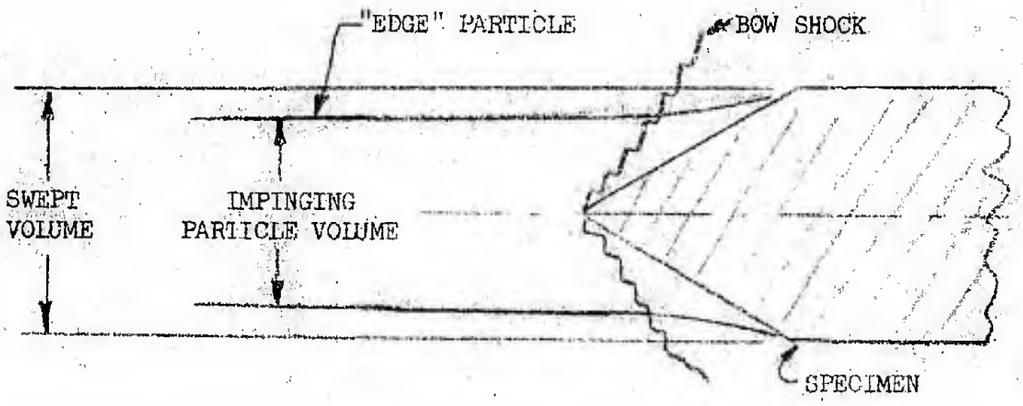

FIGURE 2 Model Collection Efficiency

Using a sharp cone as the critical configuration, with air as an ideal gas, a conical flow field was developed using the Taylor-Maccoll equation. The analysis then computed the change in the particle trajectory (using the drag equations mentioned above) and determined which particle would just touch the shoulder of the core. This "edge" particle then establishes the ratio of volumes which is the desired correction factor. This procedure revealed that

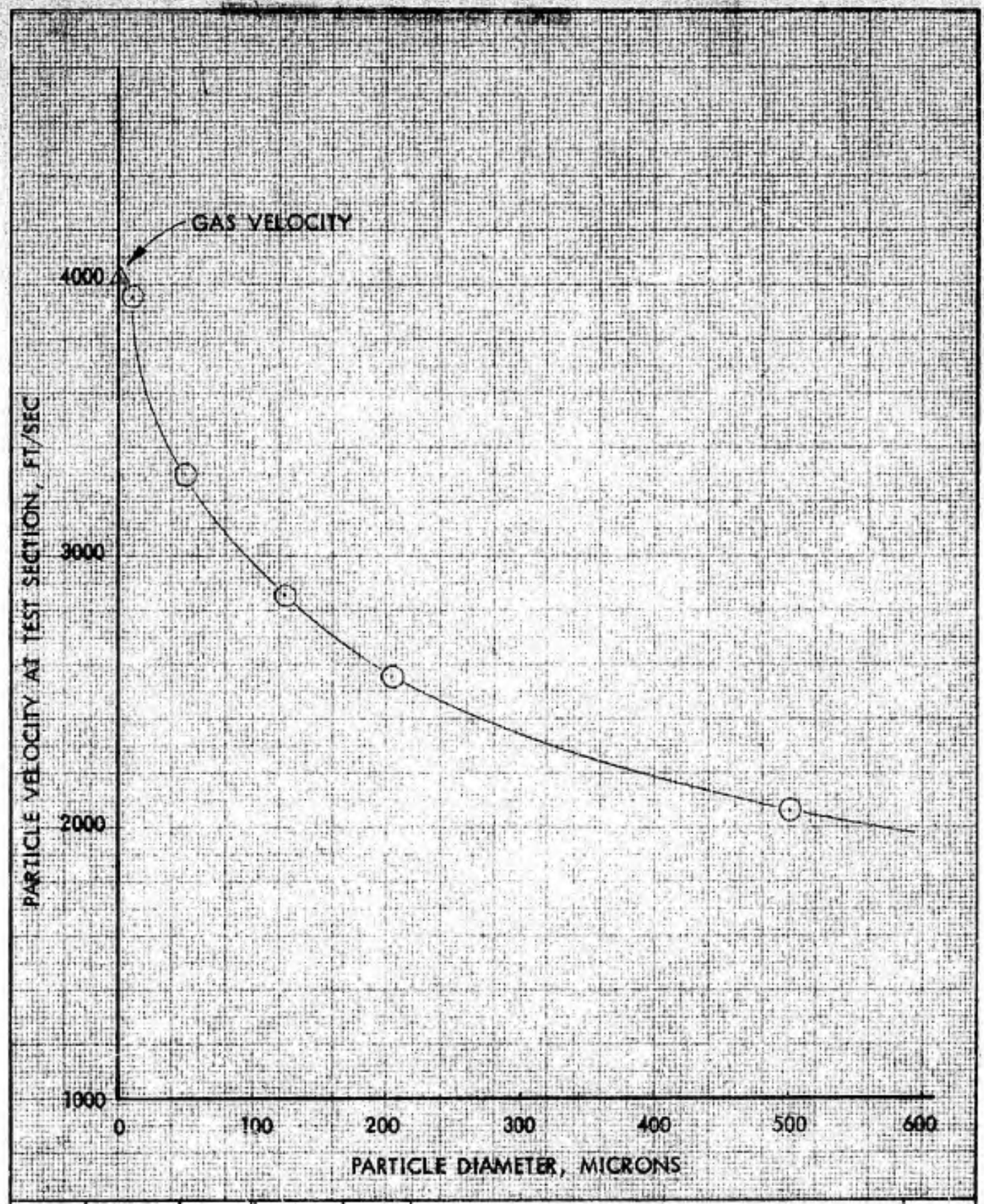

	INITIALS	DATE	REV BY INITIAL	DATE	TITLE	MODEL
CALC					COMPUTED PARTICLE VELOCITIES IN THE TEST SECTION OF THE BOEING HYPERSONIC WIND TUNNEL	Fig. 1
CHECK						
APPD.						
APPD.						

U3 4013 8000 REV 1/66

the correction factor was 0.999 for a particle with a diameter of 12.5 microns. Since 50 micron glass-beads were the smallest particles used in this test it is apparent that a collection efficiency correction factor was unity.

3.1.3 Aerodynamic Parameters

All of the aerodynamic parameters required for simulation estimates; wind shear, heat flux, heat transfer coefficient and surface temperatures were computed by the CHAP computer program. (Reference 18)

3.2 TEST FACILITY

3.2.1 Basic Tunnel Capabilities

The experiments were conducted in the Boeing 12 inch Hypersonic Wind Tunnel located at the Plant II tunnel complex. This is a standard intermittent blow-down facility with nozzles for Mach 5.0, 6.05, 6.5 and 7.0 flow. The nozzle exits are 12 inches in diameter with a useable flow core, dependent upon the Mach Number, between 8 and 9 inches in diameter. This facility has a wide operating range of total pressure and total temperature with maximums of 1200 PSIG and 1000°F. Run time, again dependent upon the Mach Number, is on the order of $1\frac{1}{2}$ to 2 minutes, sufficiently long for these tests.

The general tunnel configuration is shown in Figure 3. This sketch shows the pod injection mechanism which can rapidly inject and retract specimens in and out of the test stream. This feature is required for good heat transfer measurements and has proven to be indispensible in the conduction of these erosion tests. The test chamber shell has three viewing ports which permit easy visual observations as well as motion picture and Schlieren/shadowgraph photography.

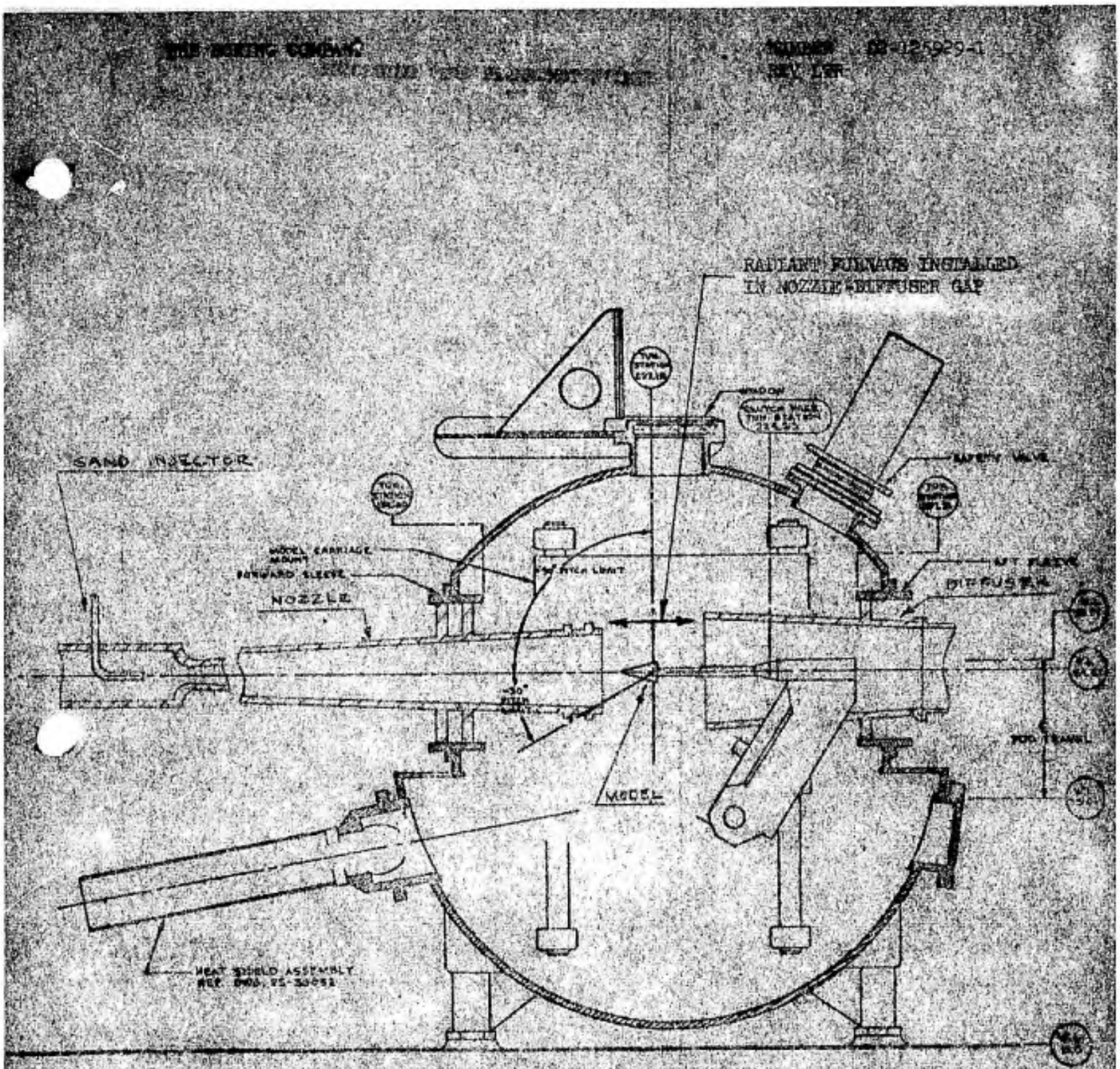

BOEING HYPERSONIC WIND TUNNEL MODIFIED FOR PARTICLE EROSION TESTING

Figure 3

3.2.2 Dust Injection Mechanism

The basic wind tunnel was slightly modified to accommodate the installation of the dust injection equipment. The installation in its final form is pictured in Figure 4. It consists primarily of a pressurized sand storage can with an electrically driven rotary spool at the base. This rotating spool allowed a slight advance of the gas flow (high pressure bottled nitrogen) followed by the dust flow. The latter was regulated by the dome pressure and by the size of the adjustable orifice at the base of the can. The rotating spool also provided for a slight delay in the gas flow at shut-down to allow a purging of the delivery tube.

The latter (seen on the right of the container) runs from the container base, through the tunnel wall and bends 90° to point directly downstream and directly at the throat section. The end of the tube was designed with a four-way opening that provided a spraying effect for dispersion of the dust particles. The end of this tube was located approximately 18 inches upstream of the throat section.

The system pressurization was controlled by a solenoid valve. This valve and the motor driving the rotary spool were controlled by an electric timing device that was accurate to 1/100th of a second.

3.2.3 Auxiliary Radiant Furnace

The Boeing Hypersonic tunnel has a maximum operating total temperature of 1000°F. With this total temperature limitation, the nominal maximum specimen surface temperature is 850 to 900°F. This temperature will char low temperature ablators such as cork and carborazole, but it will produce little or no

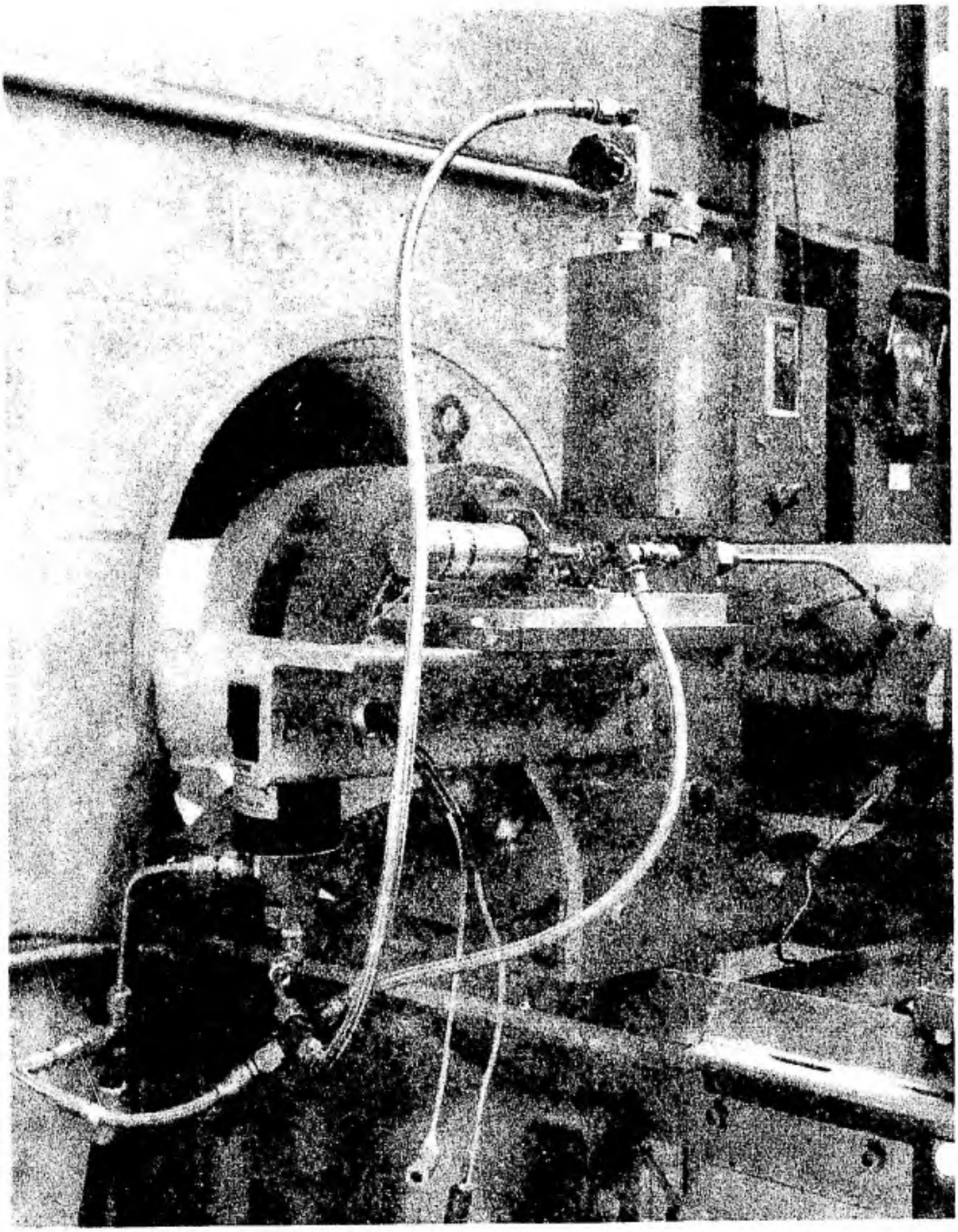

DUST INJECTION MECHANISM LOCATED IN WIND TUNNEL SECTION DIRECTLY UP STREAM OF THROAT

FIGURE 4
D2-125929-1
Sheet 106

char on higher temperature ablators such as silicone rubber. As a consequence, for these materials, the erosion effects will be those associated with the heated virgin material.

In order to produce a char on the surface of these high temperature ablators and more closely simulate the more severe heating conditions for certain trajectories, an auxiliary radiant furnace was installed surrounding the wind tunnel test section. As shown in Figure 5 this furnace encloses all of the test section except for a slot at the bottom. This slot is required for injection of the test specimens. The furnace is composed of a water cooled shell with 72 quartz heating elements lining the inside surface. Prior to installation in the wind tunnel the furnace was calibrated with the voltage vs. heat flux results as shown in Figure 6. The maximum heat flux, 37.5 BTU/FT^2-SEC, when imposed upon a test specimen in the stream flow will produce a surface temperature, dependent upon the thermal properties of the material, of approximately $2100^{\circ}F$. Therefore this auxiliary device is an extremely valuable addition to the over-all tunnel installation by permitting a wide range of surface temperatures for ablation and erosion-ablation testing.

PRECEDING PAGE BLANK-NOT FILMED

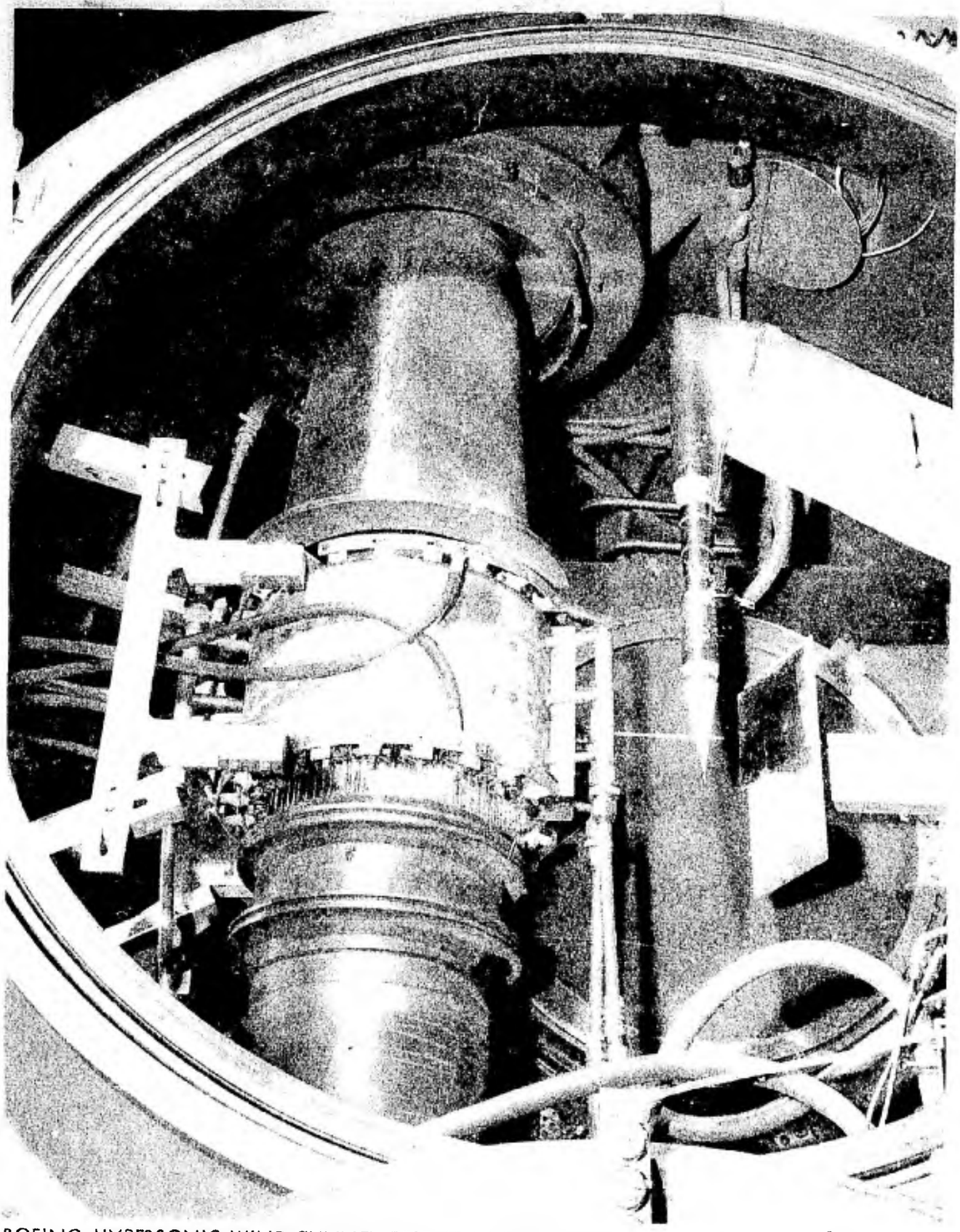

BOEING HYPERSONIC WIND TUNNEL TEST SECTION SHOWING INSTALLATION OF THE AUXILIARY RADIANT FURNACE

FIGURE 5
D2-125929-1

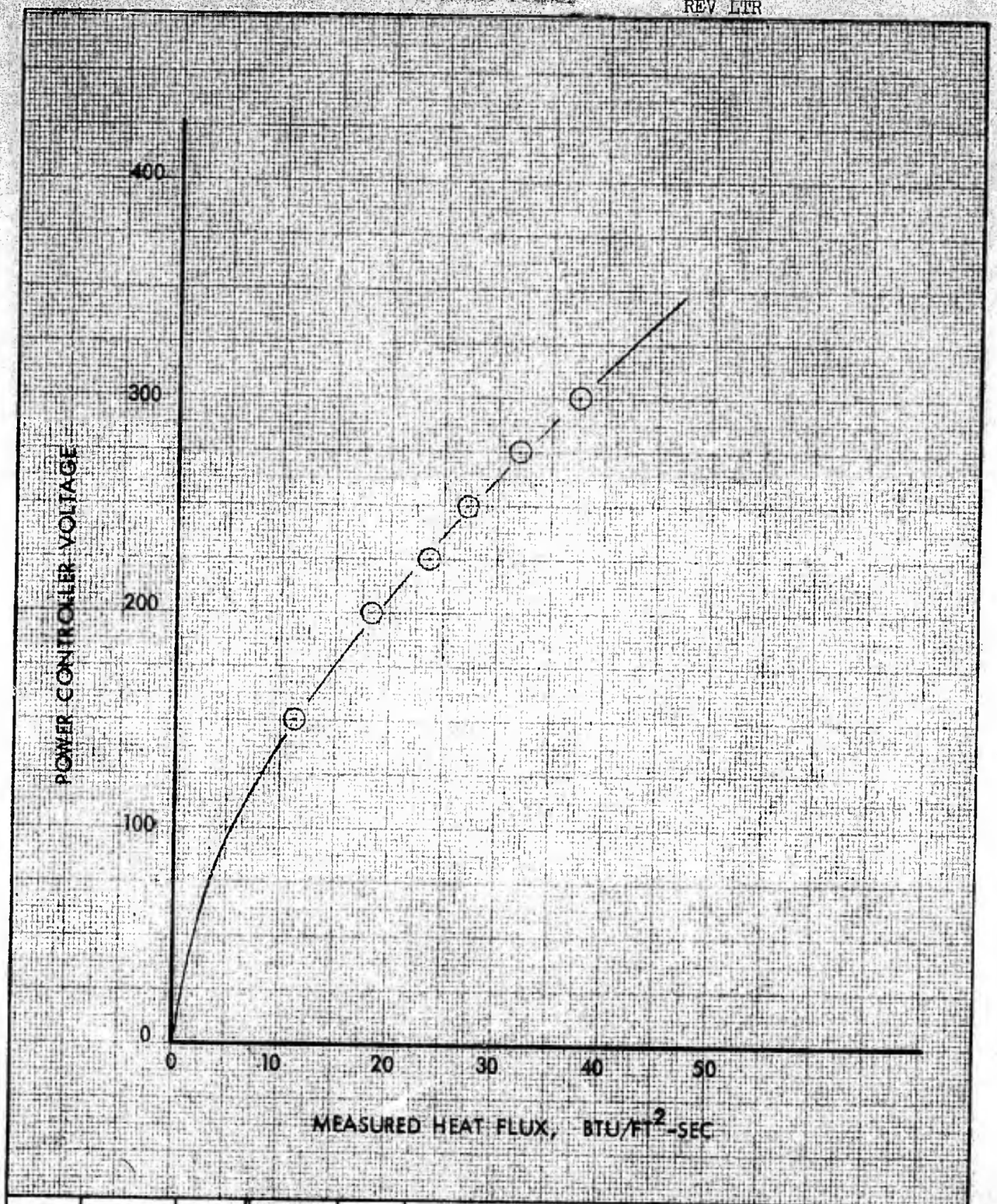

	INITIALS	DATE	REV BY INITIAL	DATE	TITLE	MODEL
CALC					WIND TUNNEL FURNACE CALIBRATION	Fig. 6
CHECK						
APPD.						
APPD.						

U3 4013 8000 REV 1/66

3.3 TEST CONDITIONS

3.3.1 Tunnel

Tests were conducted under conditions noted in the table below:

	PHASE I	PHASE II	PHASE III
MACH NO.	6.50	6.05	6.05
GAS VELOCITY, FT/SEC	4020	3800	3960
TOTAL PRESSURE, PSI	1150	850	1000
TOTAL TEMPERATURE, ^{o}F	1000	1000	1000
Re/FT x 10^{-6}	8.0	7.2	8.5
RADIANT HEATING	NONE	NONE	TO 37.5 BTU/FT^2 SEC

Phase I was conducted with the Mach 6.50 nozzle because the latter was considered to be expendable. Therefore, any damage incurred by the particles passing through the throat would have little consequence. When the damage factor was found to be negligible, and the Mach 6.50 nozzle was required for another test, testing was switched to the Mach 6.05 nozzle. The total pressure was reduced during Phase II operations in order that the specimen heating rates would be the same in each case. Since the auxiliary furnace was not installed at this time, the specimen surface temperatures would have been approximately 850 to 900^{o}F.

The Phase III tests were conducted in order to help resolve a wind tunnel contamination problem incurred during the AGM ablation testing. These tests required surface temperatures in excess of 900^{o}F and as a result led to the design and installation of the radiant furnace. The total pressure was raised to 1000 PSI in order to generate the highest wall shear possible.

The variations in Mach Number and total pressure had a slight effect upon the test section gas velocity and a negligible effect upon the test section particle velocities.

3.3.2 Dust Cloud

The two main factors associated with the simulation of a dust cloud are: (1) the mass density of the contaminants and (2) the size of the particles. Based upon various analyses performed by the Physics Technology staff it was determined that the expected range of densities in nuclear dust clouds was within the range which could be simulated by the dust injection device in the hypersonic tunnel. A range of particle sizes typical of those expected in nuclear dust clouds was selected for these tests.

A convenient contaminant with a mean diameter of 125 microns was found to be an olivine casting sand which is used in the Boeing Foundry. In order to determine the effects of particle size larger and smaller sizes were tested. For the larger particles a silica casting sand with a mean size of 210 microns was selected. Finding an earth-like material of a smaller size proved to be more difficult and therefore 50 micron glass beads were substituted.

3.4 MODEL DESIGN

The configurations of the models tested are shown in Figure 7. They consisted of four basic shapes; (1) hemisphere, (2) 25° half-angle cone with a 3/8 inch nose radius, (3) a 15° half-angle cone with both sharp and blunt noses and (4) a 9° half-angle cone with sharp and blunt noses. All of the models had a 1.8 inch base diameter, a dimension which coincided exactly with the opening in the cloud sampling device. The sharp nosed versions had a boundary layer trip strip consisting of .030 steel balls spot welded with a spacing of one diameter.

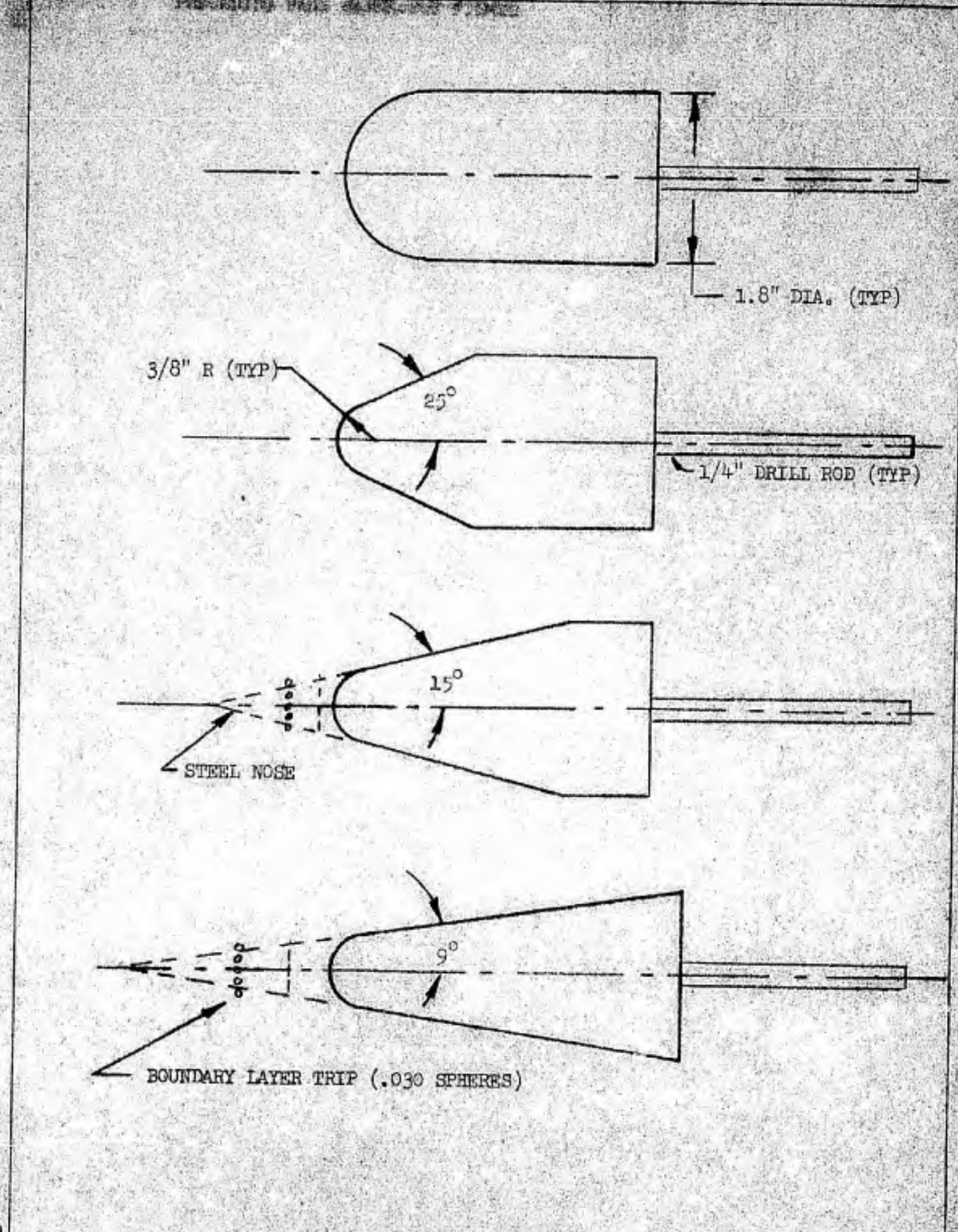

DETAILS OF PARTICLE EROSION MODELS

FIGURE 7

This trip strip insured the existence of a turbulent boundary layer over the surface of these cones. All of the cones were molded around a sting mount that was simply a piece of $\frac{1}{4}$ inch drill rod.

The models were made of three materials; cork, Dow Corning DC 93-072 silicone rubber, and a Boeing developed compound referred to as Carborazole.

The only models that were instrumented was a group of 9° cones made of silicone rubber. These specimens had four horseshoe shaped foil thermocouples molded at specific depths - .010 to .050 inch - below the surface. These models were used to determine the surface temperatures of the silicone rubber specimens when they were subjected to the combined effects of tunnel flow and external radiant heating.

3.5 TEST PROCEDURE

3.5.1 Dust Cloud Calibration

The success of this test program was largely dependent upon a reasonably accurate determination of the mass of material impinging upon the test specimens. Because of particle stratification in the tunnel flow, concurrent specimen testing and cloud sampling was not reliable and feasible. Therefore many repetitious sampling runs were conducted. These runs included a horizontal and vertical cloud survey to determine the best model location. The average of these runs provided a reliable ratio between the material impinging to the amount dispensed. After considerable experimentation a dispensing technique was developed where this ratio was repeatable within 5%. It was then assumed that this ratio also prevailed during a specimen run; i.e., the weight of material dispensed multiplied by this ratio determined the amount of material

that struck the specimen. A ratio was determined, in this manner, for each of the three particle sizes tested.

The cloud sampler design that proved to be the most effective is shown in Figure 8. It is quite simply an "L" shaped tube with the short leg open and the long end closed. The open end, equipped with a hardened steel nose-ring of an inside diameter identical (1.8") to the specimens', was positioned in the tunnel flow. Particles flowing down the nozzle and into the test section passed through the sampler bow shock, entered the tube and were collected at the closed end. At the conclusion of the run the material collected was removed from the sampler and weighed. Therefore, the relationship, $\eta_c = \frac{W_c}{W_i}$ was established for each of the particle sizes. Figure 9 is an indication of the vertical and horizontal variations in the test section dust cloud.

3.5.2 Specimen Testing

The test specimens were tested in three manners. These were: (1) ablation runs, (2) ablation-erosion runs and (3) surface temperature runs.

In the ablation runs, the specimens were simply exposed to the tunnel flow, or combined tunnel flow-radiant heating conditions, for a specific length of time. These runs established the amount of basic weight loss and configuration change due to heating and shear.

Ablation-erosion runs were conducted using three modes of operations. These three modes result in the erosion testing of three initial surface conditions: (1) a hot-char surface, (2) a cold-char surface and (3) a virgin or uncharred surface.

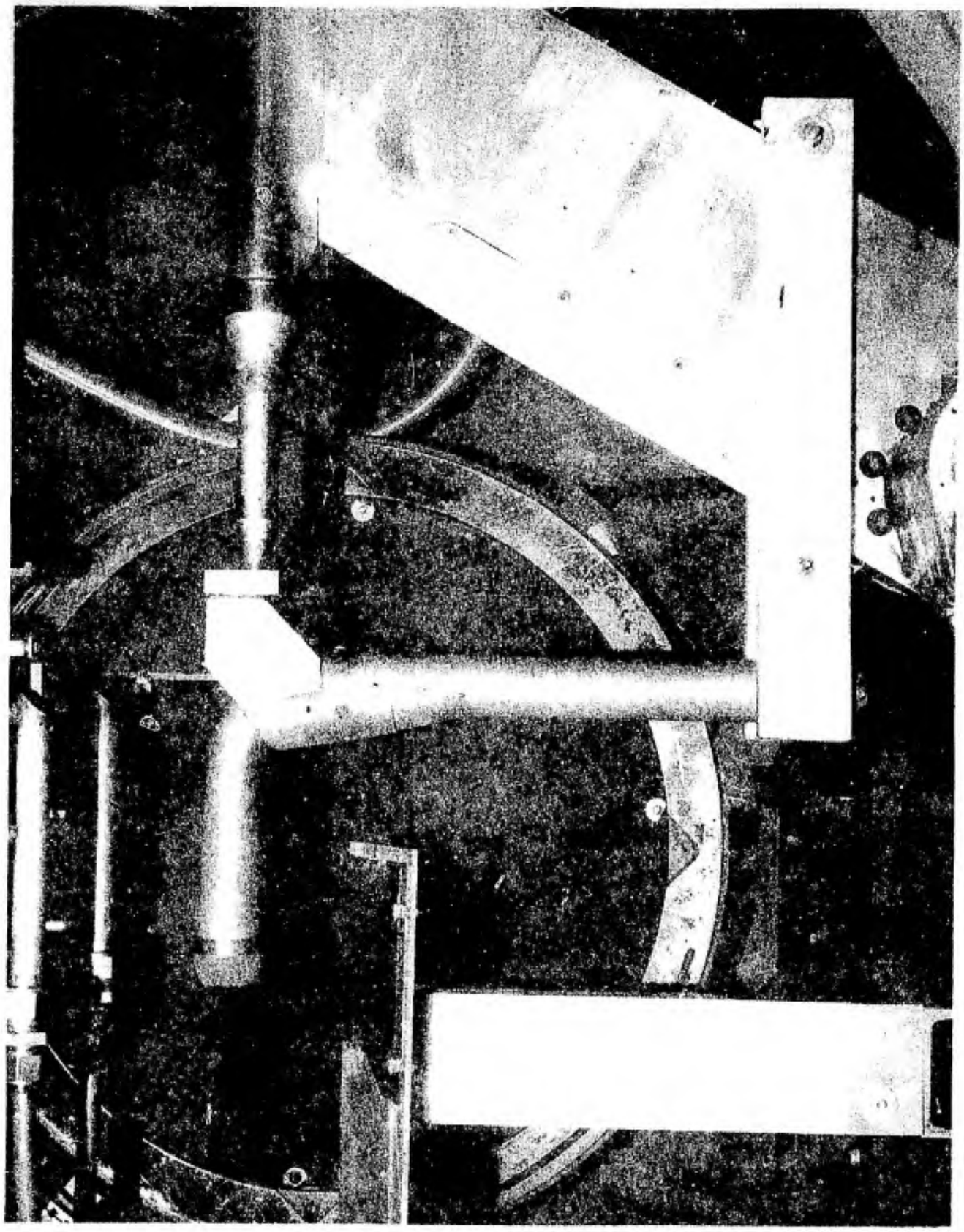

DUST CLOUD SAMPLER SHOWN IN STOWED POSITION

FIGURE 8
D2-125929-1
Sheet 35

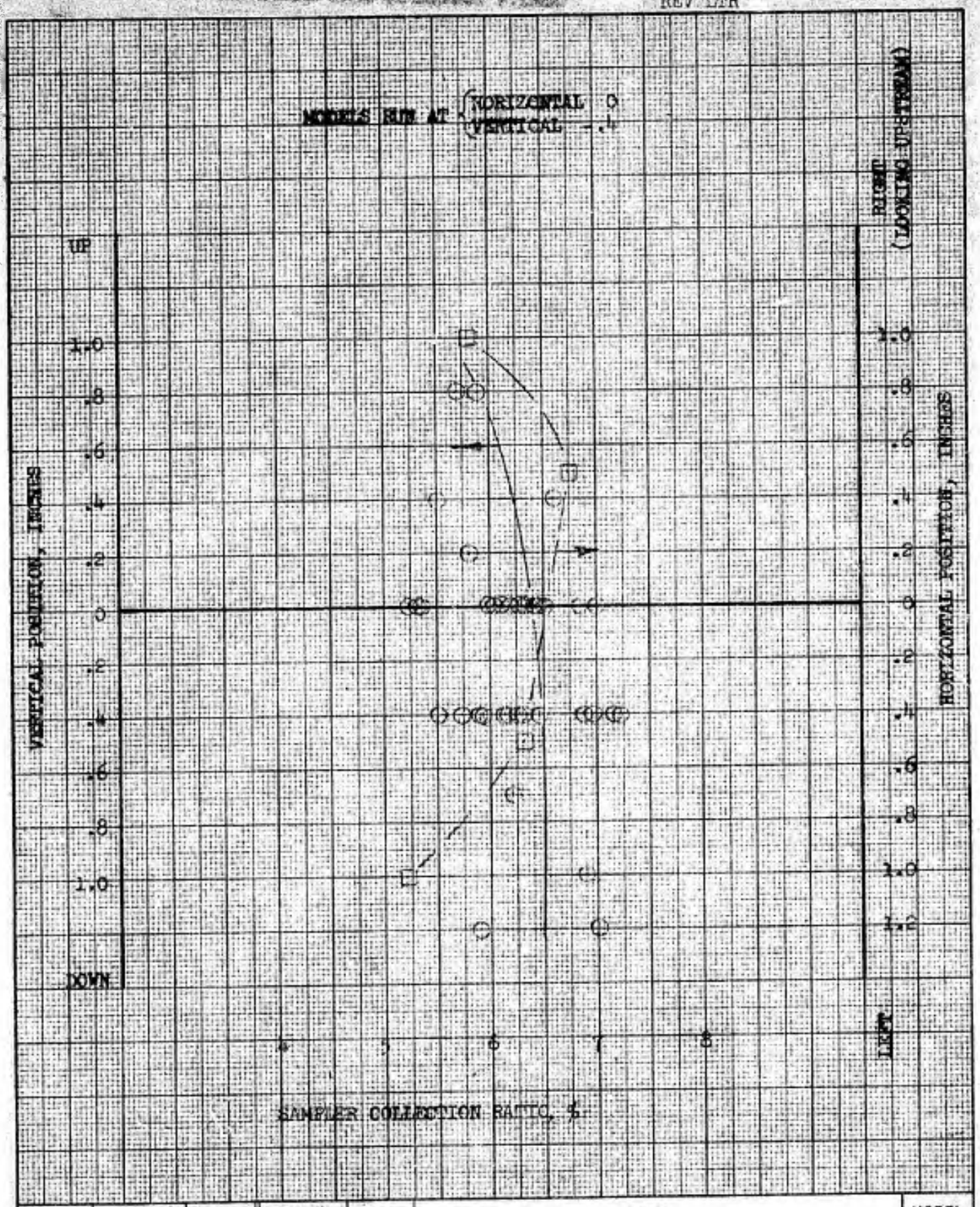

	INITIALS	DATE	REV BY INITIAL	DATE	TITLE	MODEL
CALC					CALIBRATION CURVES OF DUST CLOUD IN WIND TUNNEL TEST SECTION FOR 125 μM OLIVINE CASTING SAND	Fig. 9
CHECK						
APPD.						
APPD.						

A hot-char run is made by exposing the specimen to the test environment for a specific period of time (usually 10 seconds) prior to exposure to the dust cloud. This mode would be representative of missile entry into the dust cloud at the higher altitudes and hotter portion of the trajectory.

The cold-char mode consists of exposing a previously charred but not eroded specimen to the dust cloud at the instant the model arrived at the tunnel centerline. This results in a concurrent reheating of the char while erosion is taking place. This mode was tested in order to evaluate the relative resistance of a hot and cold char and not to simulate flight conditions.

When the above test procedure was employed using a new uncharred specimen it was considered to be a virgin run. This mode would be representative of the missile entry into a dust cloud at lower altitudes while the missile is still relatively cool. During this procedure the surface is concurrently being charred and eroded.

The surface temperature runs were conducted with the instrumented silicone rubber models. These models were exposed to the combined tunnel flow-radiant heat environment. Each model was run with an increase in the radiant heat flux until the maximum level of 37.5 BTU/FT^2-SEC was achieved. During these runs the thermocouple temperatures were recorded on strip charts revealing the temperature profiles at four surface depths. This temperature data was analyzed to obtain surface temperatures versus heat flux as described later.

4.0 DATA REDUCTION

4.1 CONTAMINATION RATES

The weight of dust or sand dispensed into the tunnel was determined by placing a 300 gram sample in the sand storage can prior to a run and weighing the residue after the run. Therefore,

$$W_d = 300 - W_A$$

As mentioned previously, the amount of sand presumed to have impinged upon a specimen, W_i, was the product of the amount dispensed and the impingement ratio,

$$W_i = \eta_c \times W_d$$

4.2 ABLATION LOSSES

The loss of material due to stream and radiant heating effects was determined by simple before and after weight measurements;

$$MW_{AB} - MW_B = MW_A$$

The ablation only losses, as a function of time, for cork and carborazole are shown in Figure 10. This loss for the silicone rubber, Figure 11, is shown as a function of surface temperature.

4.3 ABLATION - EROSION

The specimen material lost during an ablation (pre-char) interval followed by erosion is also a measurement of before and after weights. To obtain the weight loss due to erosion alone, either of two analysis methods can be employed: (1) to subtract just the pre-char ablative losses or (2) to subtract the ablative loss for the entire exposure period. For example, if a model were subjected to 10 seconds of pre-char and 10 seconds of erosion, the pre-test weight could be reduced by either 10 seconds or 20 seconds of ablative weight loss per Figure 10.

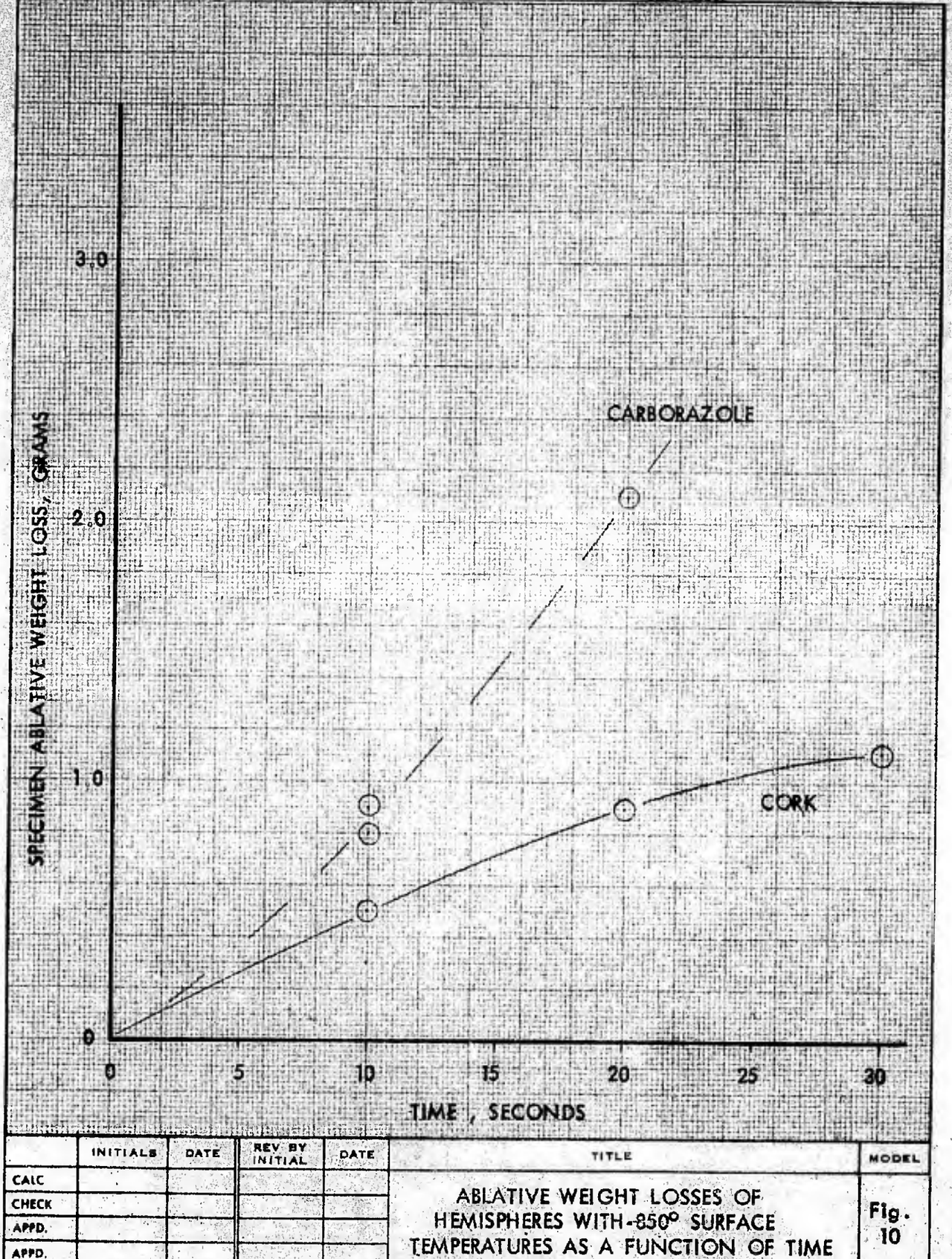

	INITIALS	DATE	REV BY INITIAL	DATE	TITLE	MODEL
CALC					ABLATIVE WEIGHT LOSSES OF HEMISPHERES WITH -850° SURFACE TEMPERATURES AS A FUNCTION OF TIME	Fig. 10
CHECK						
APPD.						
APPD.						

U3 4013 8000 REV. 1/66

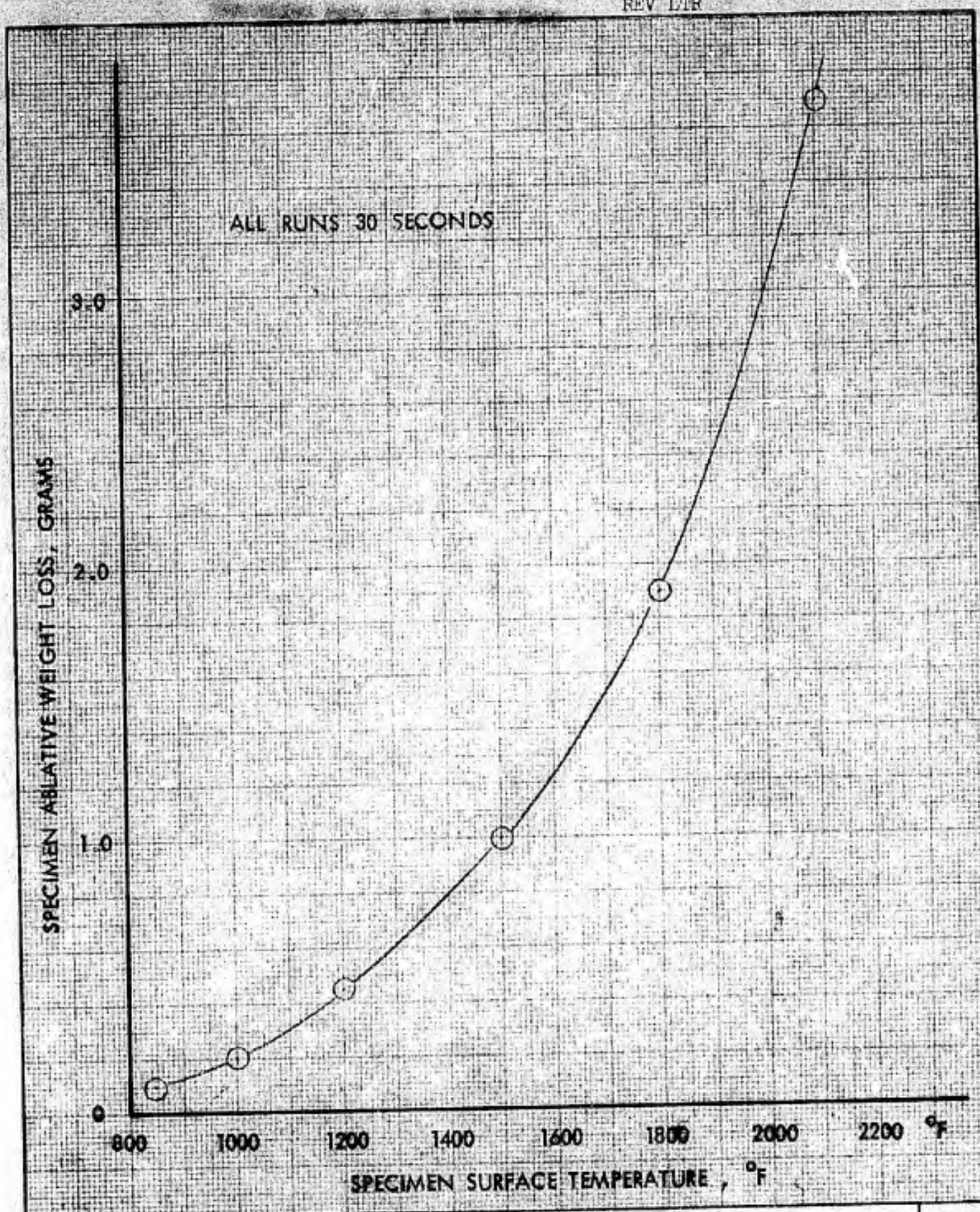

	INITIALS	DATE	REV BY INITIAL	DATE	TITLE	MODEL
CALC					WEIGHT LOSS OF SHARP 9° CONES, DC-93-072 SILICONE RUBBER, ABLATION ONLY	Fig. 11
CHECK						
APPD.						
APPD.						

U3 4013 8000 REV. 1/66

REV LTR_____

Neither approach is absolutely correct because during the erosion phase the losses are due to the combined effect of ablation and erosion. However, since the two effects cannot be separated and extended pre-char ablative losses are not available for all specimen configurations, method (1) above has been used in the analysis of these data. The effects of including and excluding the weight loss can be seen in Figure 12, where the data for the hemisphere models for each method is shown.

Specimens subjected to the combined effects of ablation and erosion quite often suffer a considerable change in shape. In order to record this shape-change a profile measuring device was devised. This device, referred to as a comparitor, consisted of a spark gap generator, a columnating mirror and a polaroid film holder. The before and after profile shadows of the specimens were projected upon the film by the short time duration spark gap. The result is a black profile of the remaining configuration superimposed upon a gray profile of the original shape. Several examples of the comparitor results are shown in Figure 13. With these records, shape changes as a function of erosion rates could be analyzed.

4.4 WEAR ANALYSIS

Some of the hemispherical cylinder erosion data was analyzed using the method of Neilson and Gilchrist, Reference 10. The details of the procedure as applied to these specimens can be found in Appendix A. Briefly the method consisted of dividing the total erosive wear into two wear factors, impact wear and cutting wear. The hemisphere cylinder data were used in this manner by dividing the total eroded volume into sections and assuming an average λ, particle impingemen ngle, for each of the volumes. Thus, by knowing the

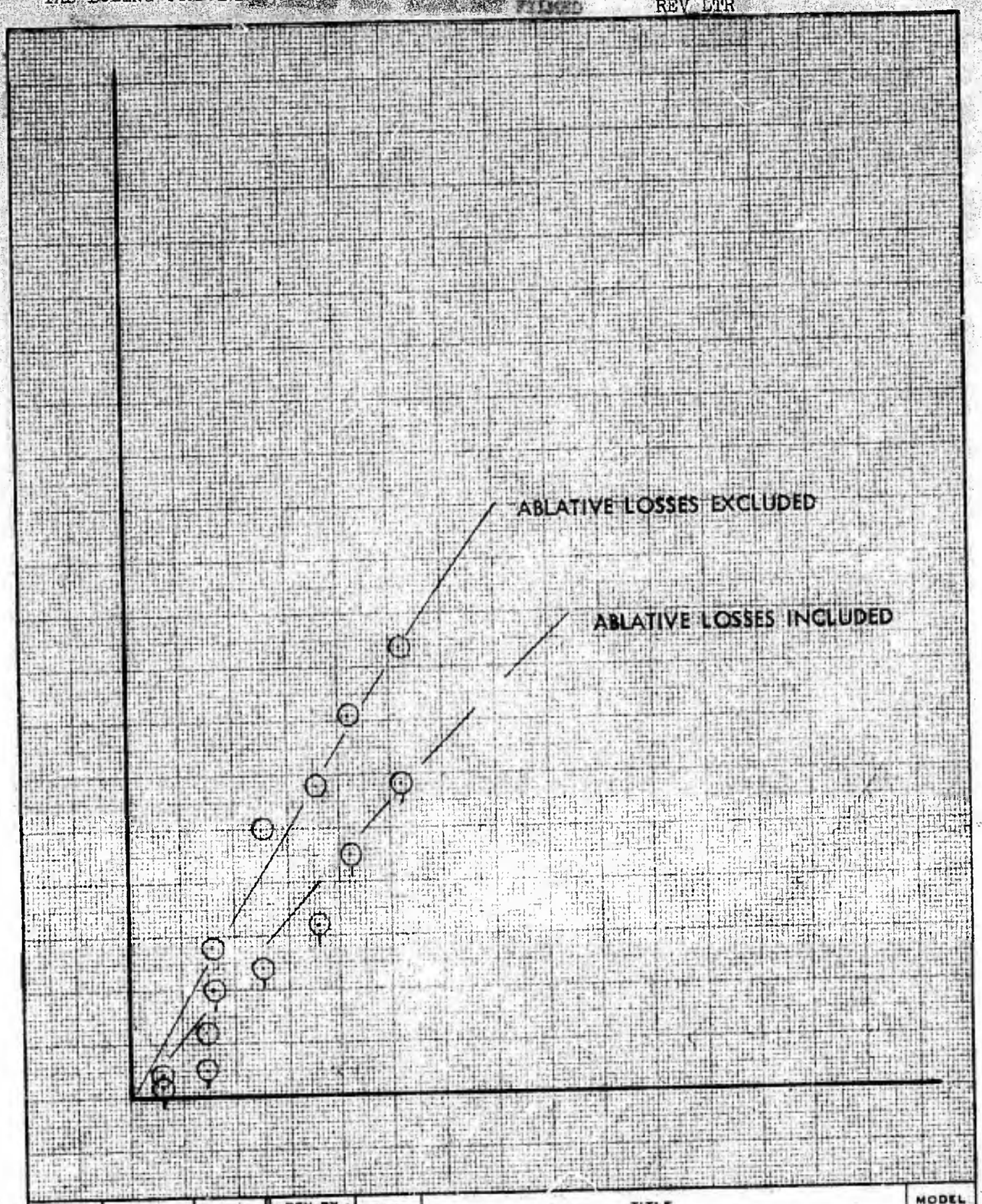

	INITIALS	DATE	REV BY INITIAL	DATE	TITLE	MODEL
CALC					CARBORAZOLE	Fig. 12A
CHECK						
APPD.						
APPD.						

U3 4013 8000 REV. 1/66

REV LTR

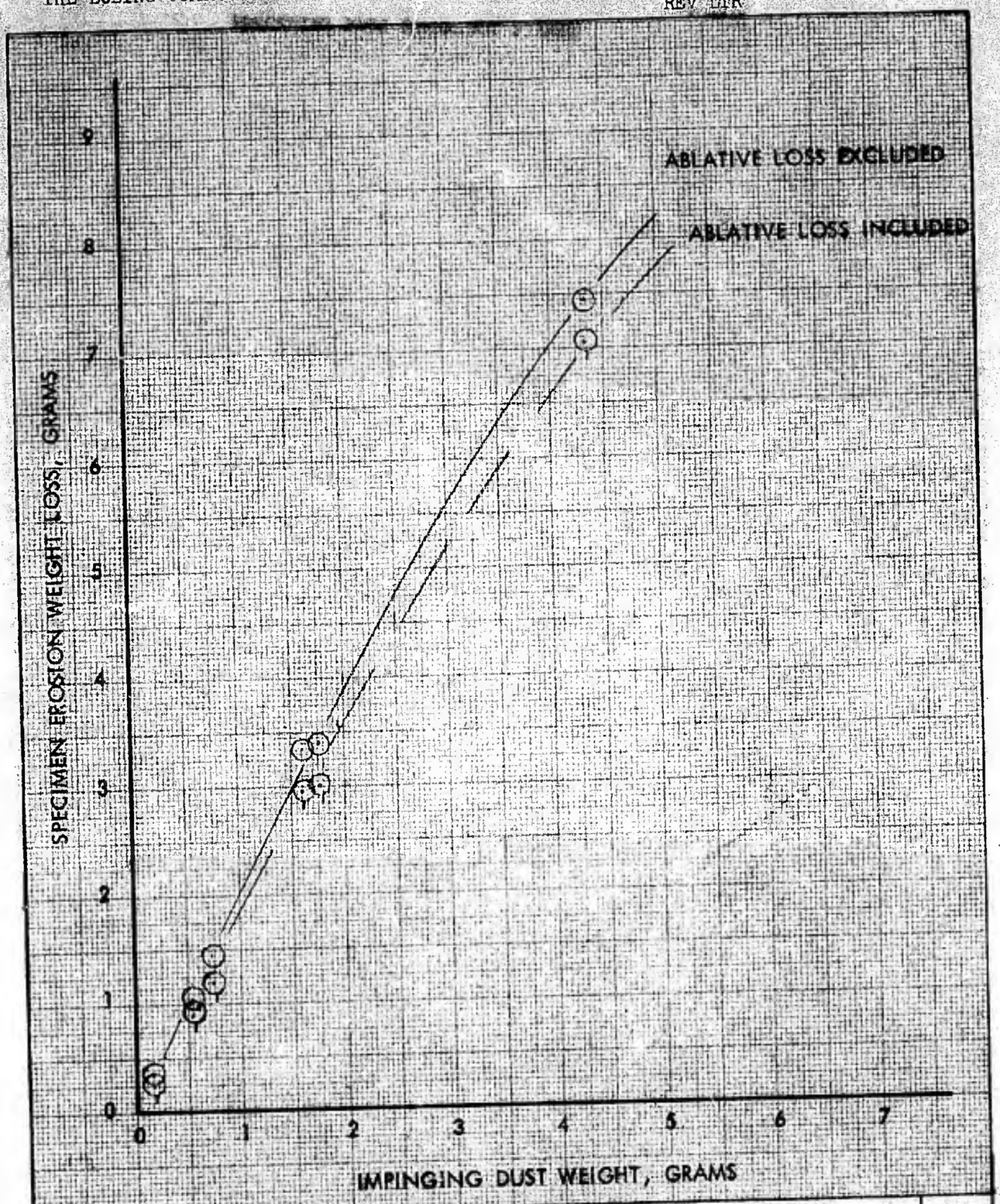

	INITIALS	DATE	REV BY INITIAL	DATE	TITLE	MODEL
CALC					COMPARISON OF CORK HEMISPHERE DATA ANALYSIS METHOD	Fig. 12B
CHECK						
APPD.						
APPD.						

U3 4013 8000 REV. 1/66

REV LTR

BOEING NO. D2-125929-1

SH. 43

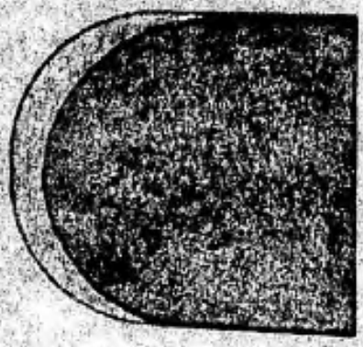

CORK HEMISPHERE

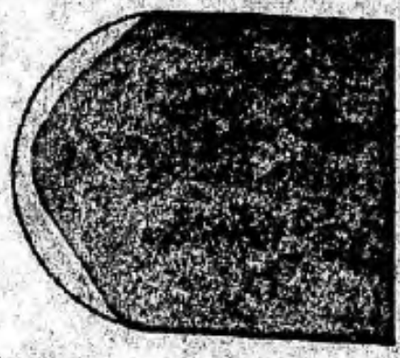

CARBORA 20LE HEMISPHERE

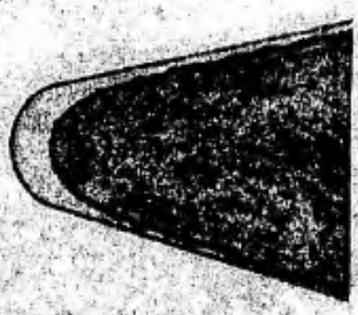

CORK 15° HALF-ANGLE

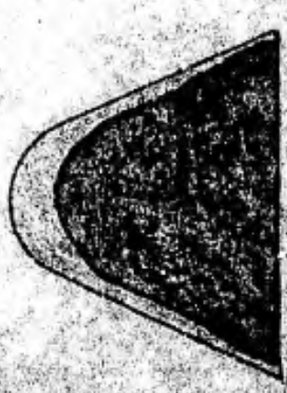

CARBORA 20LE 25° HALF-ANGLE

TYPICAL "COMPARITOR" PROFILES OF VARIOUS EROSION SPECIMENS

FIGURE 13

weight of ablation material eroded and the weight of the impacting dust particles, the wear attributable to each factor can be derived. The exact procedure is outlined in Appendix A and the data derived is shown in a following section.

4.5 SURFACE TEMPERATURE EXTRAPOLATION

As mentioned previously, the instrumented silicone rubber models had four foil thermocouples imbedded beneath the surface at known depths. The temperatures recorded by these thermocouples were plotted, as a function of depth, temperature and time, as shown in the example of Figure 14. This was done for each of the radiant heat flux rates. This resulted in a specimen surface temperature plot as a function of exposure time as is shown in Figure 15.

4.6 CONVERSION OF DATA TO C_N VALUES

The notation C_N, in the units of Joules per gram of material removed, is often used in expressing a degree of erosion loss. (It would be found, for instance, in Reference 15.) The data shown in this report can be expressed in terms of C_N by the use of the equation

$$C_N = \frac{4.63 \times 10^{-5} \times V_p^2}{\text{Loss Ratio}}$$

where the loss ratio is the specimen weight loss divided by the weight of the impinging dust.

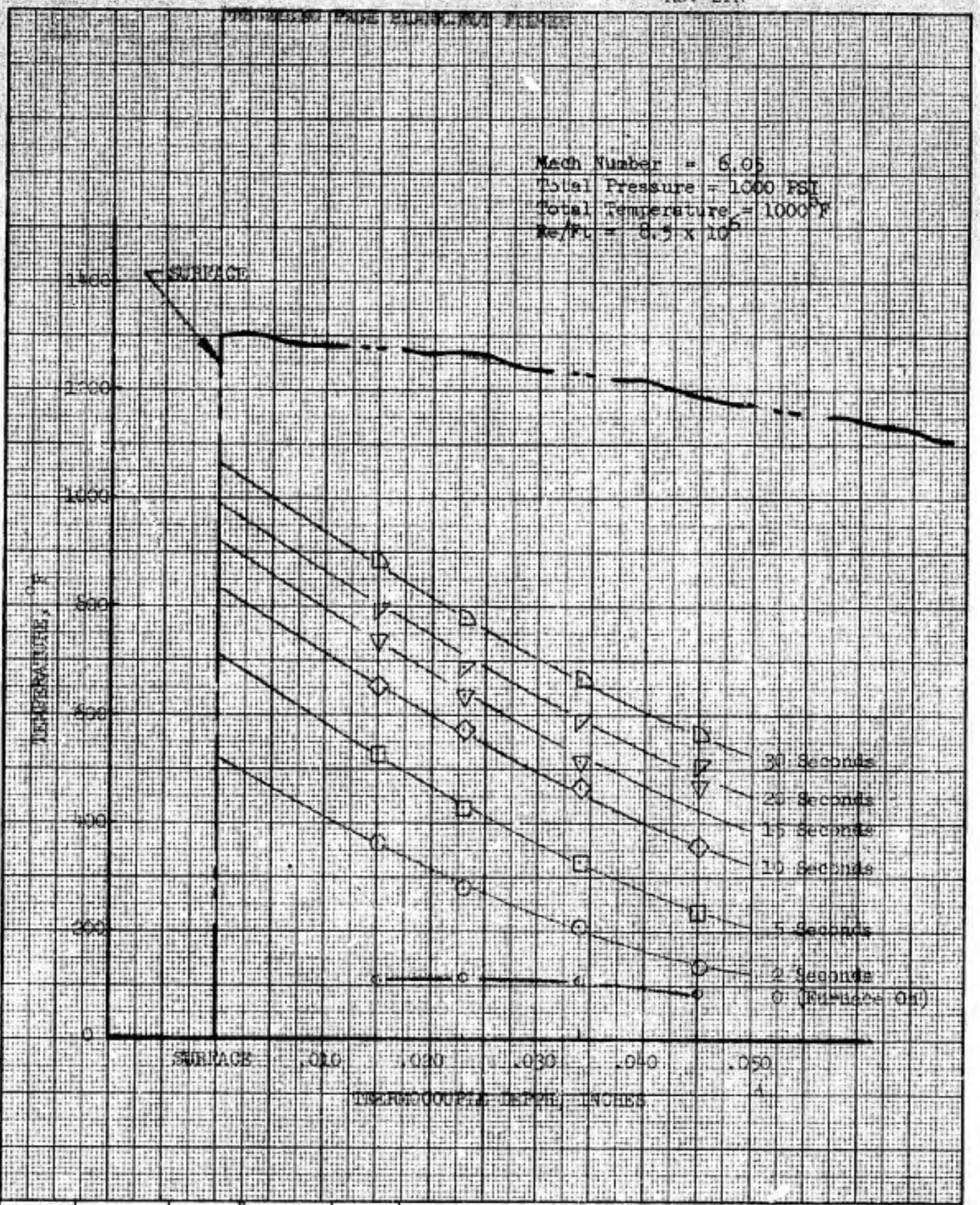

	INITIALS	DATE	REV BY INITIAL	DATE	TITLE	MODEL
CALC					SILICONE RUBBER MODEL TEMPERATURES IN TUNNEL FLOW AUGMENTED BY A RADIANT HEAT FLUX OF 5 BTU/FT^2-SEC	Fig. 14
CHECK						
APPD.						
APPD.						

US 4013 8000 REV. 1/66

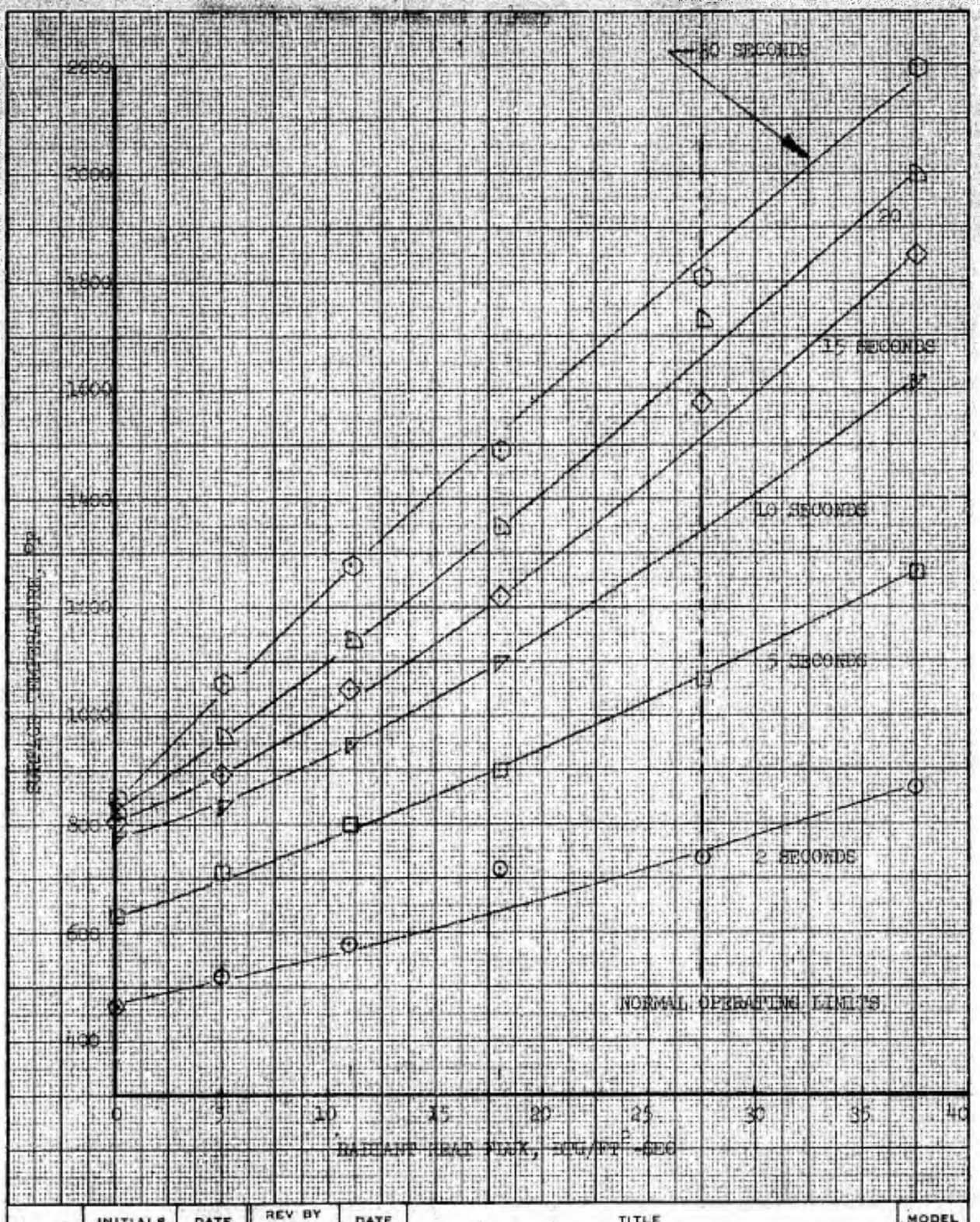

	INITIALS	DATE	REV BY INITIAL	DATE	TITLE	MODEL
CALC					SILICONE RUBBER MODEL SURFACE TEMPERATURES AS A FUNCTION OF TIME AND RADIANT HEAT FLUX	Fig. 15
CHECK						
APPD.						
APPD.						

5.0 TEST RESULTS

5.1 PARAMETER EFFECTS

5.1.1 Temperature

The dramatic increase in the erosion rate of Dow Corning DC-93-072 silicone rubber as the surface temperature is elevated from 850°F to 1800°F is shown in Figure 16. The erosive effects are rather insignificant below a surface temperature of approximately 1000°F. The material is relatively uneffected (notable in Figure 11) at these lower temperatures and acts essentially like the tough virgin material. However, at temperatures above 1000°F the rubber surface begins to take on the appearance of a dried "mud-flat" and becomes rather soft and brittle. This surface is very susceptible to particle impact and the erosion rate rises very rapidly, as can be noted in Figure 16B. The effect of a small amount of contamination is notable in the cross-plotted data of Figure 16C where an impaction rate of 0.5 grams (1.67×10^{-2} grams/sec) results in an increase of specimen weight loss of several factors; e.g., 5 at 1500°F. This same data is presented in Figure 16D, where the total specimen weight loss is normalized by the uncontaminated ablation loss, revealing that the effect of increasing the particle impingement rate diminishes as the surface temperature of the rubber is elevated beyond 1200°F. This can be attributed to the increasing significance of the pure ablation loss as the surface temperature is elevated beyond 1200°F.

The effects of elevated surface temperatures on the particle erosion of cork are shown in Figure 17. Because cork forms a surface char at a lower temperature than silicone rubber, it shows a relatively high loss ratio at 850°F. At a temperature of 1250°F, the only other data point, the cork loss ratio increases by a factor of 2 to 3. However, the curve indicates that as the particulate mass density increases, the char is removed faster than it is formed and the loss ratio approaches an asymptote. The cork elevated temperature data is limited to this one curve and no tests were conducted with carborazole at elevated temperatures.

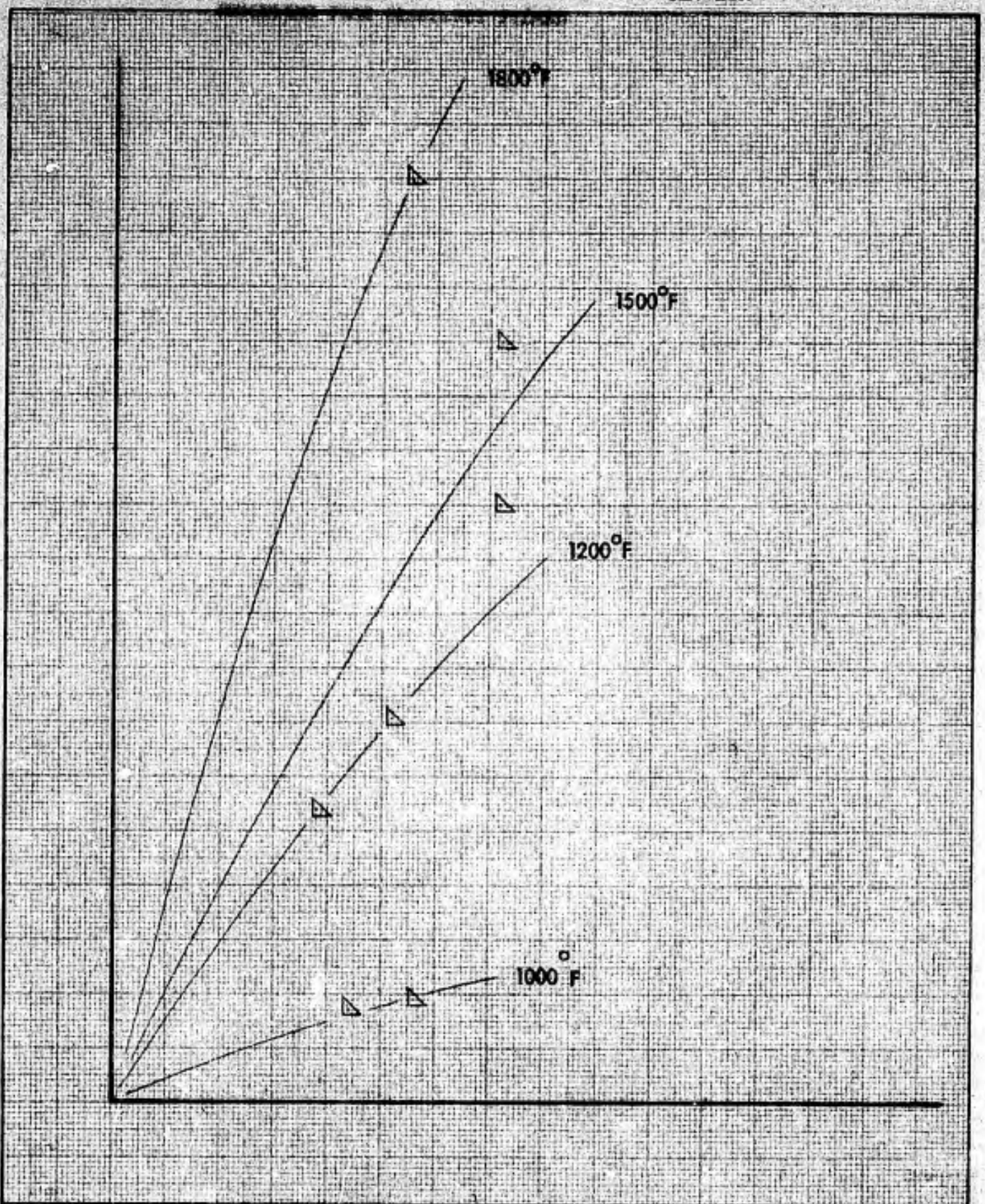

	INITIALS	DATE	REV BY INITIAL	DATE	TITLE	MODEL
CALC					50 MICRON GLASS BEADS	Fig. 16A
CHECK						
APPD.						
APPD.						

U3 4013 8000 REV 1/66

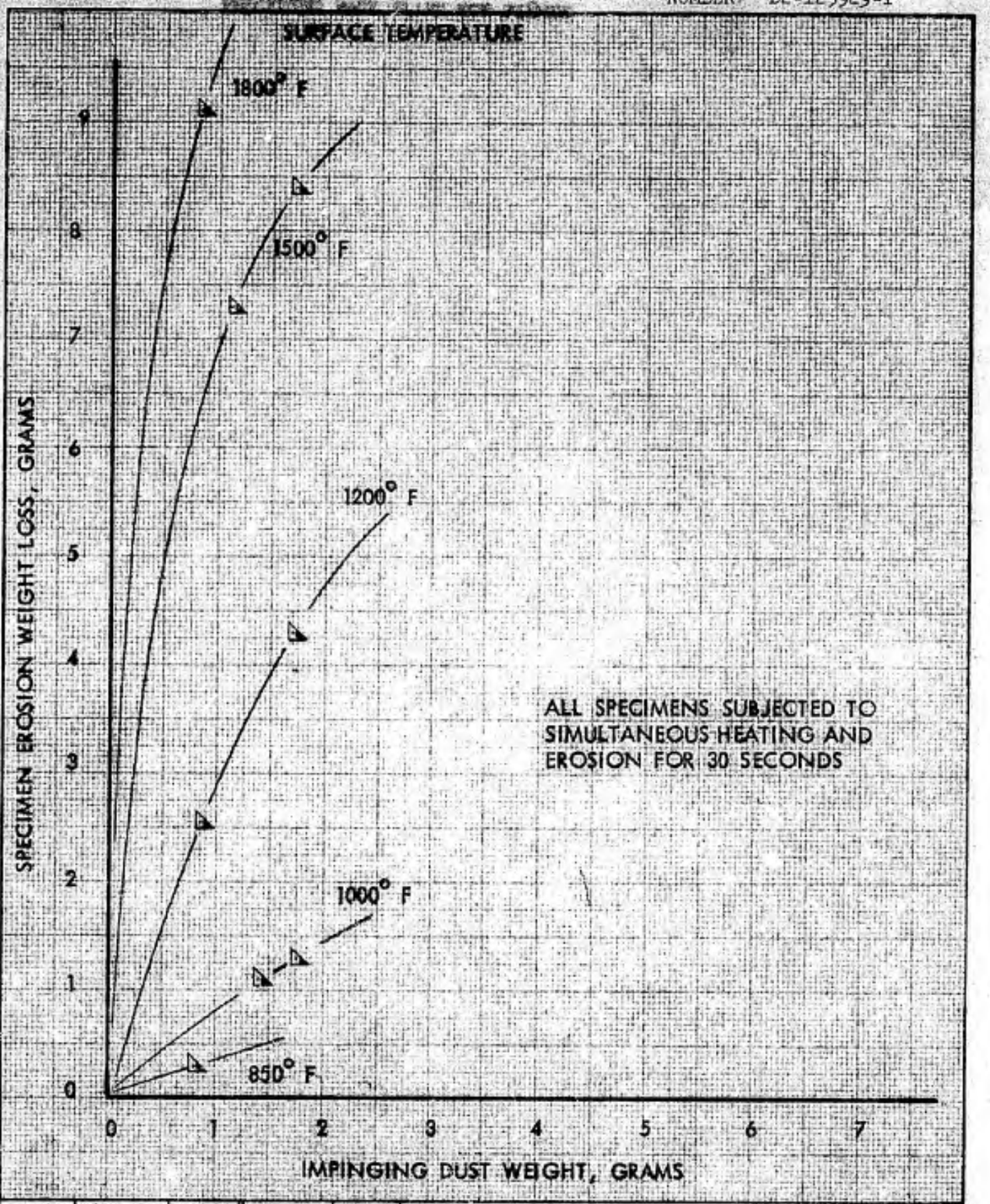

	INITIALS	DATE	REV BY INITIAL	DATE	TITLE	MODEL
CALC					WEIGHT LOSS OF SHARP 9° CONE, DC-93-072 SILICONE RUBBER, IMPACTED BY 125 MICRON OLIVINE SAND	Fig. 16B
CHECK						
APPD.						
APPD.						

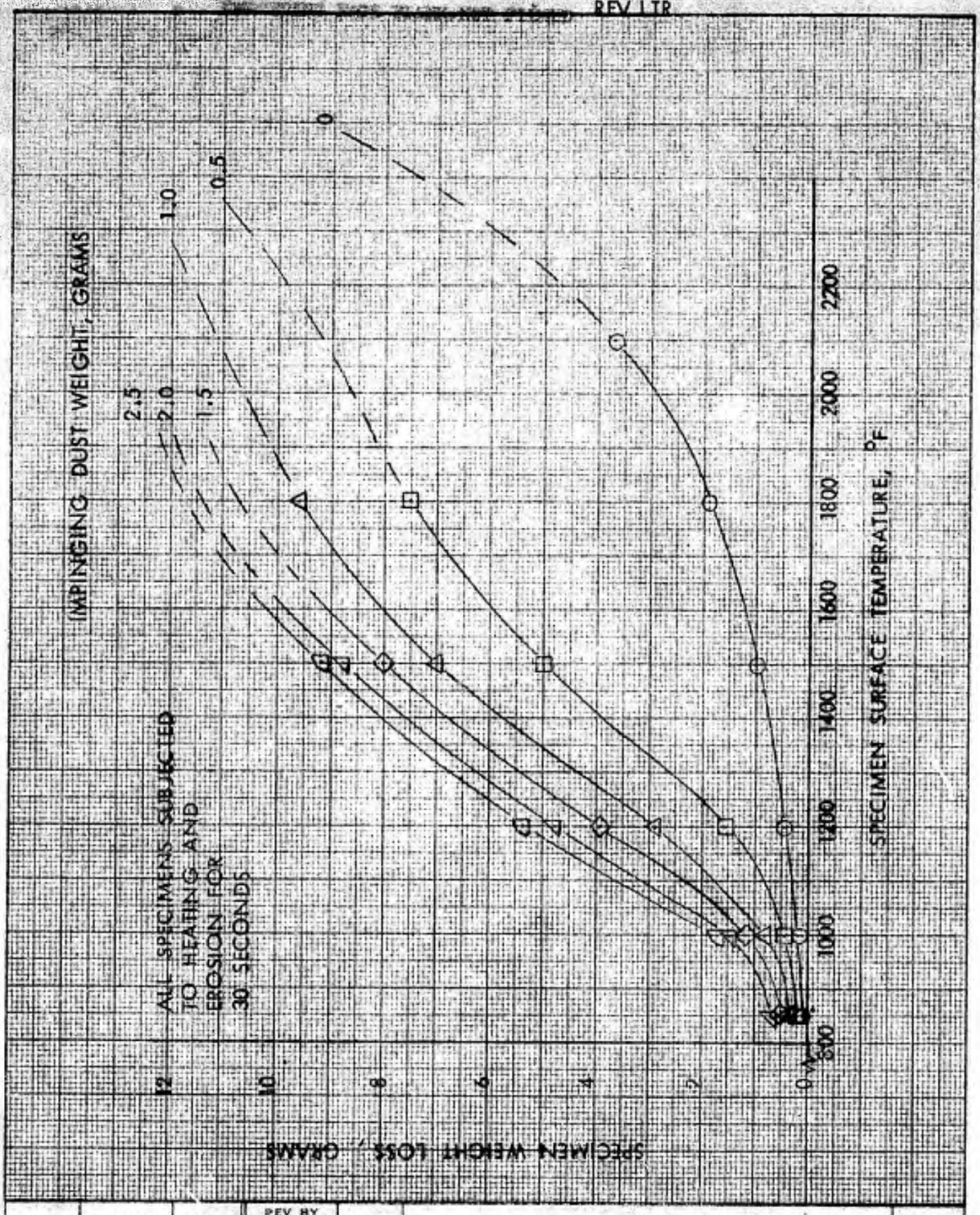

	INITIALS	DATE	REV BY INITIAL	DATE	TITLE	MODEL
CALC					WEIGHT LOSS OF SHARP 9° CONES, DC-93-072 SILICONE RUBBER, IMPACTED BY 125 MICRON OLIVINE SAND	FIG. 16C
CHECK						
APPD.						
APPD.						

U3 0013 8000 REV. 1/66

REV LTR

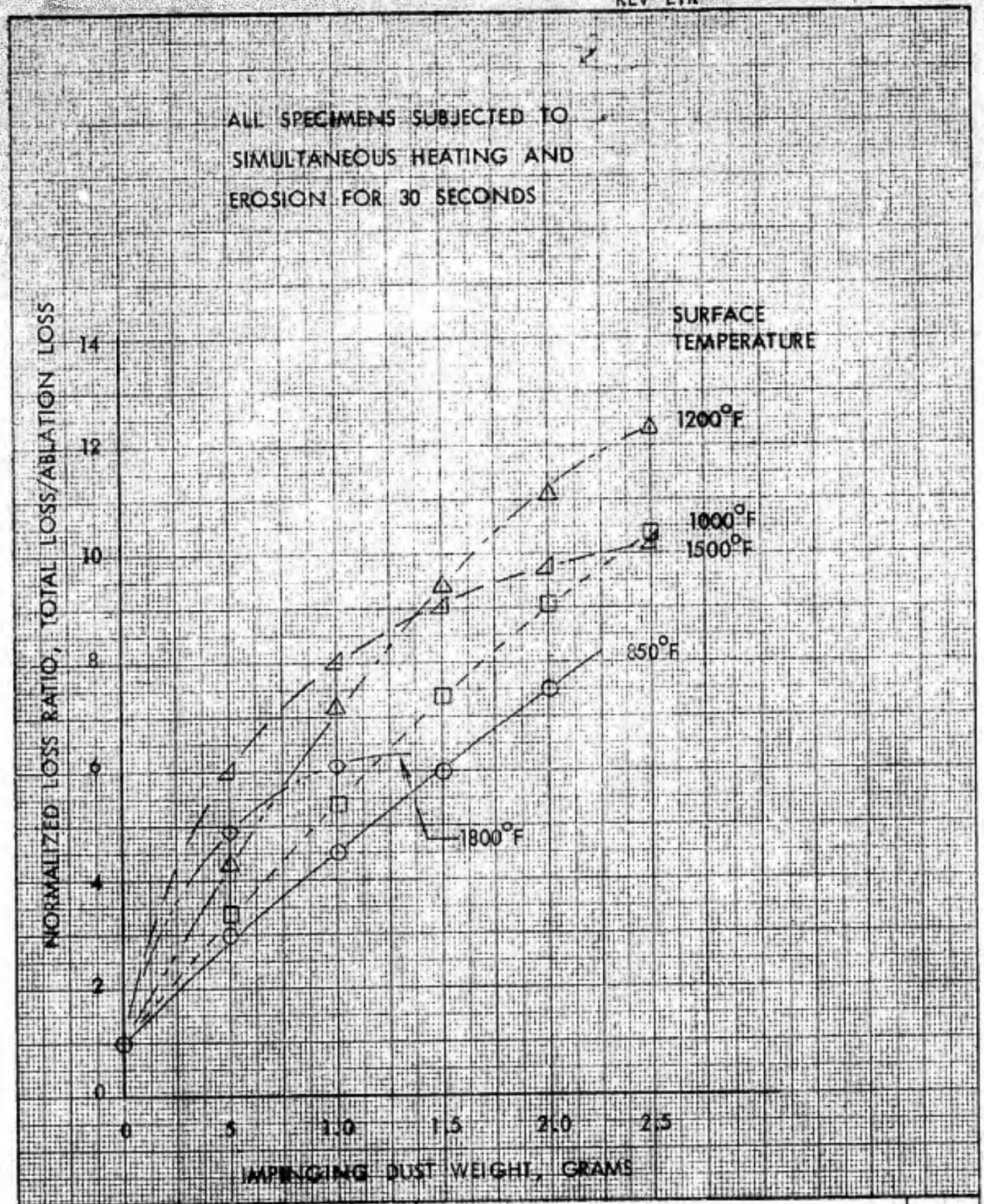

	INITIALS	DATE	REV BY INITIAL	DATE	TITLE	MODEL
CALC					NORMALIZED SILICONE WEIGHT LOSS RATIO SILICONE RUBBER CONES IMPACTED BY 125 MICRON OLIVINE SAND	FIG. 16D
CHECK						
APPD.						
APPD.						

U3 4013 8000 REV. 1/66

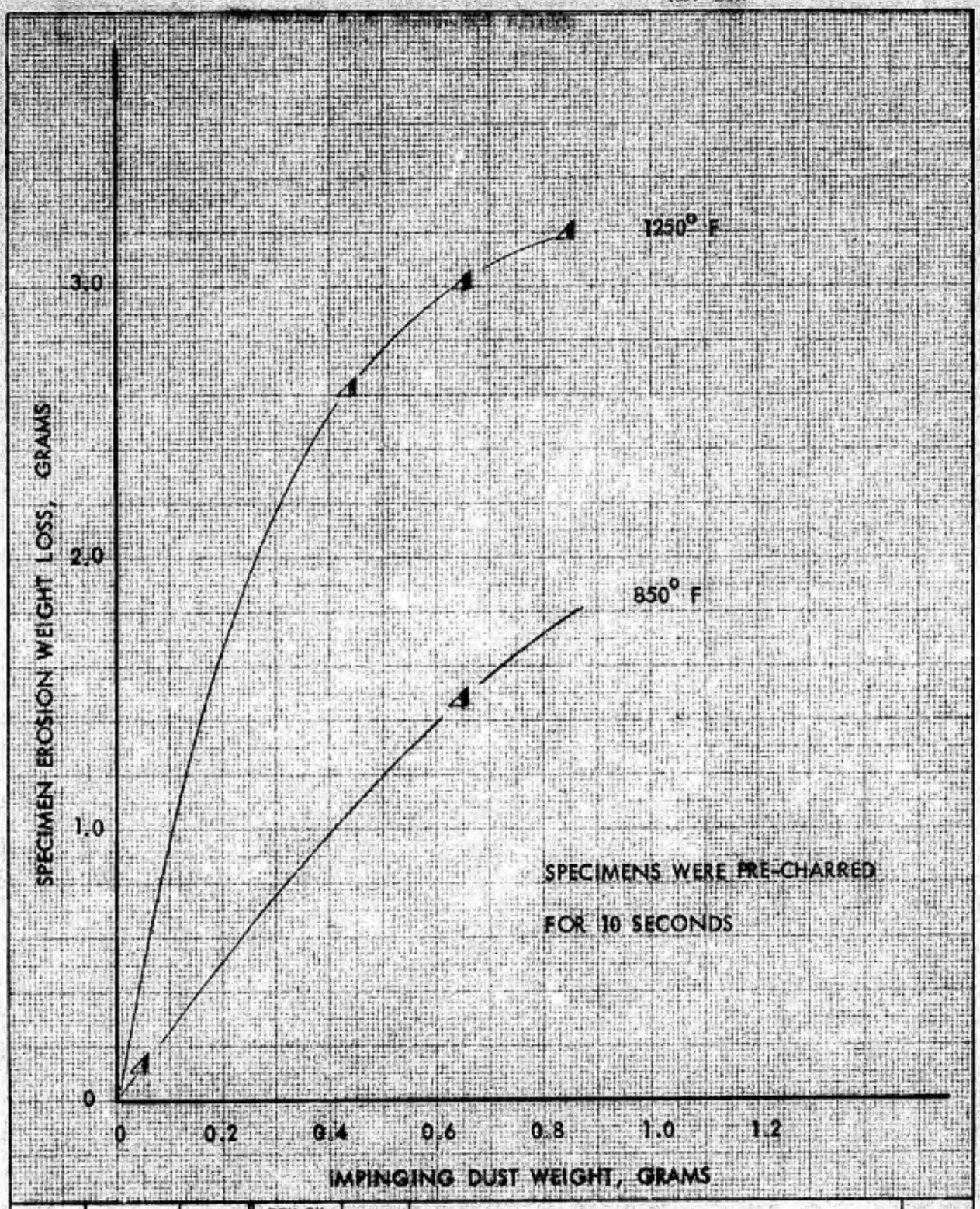

	INITIALS	DATE	REV BY INITIAL	DATE	TITLE	MODEL
CALC					WEIGHT LOSS OF SHARP 15° CORK CONES ERODED BY 125 MICRON SAND AS A FUNCTION OF SURFACE TEMPERATURE	Fig. 17
CHECK						
APPD.						
APPD.						

U3' 4013 8000 REV 1/66

REV LTR_____

5.1.2 Particle Size

The effect of particle size can be noted in most of the plotted data, especially in Figures 16 and 18. The latter illustrates the weight loss incurred by the cork and carborazole hemispheres when impacted by the three particulate sizes. It is notable that the 125 and 210 micron data fall on the same loss ratio line with a marked reduction in the 50 micron glass data. The latter was unexpected because one could anticipate that the greater surface area to mass ratio would result in an increasing volume removal per unit mass of abrasive. However, considering the analytical method of FINNIE [7] it would appear, that at similar energy levels, angular particles should produce more erosion than sphere-like particles. This is confirmed by test data from Reference 19 where sandblasting with "sharp" sand produced four times the wear of round sand. Viewed through a microscope the 125 micron olivine sand and 210 silica sand are very angular and the glass beads are spherical and smooth. Therefore, it is concluded that the particle size effect noted in these data can also be attributed to the particle shape rather than size.

5.1.3 Material

The relative abrasion resistance characteristics of the three materials can be seen in Figure 18. Here the data derived from the hemisphere specimens of cork and carborazole can be compared. It will be noted that at the 850°F surface temperature condition, the carborazole is slightly more resistant to the sand particles and considerably more resistant to the glass beads. The same effect can be noted in Figure 19 where the data is more extensive. For added comparison, the resistance of the virgin silicone rubber is referenced, indicating its superior abrasion resistance at these low surface temperatures.

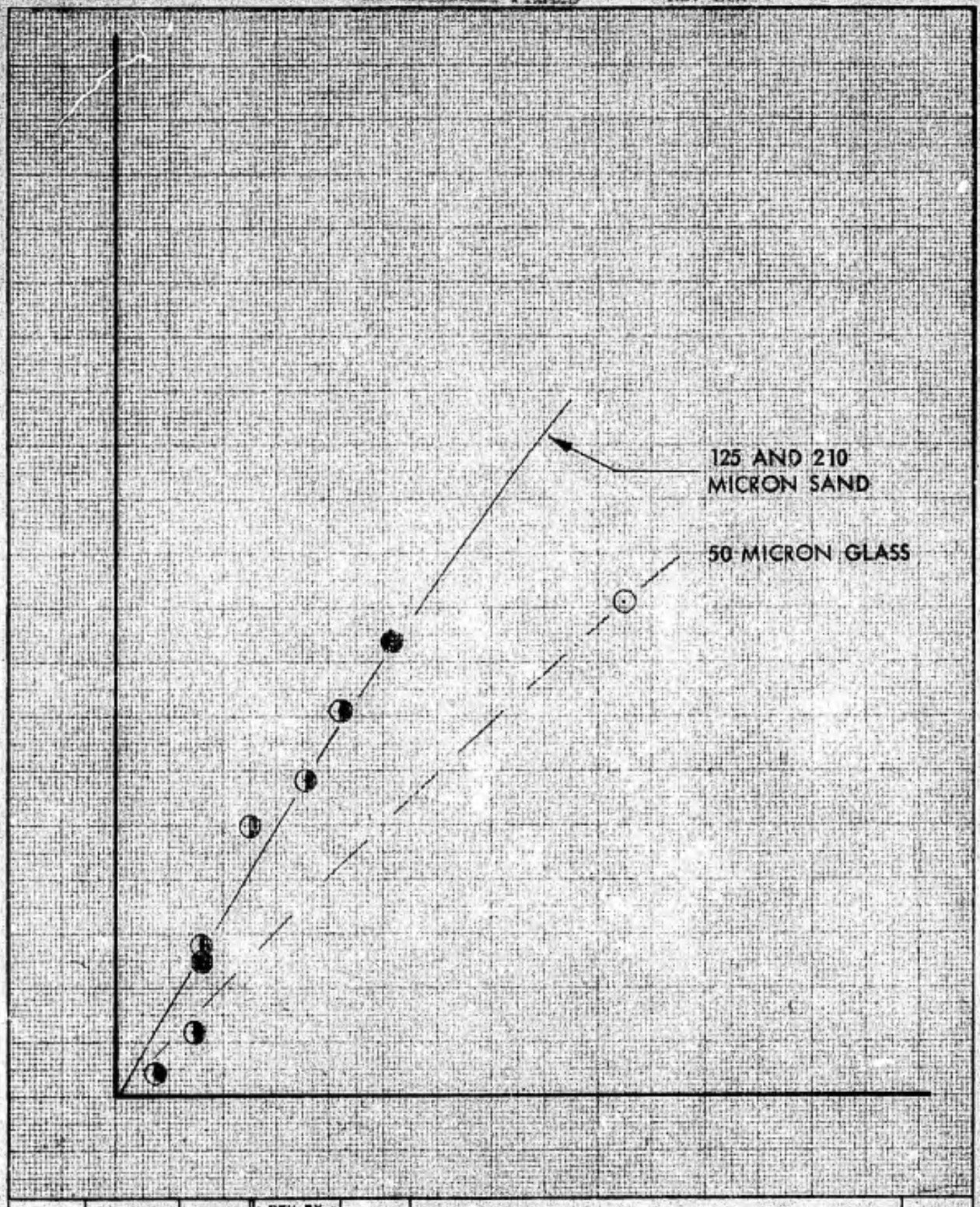

	INITIALS	DATE	REV BY INITIAL	DATE	TITLE	MODEL
CALC					CARBORAZOLE	Fig. 18A
CHECK						
APPD.						
APPD.						

U3 4013 8000 REV. 1/66

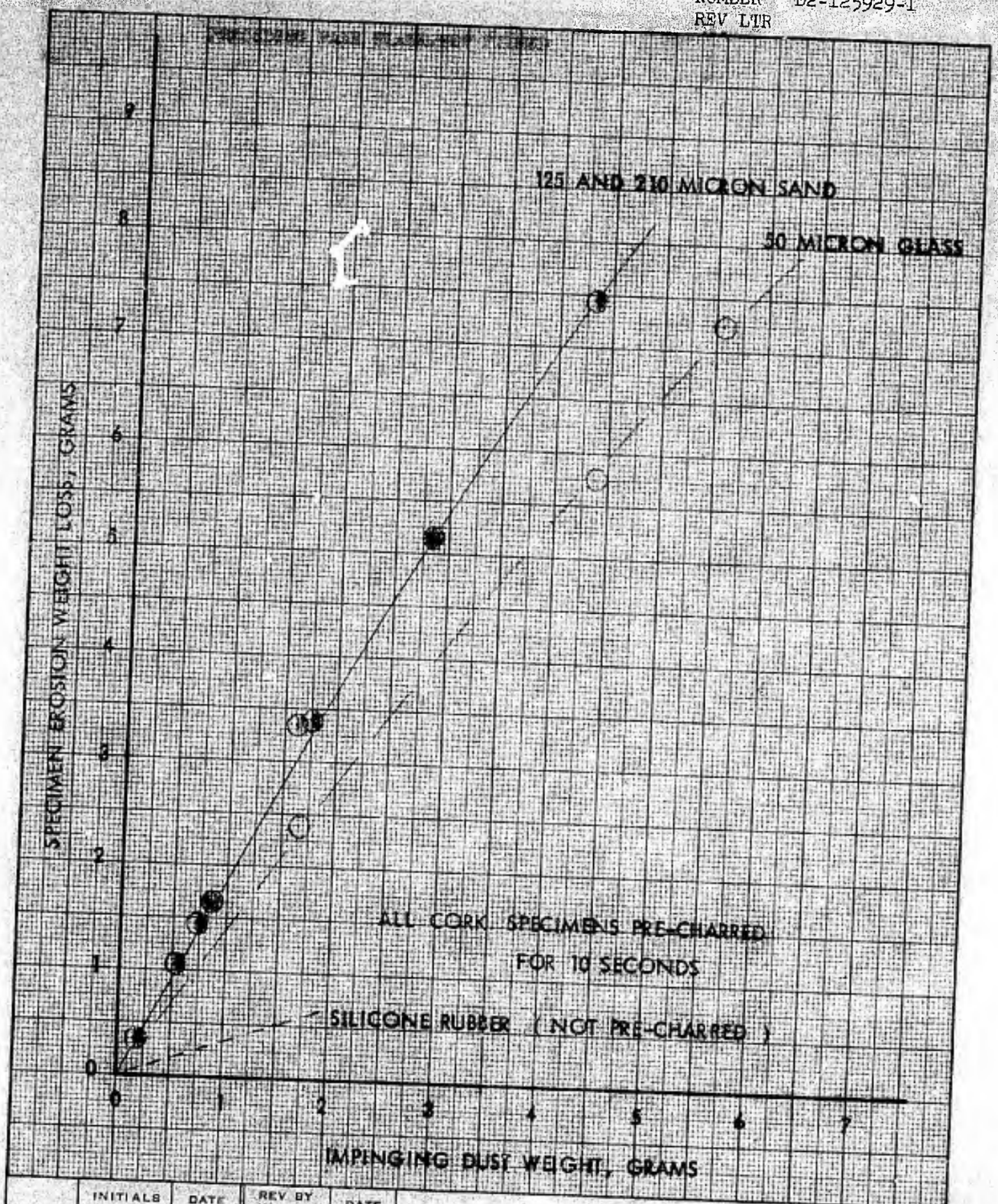

	INITIALS	DATE	REV BY INITIAL	DATE	TITLE	MODEL
CALC					EROSION WEIGHT LOSS OF CORK HEMISPHERES WITH A SURFACE TEMPERATURE OF 850° F	Fig. 18B
CHECK						
APPD.						
APPD.						

03 4013 8000 REV. 1/66

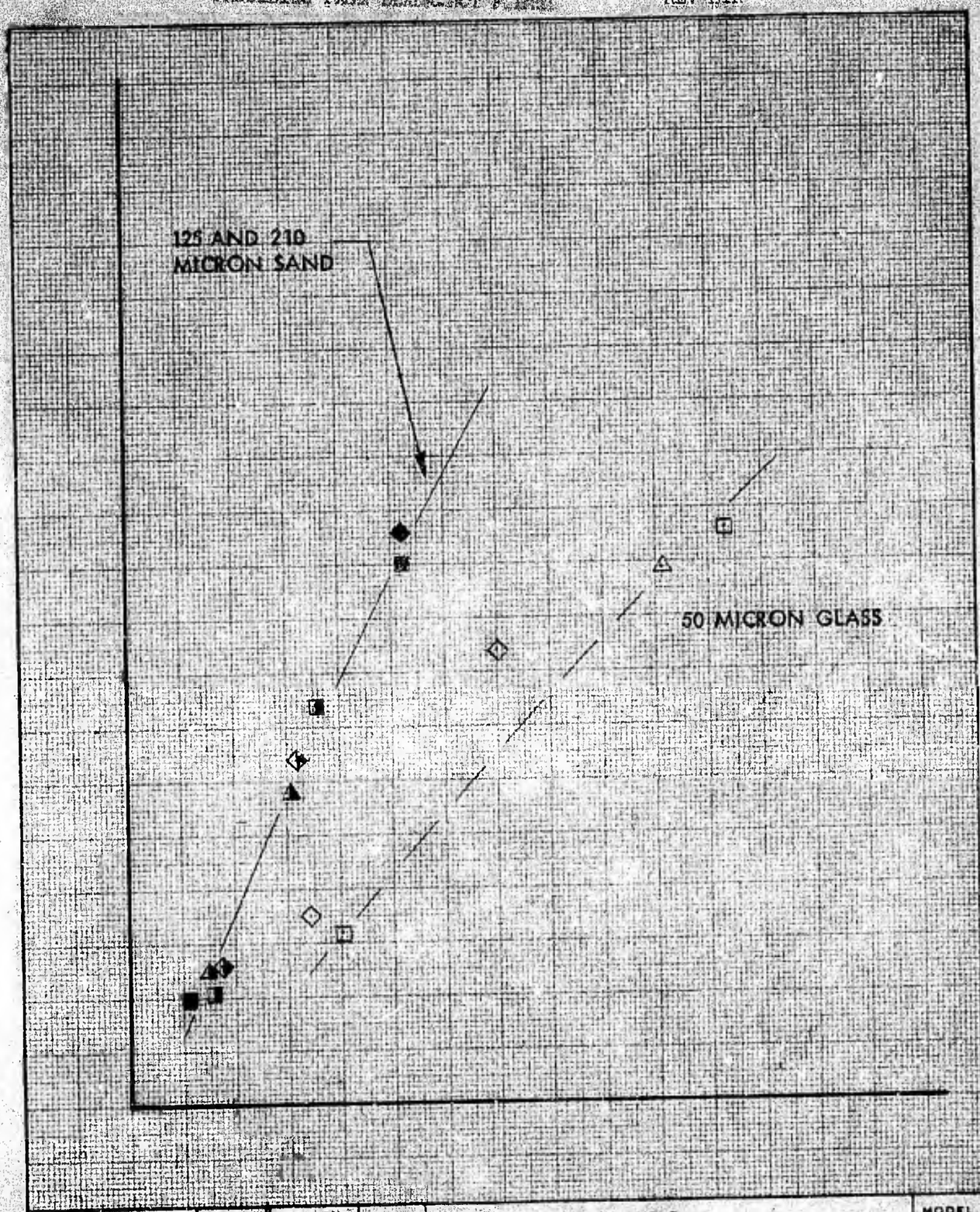

	INITIALS	DATE	REV. BY INITIAL	DATE	TITLE	MODEL
CALC					CARBORAZOLE	Fig. 19A
CHECK						
APPD.						
APPD.						

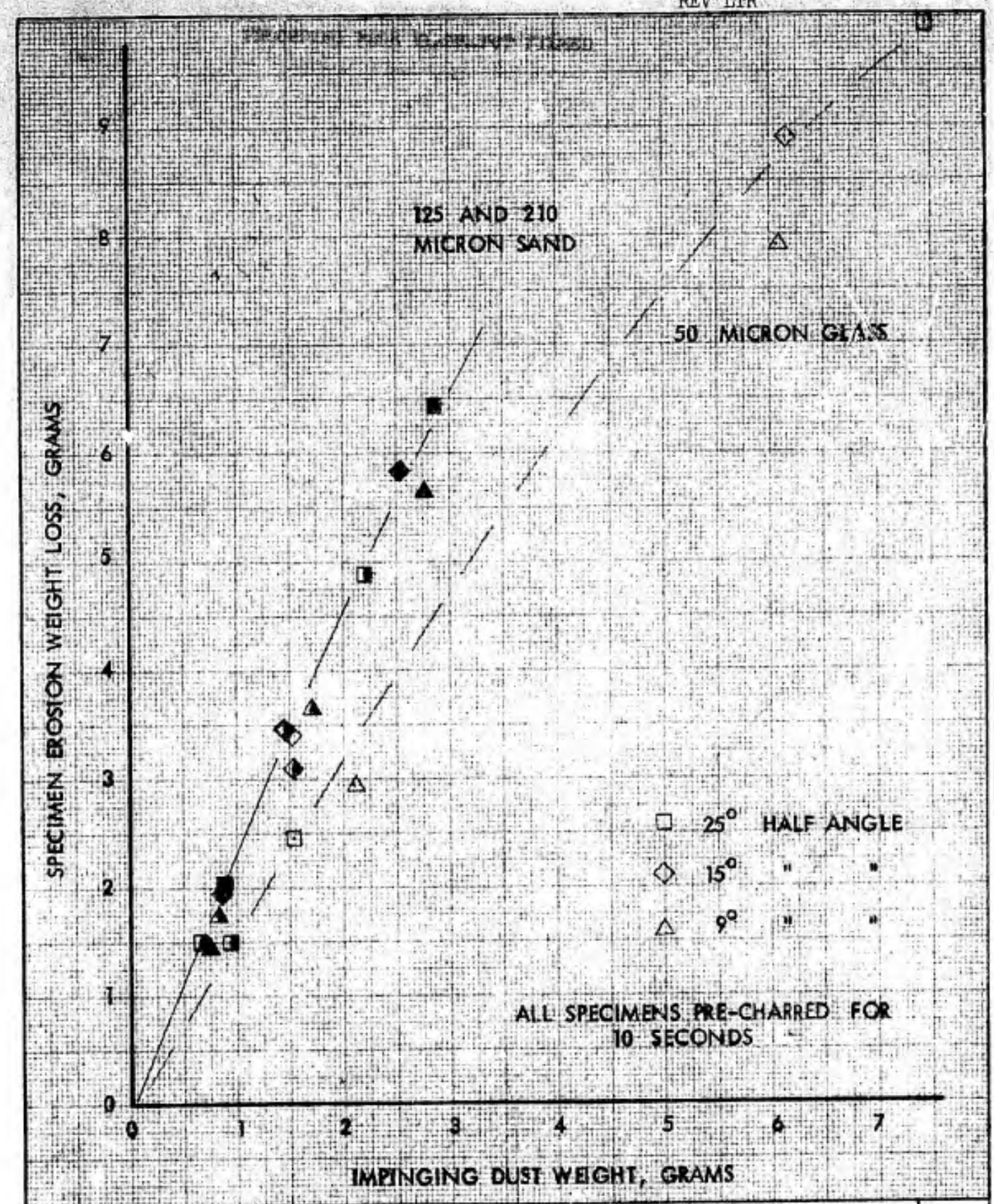

	INITIALS	DATE	REV BY INITIAL	DATE	TITLE	MODEL
CALC					WEIGHT LOSS OF BLUNT CORK CONES WITH A SURFACE TEMPERATURE OF 850° F	Fig. 198
CHECK						
APPD.						
APPD.						

5.1.4 Impingement Angle

The testing of impingement angle was limited to angles between 9 and 25 degrees. This limitation was imposed because the missile surfaces protected by these ablation-insulation materials are essentially within these limits. Figure 19 is a result of tests conducted with cone specimens with half-angles of 9, 15 and 25 degrees.

The data verify the previously noted effects that carborazole is slightly more resistant than cork and also that the smaller glass beads produce less wear. However, concerning the effect of impingement angle, the data indicate that there was very little difference between the three angles. This was especially true regarding the more extensive data existing for the larger particle sizes. The cork and carborazole data show loss ratio curves where all three cone angles lie essentially within the limits of experimental error. The limited data with the glass beads more vaguely indicate that the 15° angle is more susceptible in carborazole while the lower 9° angle is most critical in cork. It would be more reasonable to state that none of the angles offer any particular vulnerability over the others, at least not at the conditions tested.

In an attempt to resolve the impasse regarding impingement angle, some of the hemisphere data was reduced using the procedures outlined in Reference 10. The details of this analysis are given in Appendix A. Briefly, the hemisphere surfaces are divided into segments of average impingement angles and knowing the loss ratio for each segment, the impact wear and cutting wear can be separated. This analysis leads to an empirical solution for the angle producing the maximum total wear rate. These solutions indicate that the maximum wear curves for cork and carborazole are very flat (see Appendix A) between

$\alpha = 10^{\circ}$ and $\alpha = 30^{\circ}$. Therefore these results tend to confirm the test data by failing to reveal a critical impingement angle among those tested.

5.1.5 Specimen Surface Conditions

Specimens were tested, as noted previously, under three modes of surface conditions; (1) hot-char, (2) cold-char and (3) a new or virgin surface. The results of these runs can be seen in Figure 20. It appears that loss ratio for the cork is somewhat dependent upon the surface condition with the virgin surface being most resistant, followed by the cold-char and hot-char, respectively. The carborazole specimens did not exhibit this tendency; the loss ratio was essentially the same regardless of the surface condition. This is probably due to the sticky or tacky nature of the carborazole char; a condition that more closely resembles the virgin material.

5.1.6 Contaminant Mass-Density and Mass

During the initial phases of this research program it was discovered that the cloud dust-density or mass-density had a pronounced effect on the loss ratio. A good example of this effect is noticeable in the 1250°F curve of Figure 17. This data was generated using the same test mode, 10 seconds char followed by 10 seconds of dust. However, the total amount of dust dispensed was different for each run, producing the curve in the data. As discussed previously (Temperature Effects) this would indicate that as the cloud density on impingement rate is increased the char is essentially removed as fast as it forms. Therefore, the loss ratio curve should approach the asmyptotic value that would exist for the virgin unheated material. However, since the mass density values used in this experiment were consistent with those anticipated in a nuclear cloud; it is doubtful that this case would ever exist in actual flight.

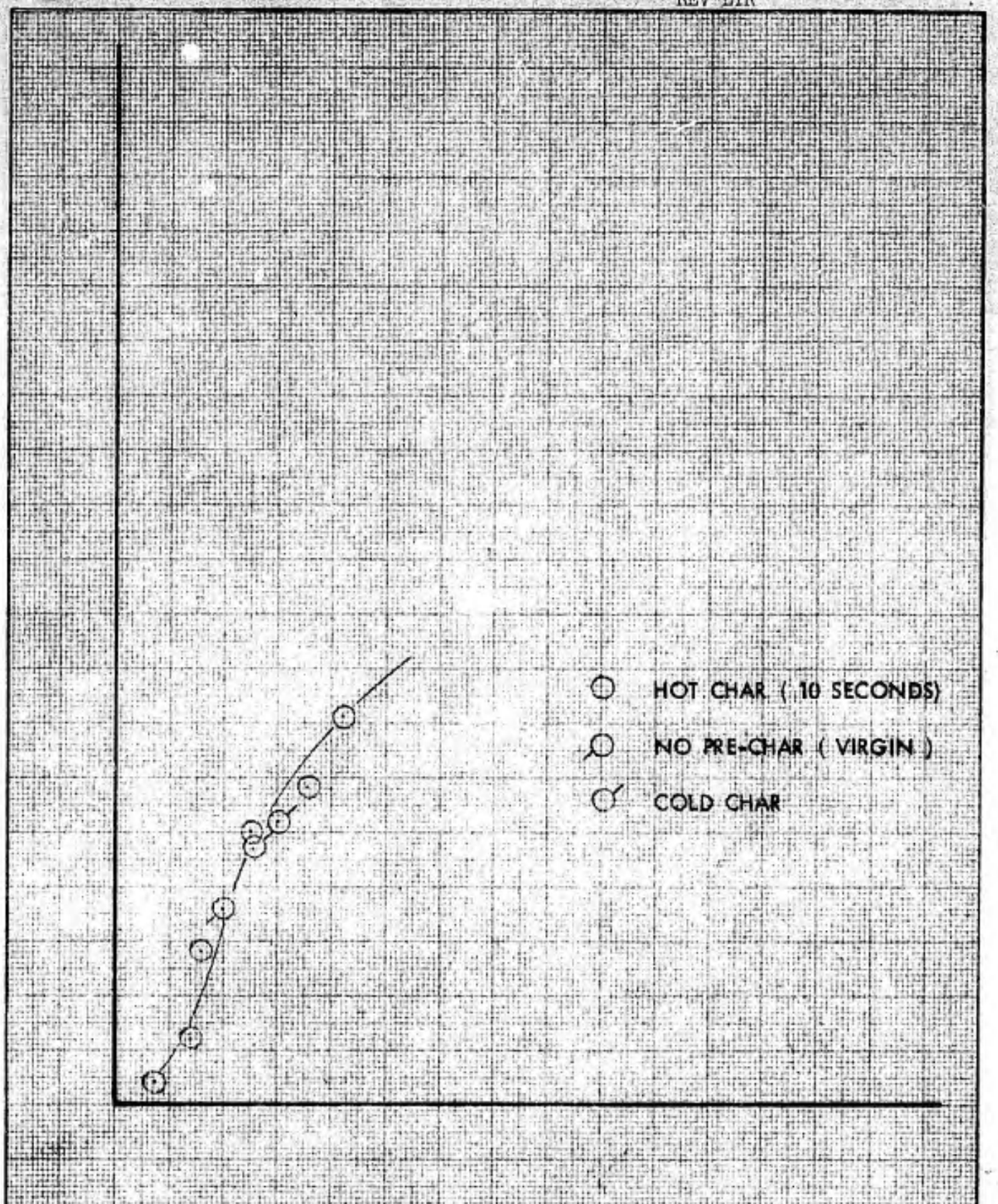

	INITIALS	DATE	REV BY INITIAL	DATE	TITLE	MODEL
CALC					CARBORAZOLE HEMISPHERES FOR ALL CHAR SURFACE CONDITIONS	Fig. 20A
CHECK						
APPD.						
APPD.						

U3 4013 8000 REV 1/66

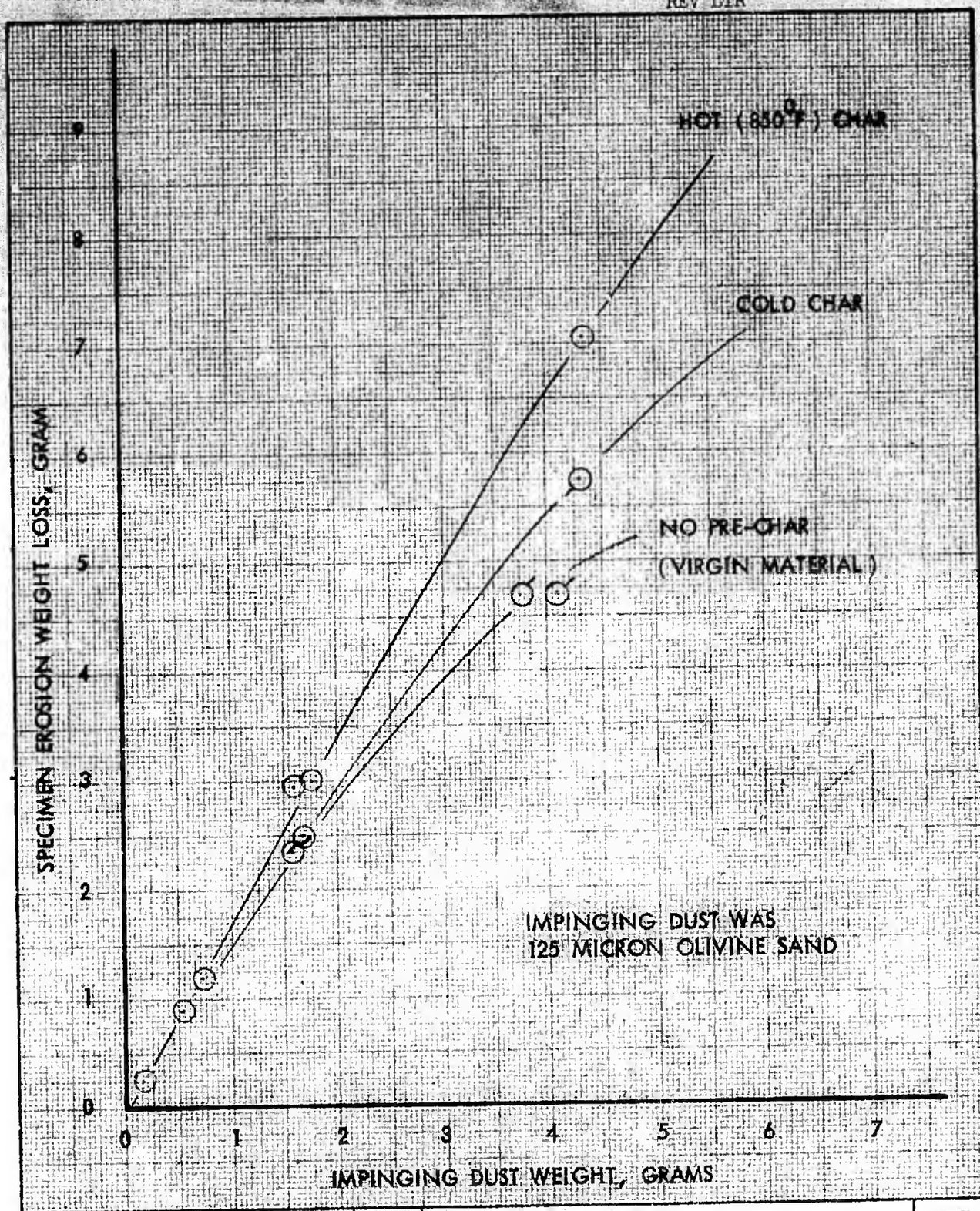

	INITIALS	DATE	REV BY INITIAL	DATE	TITLE	MODEL
CALC					EROSION LOSS OF CORK HEMISPHERES WITH NOTED CHAR SURFACE CONDITIONS	Fig. 20B
CHECK						
APPD.						
APPD.						

U3 4013 8000 REV 1/66

The data that is typified in Figures 18 and 19 illustrates the effect of changing the impinging mass while maintaining essentialiy a constant cloud-density. This was accomplished by holding a constant dispenser output setting and operating it for different lengths of time. This results in straight line data that would indicate that with a constant cloud density the material eroded is a direct function of the impinging mass.

6.0 CONCLUSIONS

1. A dust cloud with a contamination density close to predicted values can increase the weight loss in an ablative-insulative material, such as cork or silicone rubber by a factor of 5 to 10 times.

2. The erosion loss ratio is highly dependent upon the surface temperature and material characteristics. The silicone rubber used in these tests appeared to have a resistance threshold at 1000°F, beyond which the loss ratio is greatly accelerated. Cork appears to have similar characteristics at a lower temperature, however, the data is insufficient to predict the exact temperature threshold.

3. Materials that are exposed to the combined effects of ablation-erosion in the virgin-uncharred condition are the most resistant to erosion. If a char already exists on the surface of a cork specimen when the erosion process begins, the initially cold char is more resistant than a hot char.

4. With the cloud contamination density held constant (within the predicted limits) the weight of material eroded increases in direct proportion with the mass of the impinging material.

5. When the cloud particle density is increased the erosion loss ratio decreases approaching an asymptotic value that could be established with uncharred virgin material.

6. Analysis of the hemisphere data by the method of Neilson and Gilchrist indicates that charring cork exhibits the general characteristics of a material like plexiglas. Using this method the relationship between the impact wear and cutting wear were determined.

7. The tests conducted with cones with different half-angles, 9°, 15° and 25° did not produce sufficient evidence to determine which was the most vulnerable. The analysis of the hemispheres by the procedure of Neilson and Gilchrist (Reference 10, Appendix A) substantiate this conclusion by revealing very flat loss ratio curves between impingement angles of 10 to 30°.

7.0 REFERENCES

1. Belton, W. L., Gideon, D. N., and Stein, R. A., "Hyper-Velocity Impact Data Index, Part I - Bibliography.", Report No. BAT-197A-21-2 (Rev. 2), Battelle Memorial Institute, January 1967.

2. Liu, C. Y. and Stein, R. A., "Development of Hypervelocity Impact Tech" (U), Report No. BAT-197A-4-1, Battelle Memorial Institute, April 1967 (Secret)

3. Burch, G. T., "Multiplate-Damage Study" (U), Tech. Report AFATL-TR-67-116, September 1967 (Confidential)

4. Watanabe, R. K., "Velocity Measurement of Low Speed Glass and Sapphire Beads in Support of Airborne Vehicle Hardening Test", DML Report No. 27, January 1968.

5. Adair, W. R., "Airborne Vehicle Hardening - 1967 Year End Report" (U), Boeing Document D2-125690-1, April 1968 (Secret)

6. Finnie, I., "The Mechanism of Erosion of Ductile Metals", Proc. 3rd U.S. National Congress Appl. Mech., 1958, Pergamon Press, London, 1958

7. Finnie, I., "Erosion of Surfaces by Solid Particles", Wear 3 (1960) 87.

8. Holtey, H., "Uber Den Abnutzungsvorgang in Blasversatzrohren und die Frage der Bekampfung des Verschleisses", Geologie und Mijnbouw, I (1939) 209.

9. Bitter, J. G. A., "A Study of Erosion Phenomena", Parts 1 and 2, Wear, 6(1963)5, 169.

10. Neilson, J. H. and Gilchrist, A., "Erosion by a Stream of Solid Particles", Wear, 2(1968)111.

11. Fisher, M. A. and Davies, E. F., "Studies of Fly-Ash Erosion," Trans A.S.M.E., 71(1949)481.

12. Stoker, R. L., "Erosion Due to Dust Particles in a Gas Stream", Ind. Eng. Chem., 41(1945)1196.

13. Finnie, I., "An Experimental Study of Erosion", Proc. Soc. Exptl. Stress Anal., 17(2)(1960)65.

14. Neilson, J. H., and Gilchrist, A., "An Experimental Investigation into Aspects of Erosion in Rocket Motor Tail Nozzles", Wear 2(1968)123.

15. "Experimental Mass Removal and C_N of Ablating Surfaces Under Duplicated Flight Conditions" (U), DASA 01-67C-0087, 1 July 1967, Secret (SC 5677).

16. Crowe, C. T., "Drag Coefficient of Particles in a Rocket Nozzle" AIAA Journal, May, 1967.

17. Selberg, B. P., and Nicholls, J. A., "Drag Coefficients of Small Spherical Particles", AIAA Journal, March 1968.

18. Hillberg, Lauri, "The Convective Heating and Ablation Program (CHAP)", Boeing Document D2-36402-1, May 1966.

19. Rosenberg, S. J., "Resistance of Steels to Abrasion by Sand", Trans. Am. Soc. Steel Treating, 18(1930)1093.

APPENDIX A

DETAILS OF THE NEILSON-GILCHRIST EROSION ANALYSIS METHOD

The above authors, in Reference 10, have developed a simple approach to a theoretical analysis of the general erosion problem. The derived equations are correlated by experimental results and can be used to predict the erosion characteristics of various materials.

The total erosive wear sustained by a specimen can be broken down into the sum of the cutting wear and impact wear.

$$WR_t = WR_{Cu} + WR_D$$

and $$WR_t = \frac{\frac{1}{2} m \left(V_p^2 \cos^2 \alpha - v_p^2\right)}{\varphi} + \frac{\frac{1}{2} m \left(V_p \sin \alpha - k\right)^2}{\varepsilon}$$

where WR_t is the erosion produced by m pounds of particles impinging at an angle α and with a velocity V. K is the velocity component normal to the surface below which no erosion takes place and v_p is the residual parallel component of particle velocity at low αs. Due to the large magnitude of V in the Boeing tests, in relation to K and v_p, the latter are assumed to be negligible.

Therefore, $$WR_t = \frac{\frac{1}{2} m \left(V_p \cos \alpha\right)^2}{\varphi} + \frac{\frac{1}{2} m \left(V_p \sin \alpha\right)^2}{\varepsilon}$$

Now, at $\alpha = 90^\circ$ the first part of the expression, cutting wear, is zero and the impact resistance constant ε is determined by

$$\varepsilon = \frac{m V_p^2}{2 WR_t}$$

After ξ has been obtained the impact wear at all angles can be determined and by subtracting it from WR_t, WR_c and the cutting resistance constant ψ can be obtained.

Some of the hemisphere cylinder data was reduced by this method using the comparitor photographs typified in Figure 13. The hemispherical surface was divided into segments, the recession measured and the shape transformed into a series of trapezoids.

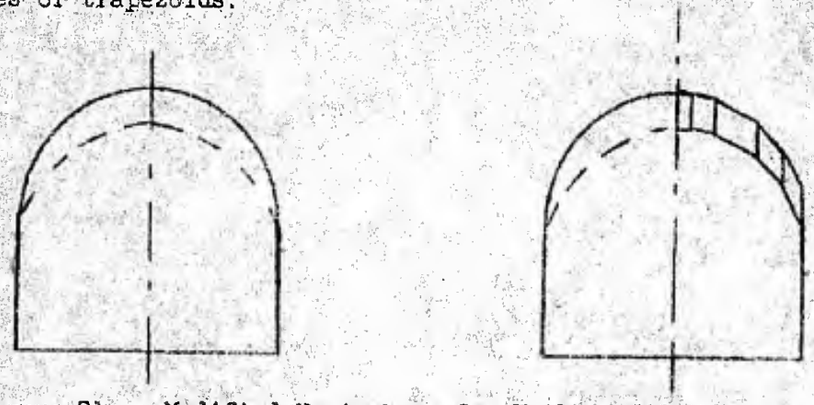

Figure 21 Modified Hemisphere for Neilson-Gilchrist Analysis

The volume of each revolved trapezoid can be determined and with the resulting volume ratio, the weight loss of each part can be found. Using a similar approach, the swept area can be ratioed and the amount of dust impinging on each segment can be determined. From this the eroded weight-impacted weight ratio for each segment is resolved.

Now, all of the quantities in the wear equation are known except the wear resistance factors, ξ and ϕ. The impact factor, ξ, was obtained from the center segment where the impingement angle is essentially 90°. The α for each of the other segments was the average across the face of the trapezoid. Using this approach, the total wear can be resolved into its two components and the angle of maximum wear can be obtained. Therefore, an approximation of the materials relative resistance to impact and cutting wear can be derived.

A BLITZ computer program was developed and a few of the specimens were analyzed by this method. The results are shown in the following Figures 22 through 28.

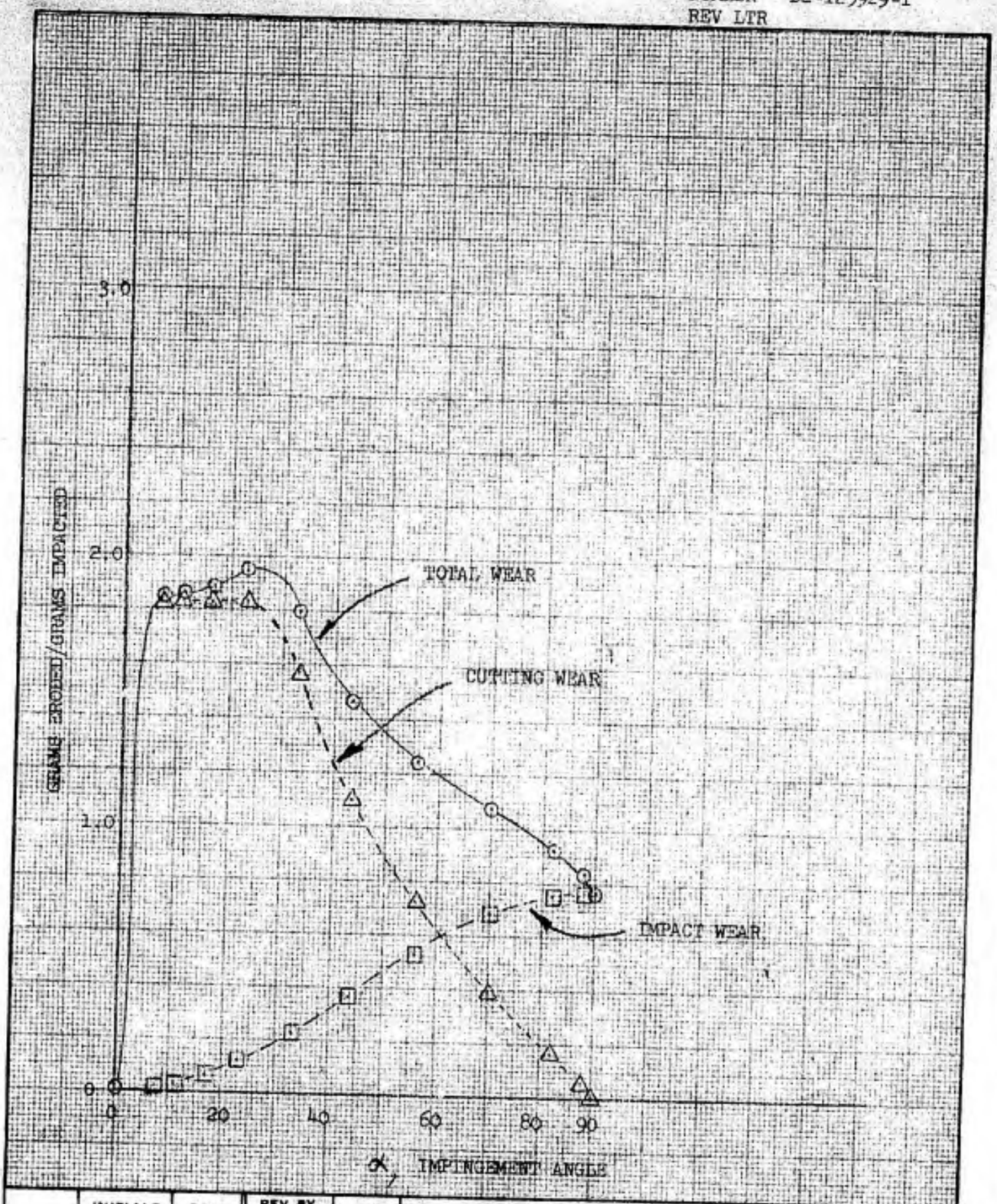

	INITIALS	DATE	REV BY INITIAL	DATE	TITLE	MODEL
CALC					EROSION RATIOS V.S. IMPINGEMENT ANGLE FOR 850°F CHARRED CORK ERODED BY 50 μ GLASS BEADS AT 3250 FT/SEC	FIG. 22
CHECK						
APPD.						
APPD.						

U3 4013 8000 REV 1/66

PRECEDING PAGE BLANK NOT FILMED

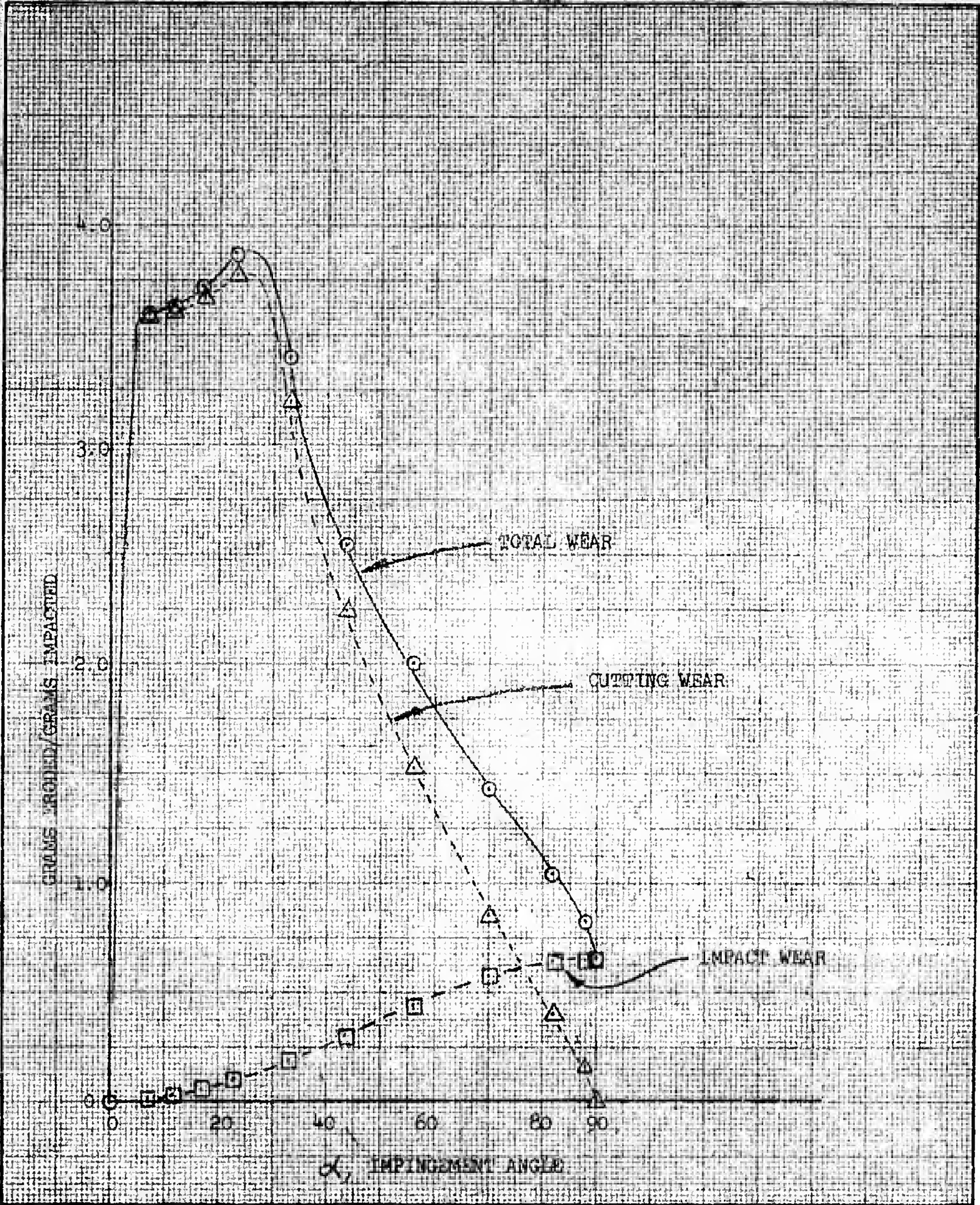

	INITIALS	DATE	REV BY INITIAL	DATE	TITLE	MODEL
CALC					EROSION RATIOS V.S. IMPINGEMENT ANGLE FOR 850°F CHARRED CORK ERODED BY 125 μ OLIVINE SAND AT 2850 FT/SEC	FIG. 23
CHECK						
APPD.						
APPD.						

U3 4013 8000 REV 1/66

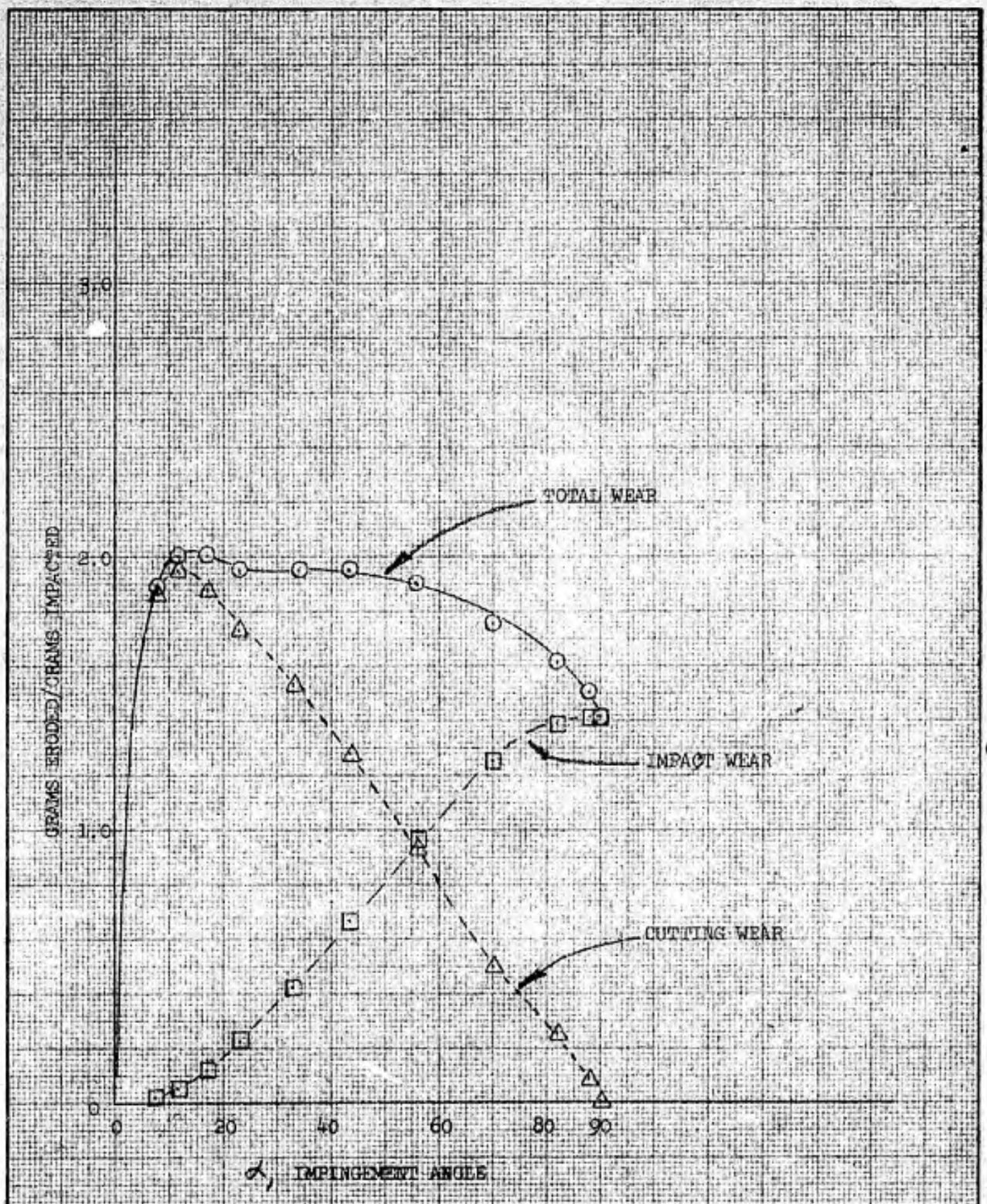

	INITIALS	DATE	REV BY INITIAL	DATE	TITLE	MODEL
CALC					EROSION RATIOS V.S. IMPINGEMENT ANGLE FOR 850°F CHARRED CORK ERODED BY 210 μ SILICA SAND AT 2550 FT/SEC	FIG. 24
CHECK						
APPD.						
APPD.						

U3 4013 8000 REV 1/66

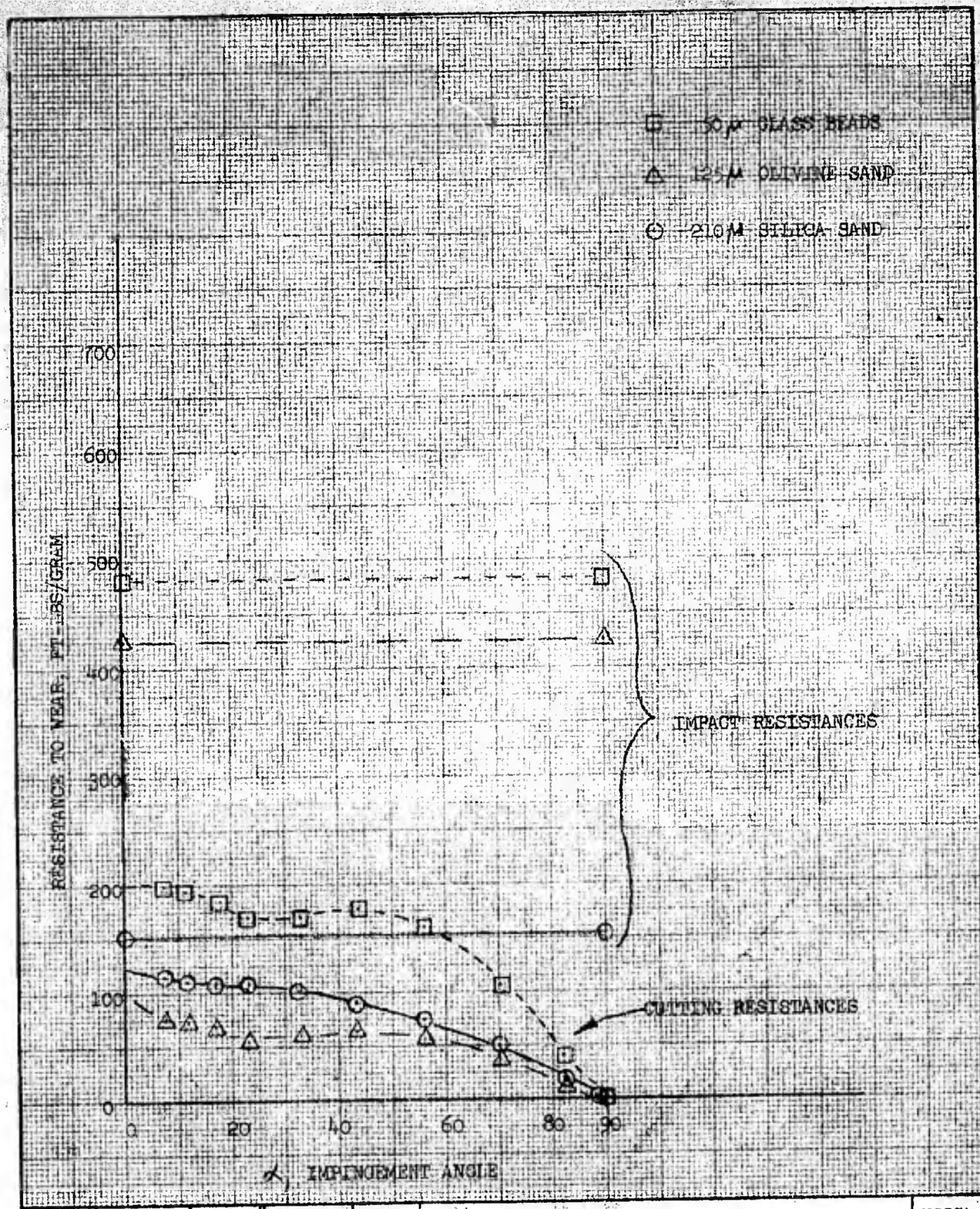

	INITIALS	DATE	REV BY INITIAL	DATE	TITLE	MODEL
CALC					MATERIAL RESISTANCE V.S. IMPINGEMENT ANGLE OF 850°F CHARRED CORK	FIG. 25
CHECK						
APPD.						
APPD.						

U3 4013 8000 REV. 1/66

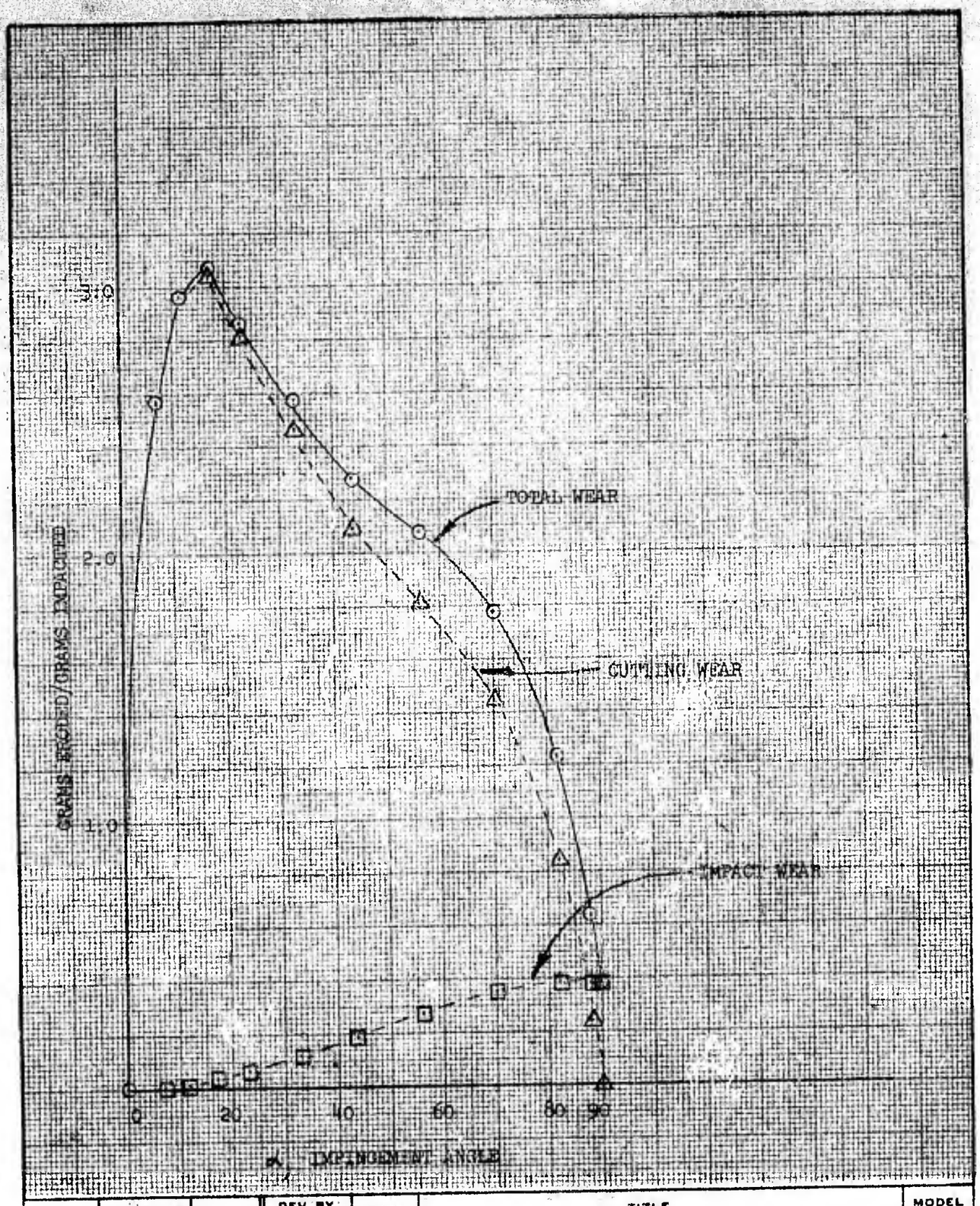

	INITIALS	DATE	REV BY INITIAL	DATE	TITLE	MODEL
CALC					EROSION RATIOS V.S. IMPINGEMENT ANGLE FOR 850°F CHARRED CARBORAZOLE ERODED BY 125 μ OLIVINE SAND AT 2850 FT/SEC	FIG. 26
CHECK						
APPD.						
APPD.						

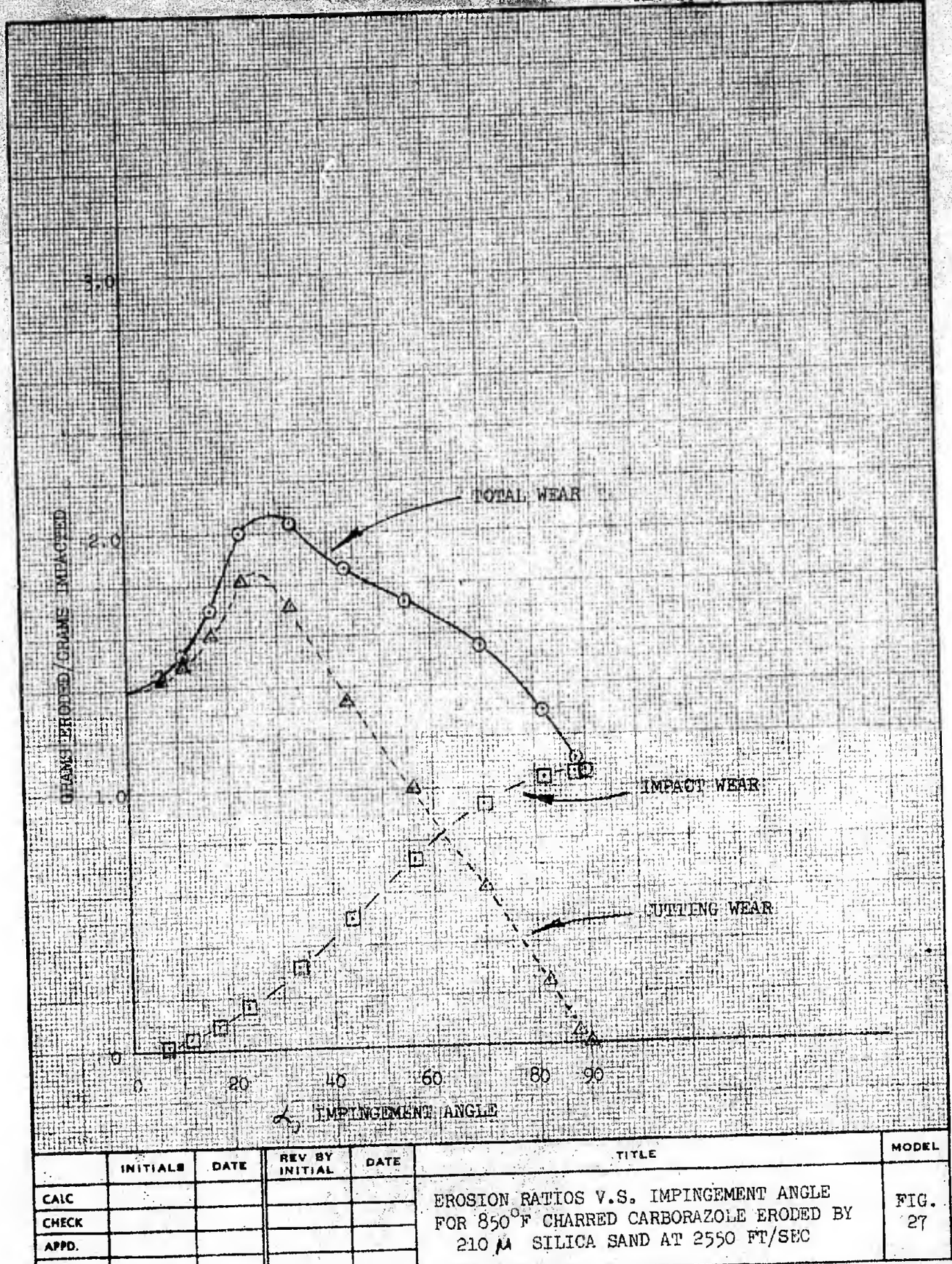

	INITIALS	DATE	REV BY INITIAL	DATE	TITLE	MODEL
CALC					EROSION RATIOS V.S. IMPINGEMENT ANGLE FOR 850°F CHARRED CARBORAZOLE ERODED BY 210 μ SILICA SAND AT 2550 FT/SEC	FIG. 27
CHECK						
APPD.						
APPD.						

U3 4013 8000 REV 1/66

REV LTR_____

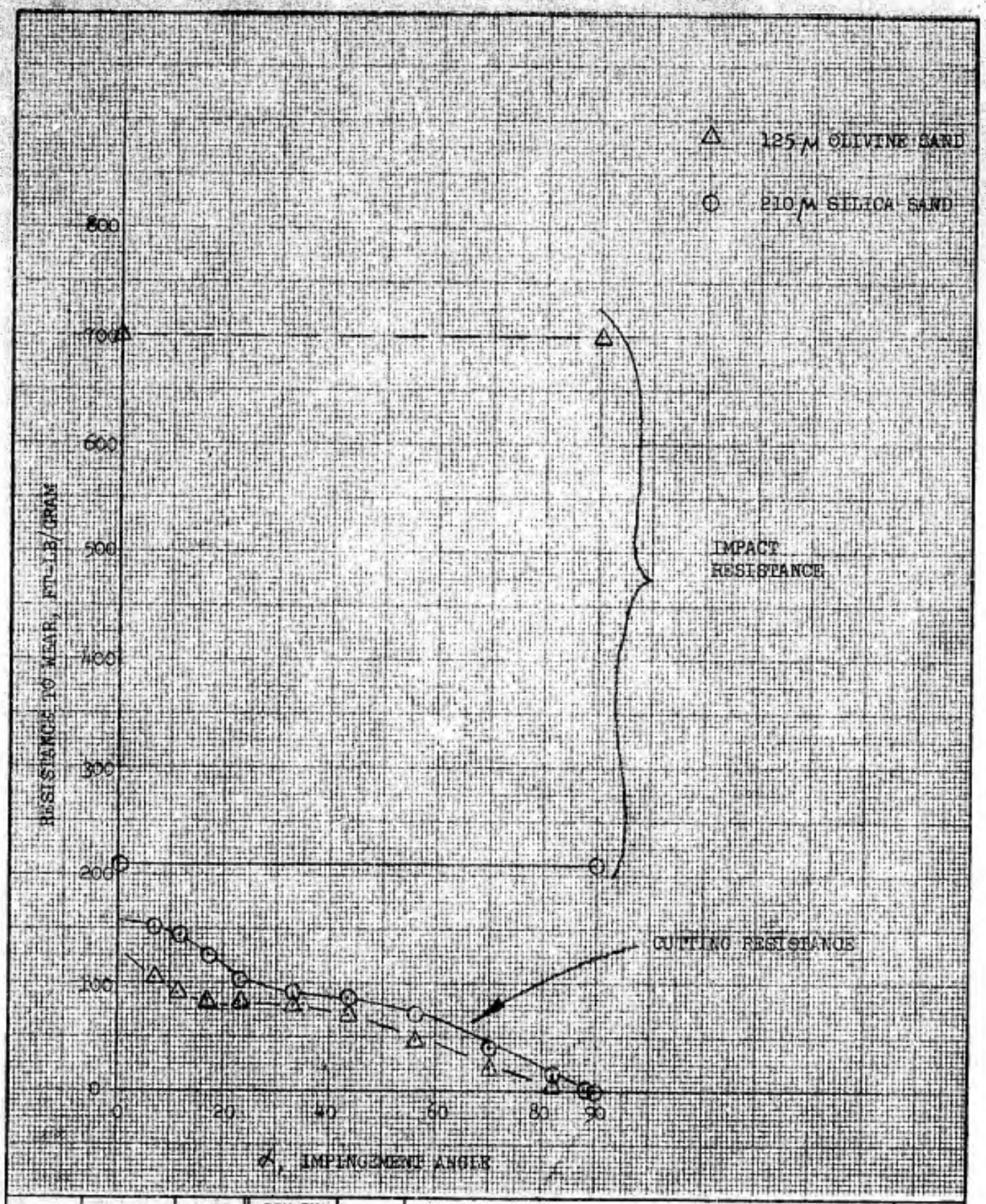

	INITIALS	DATE	REV BY INITIAL	DATE	TITLE	MODEL
CALC					MATERIAL RESISTANCE V.S. IMPINGEMENT ANGLE OF 850°F CHARRED CARBORAZOLE	FIG. 28
CHECK						
APPD.						
APPD.						

U3 4013 8000 REV 1/66

APPENDIX B

FACILITY CAPABILITIES AND NEW TESTING CONCEPTS FOR FUTURE EROSION TEST PROGRAMS

FUTURE TESTING CAPABILITIES

The test program described in this report was conducted with severe performance limitations. Before the installation of the radiant furnace, all of the tests had to be run at the maximum available total temperature, 1000°F, in order to create an ablative environment. The total temperature establishes the test section gas velocity which in turn dictates the speed that the particles will attain. Therefore, the tests were conducted under a single point condition with one particle velocity for each particle size. Figure 29 is a plot of a typical boost trajectory, in terms of velocity and pressure altitude, with the test point shown as the ◇ and ⊡ with a specimen surface temperature, T_S, of 850°F. (Mach number has a slight influence on the pressure altitude, but other than that the test points are essentially identical.)

The installation of the radiant furnace introduced a considerable degree of flexibility in the selection of test points. It permits the tunnel to be run at lower total temperatures thereby allowing the gas velocity and particle velocity to become variables. The ablative environment would be maintained or intensified by the radiant furnace with corresponding higher heat fluxes required as the tunnel total temperature was reduced. The range of test points presently available in the Boeing Hypersonic Wind Tunnel, with respect to Mach Number, pressure altitude, and surface temperatures, are shown on the left side of the trajectory curve of Figure 29. The resultant spectrum of particle velocities produced by this variety of test points is shown in Figure 30.

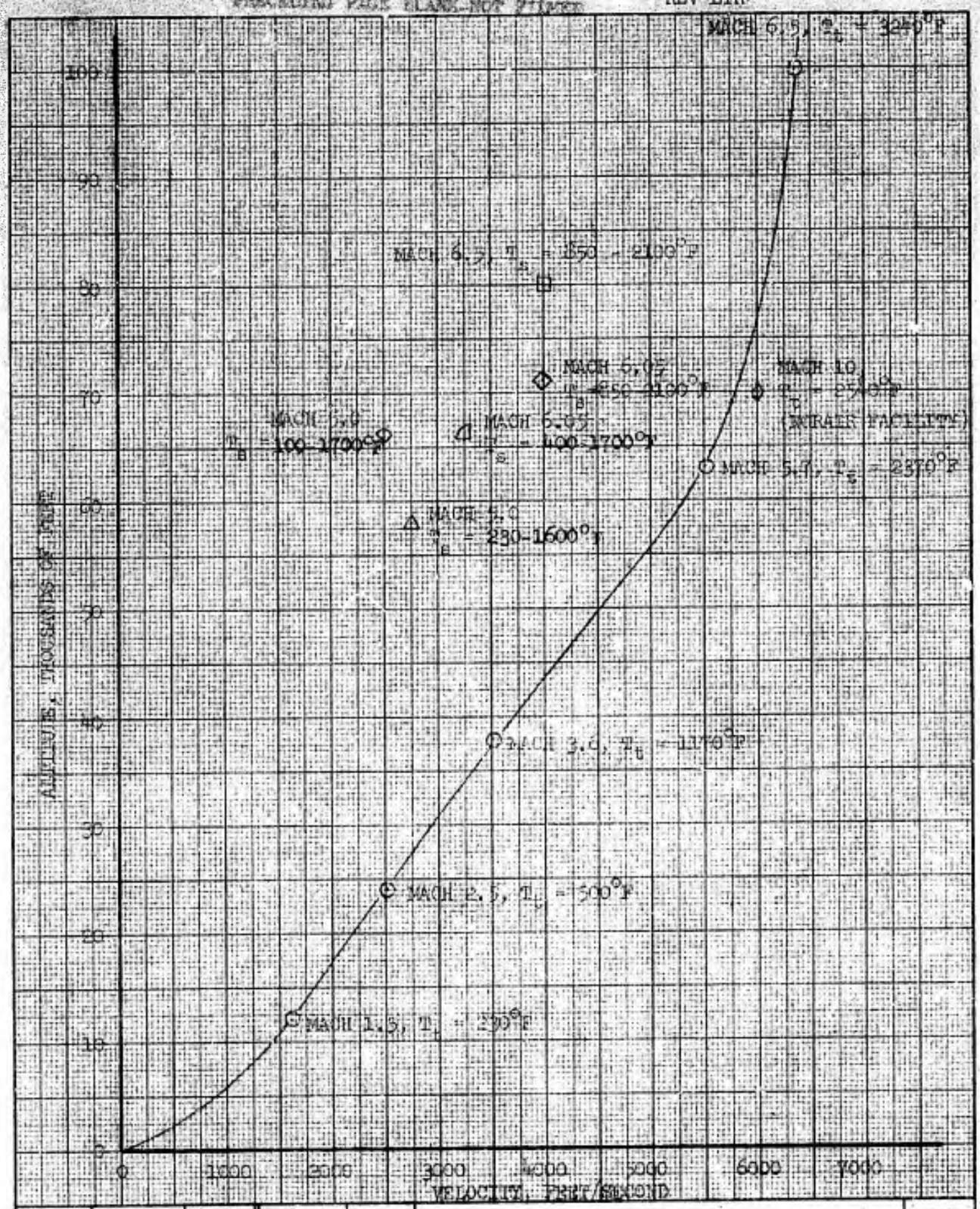

	INITIALS	DATE	REV BY INITIAL	DATE	TITLE	MODEL
CALC					COMPARISON OF RADIANT AUGMENTED WIND TUNNEL TEST CONDITIONS WITH A TYPICAL BOOST TRAJECTORY	FIG. 29
CHECK						
APPD.						
APPD.						

U3 4013 8000 REV. 1/66

REV LTR_____

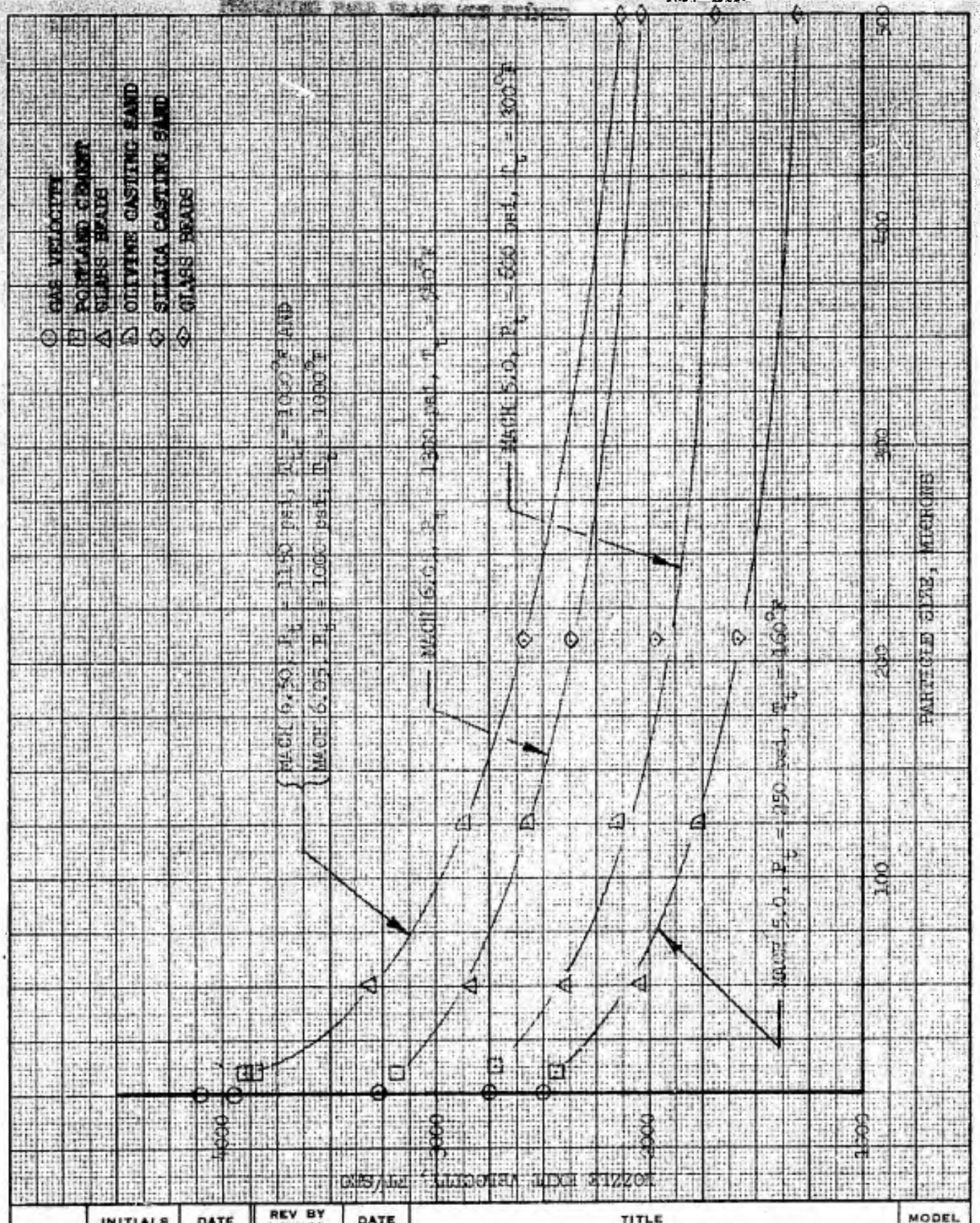

	INITIALS	DATE	REV BY INITIAL	DATE	TITLE	MODEL
CALC					COMPUTED PARTICLE VELOCITIES FOR VARIOUS TUNNEL CONDITIONS	FIG. 30
CHECK						
APPD.						
APPD.						

U3 4013 8000 REV. 1/66

In order to increase the particle velocity in the test section, a highly desirable situation, a higher tunnel total temperature is required. Since the Boeing Hypersonic is limited to 1000°F another facility would be required. A logical candidate would be a pebble bed heated facility with a total temperature in the vicinity of 3000°R. This would result in a test section gas velocity of approximately 6000 feet-per-second. The Norair Division of the Northrup Corporation has such a facility. After some exchange of information and a visit to the facility it has been established that Norair would consider conducting such tests and that alteration of the facility to include the dispensing mechanism is quite feasible.

The Norair test point is noted on Figure 29 and the range of particle velocities obtainable in the facility are shown in Figure 31.

The CHAP program (Reference 18) was utilized to determine the various aerodynamic parameters available in the Boeing Hypersonic and Norair Facility for the various test points. The results of these computer runs; (1) anticipated surface temperatures, (2) wall shear stress and (3) heat transfer coefficients are shown in Figures 32, 33 and 34.

DESIGN IMPROVEMENTS

A rather simple design for a device capable of measuring the particle velocity has been devised. It basically consists of a pointed rotating drum mounted on the test section sting. The drum, 3 inches in diameter would be rotated at a precise known RPM; e.g., 3000. As it rotates a small hole in the conical bulkhead is open to the dust flow allowing a few particles to enter the vented drum. These particles will pass down through the hollow cylinder and impinge upon a soft rear bulkhead. The angle that the resultant indentations make

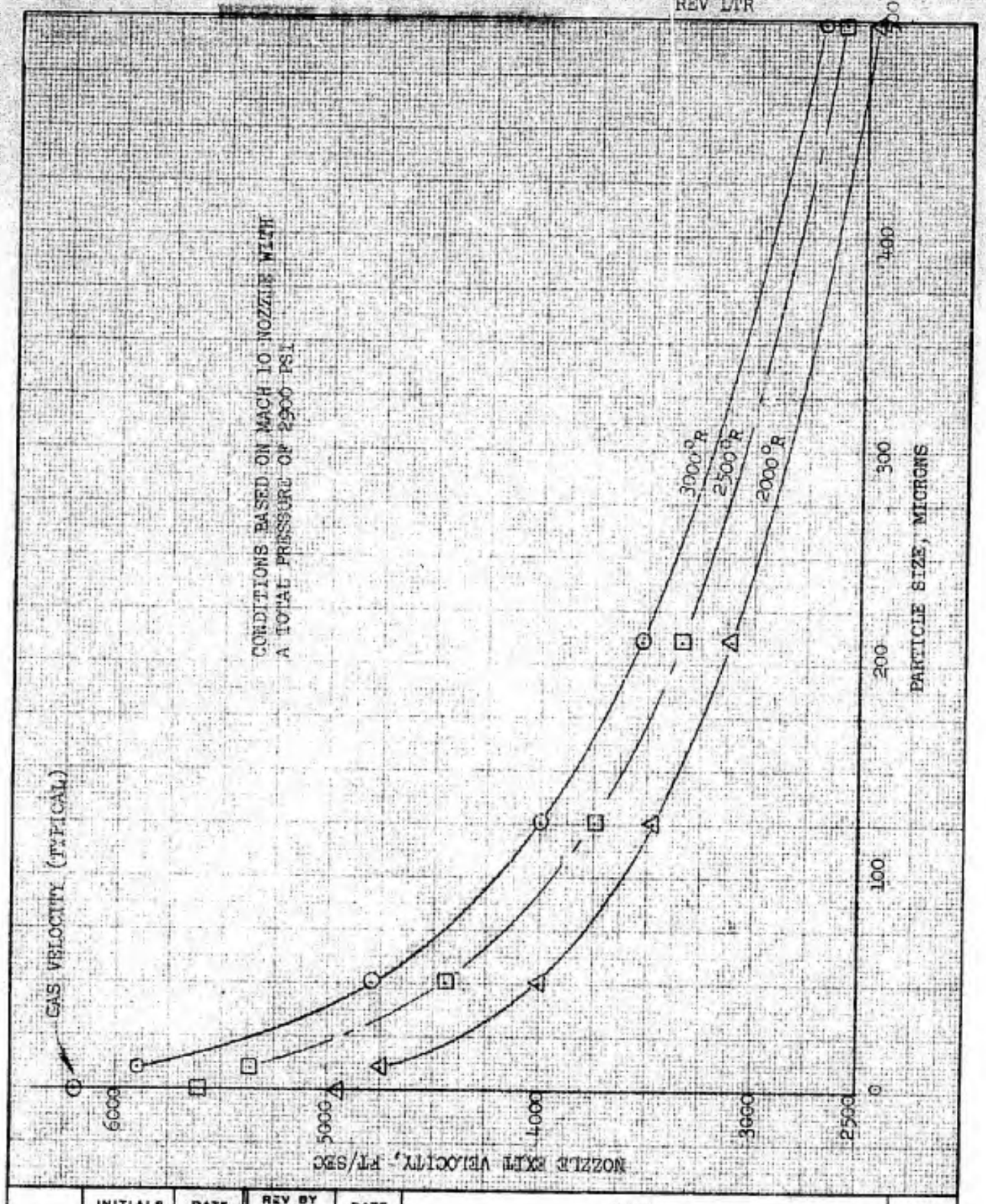

	INITIALS	DATE	REV BY INITIAL	DATE	TITLE	MODEL
CALC					COMPUTED PARTICLE VELOCITIES FOR NORAIR HYPERVELOCITY TUNNEL	FIG. 31
CHECK						
APPD.						
APPD.						

U3 4013 8000 REV 1/66

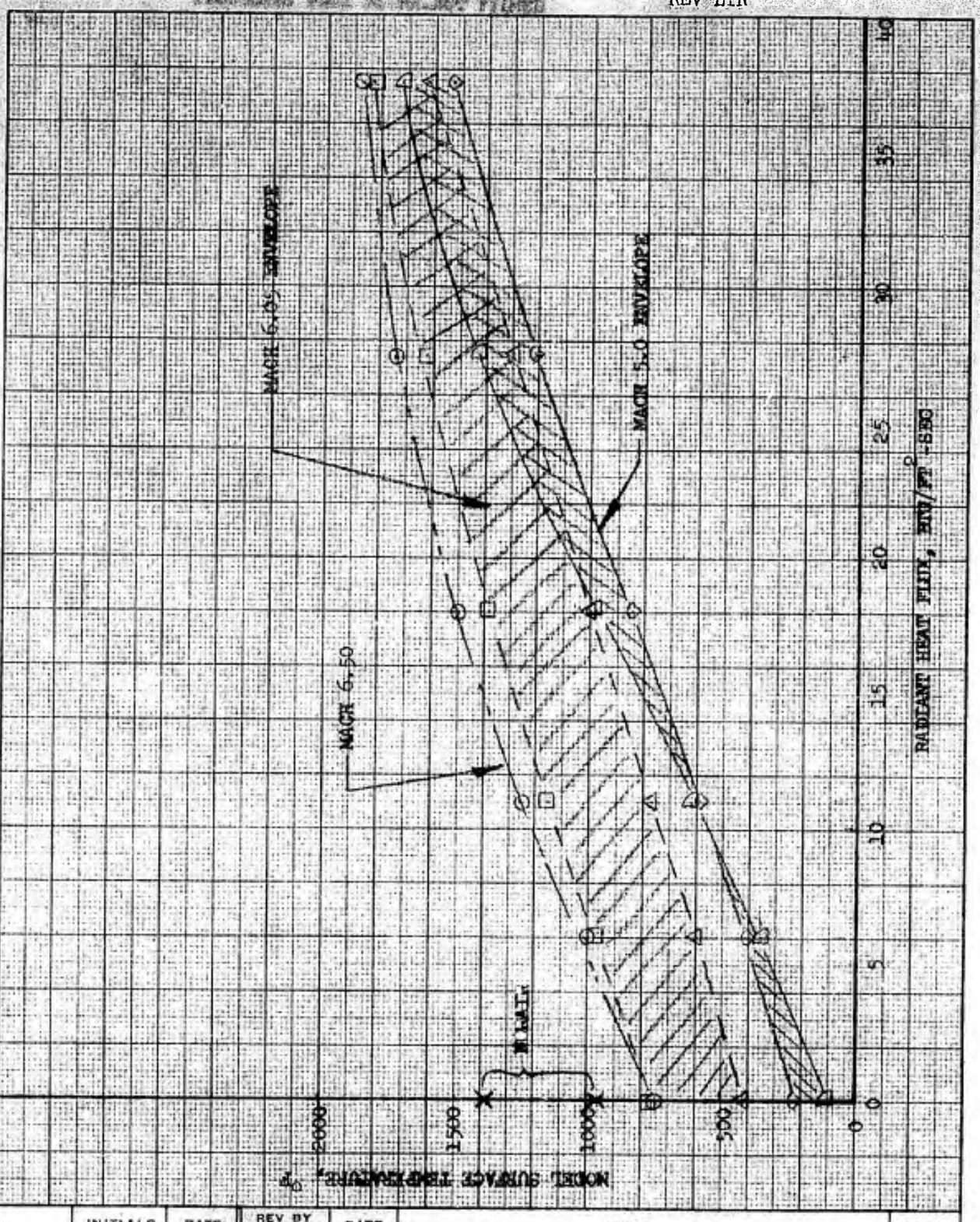

	INITIALS	DATE	REV BY INITIAL	DATE	TITLE	MODEL
CALC					COMPUTED SURFACE TEMPERATURES OF CORK CONE AS A FUNCTION OF RADIANT HEAT FLUX	FIG. 32
CHECK						
APPD.						
APPD.						

U3 4013 8000 REV. 1/66

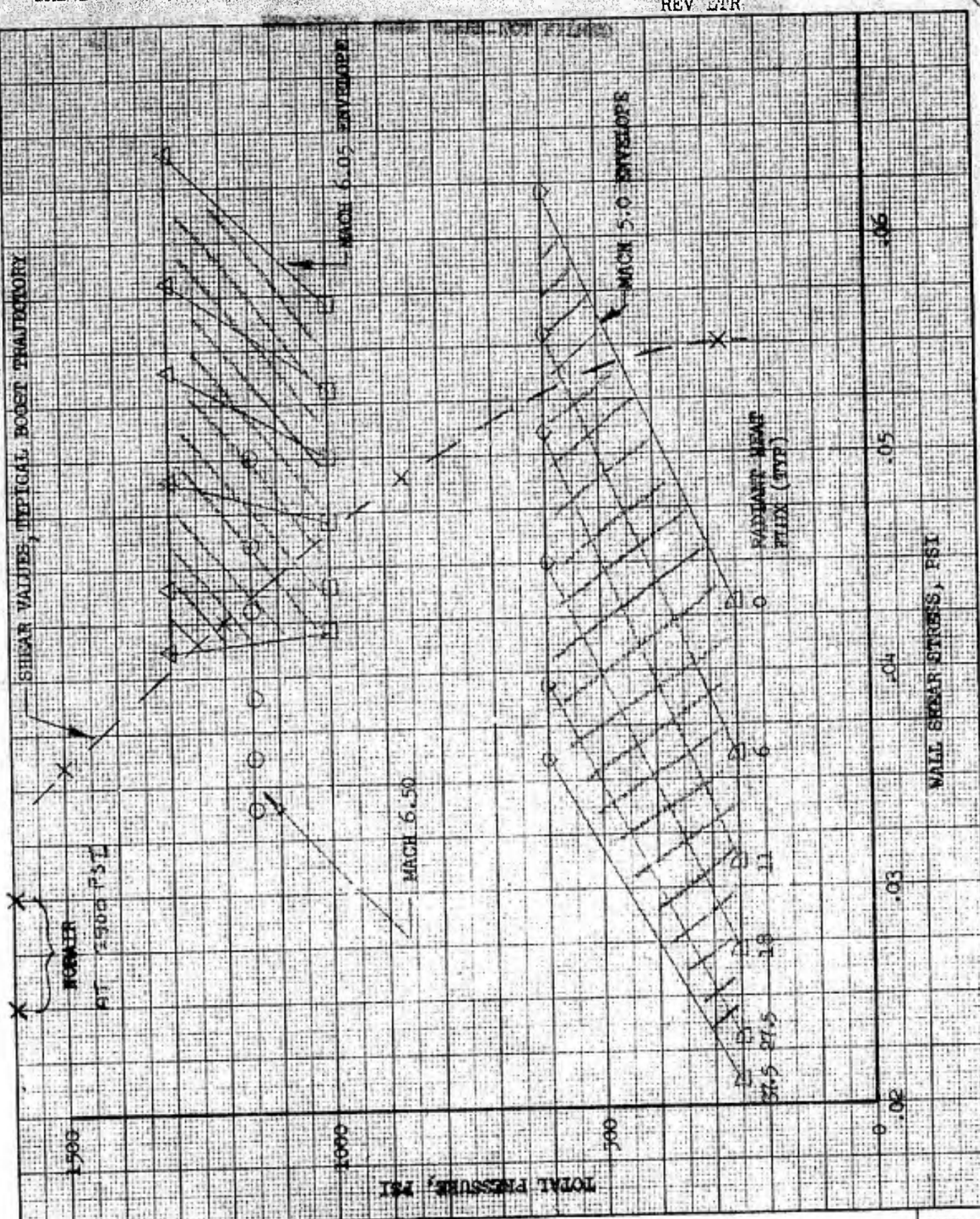

	INITIALS	DATE	REV BY INITIAL	DATE	TITLE	MODEL
CALC					WALL SHEAR STRESS AS FUNCTION OF TUNNEL TOTAL PRESSURE AND RADIANT HEAT FLUX	FIG. 33
CHECK						
APPD.						
APPD.						

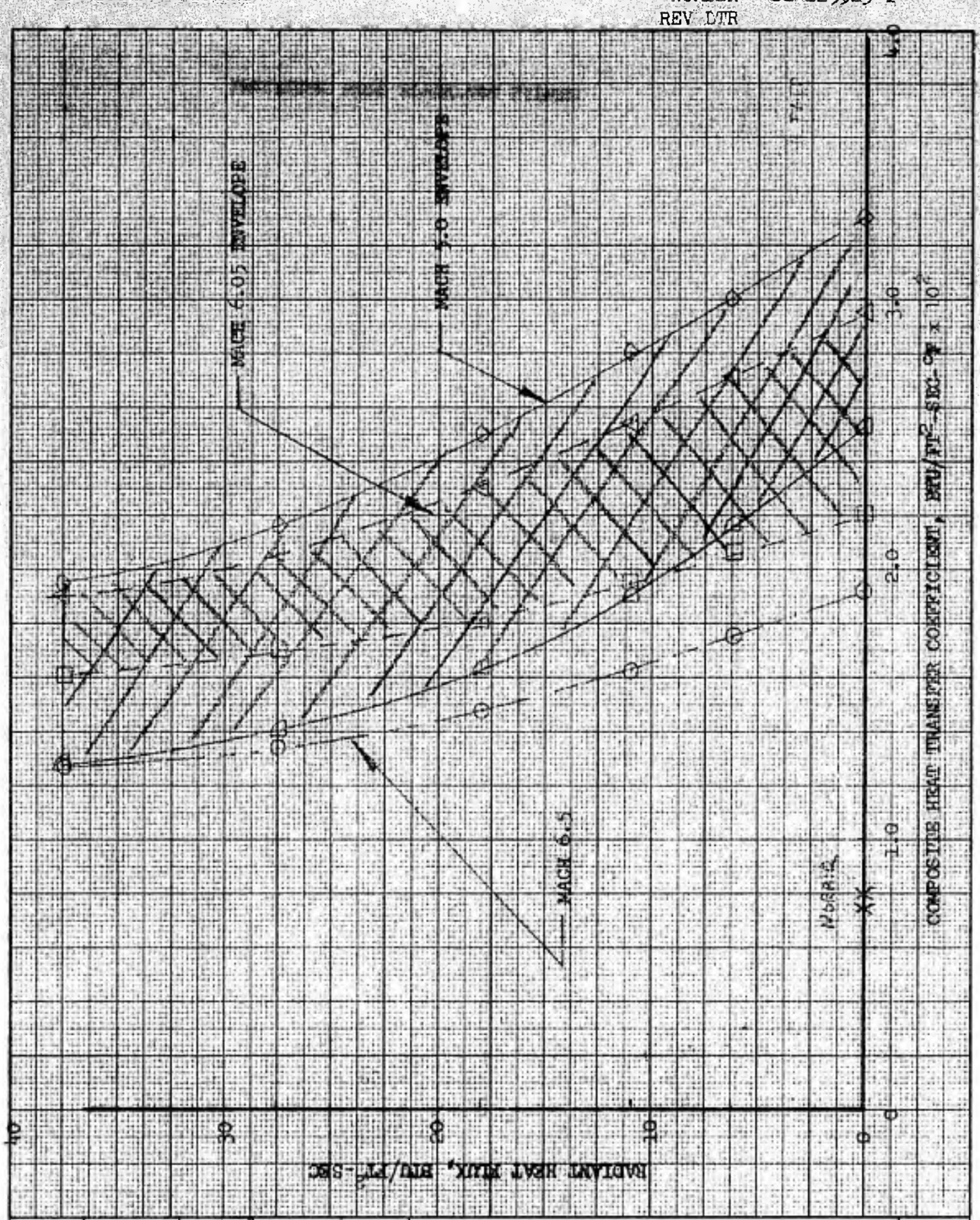

	INITIALS	DATE	REV BY INITIAL	DATE	TITLE	MODEL
CALC					HEAT TRANSFER COEFFICIENT AS A FUNCTION OF AUGMENTING RADIANT HEAT FLUX	FIG. 34
CHECK						
APPD.						
APPD.						

U3 4013 8000 REV 1/66

REV LTR_____

with the plane of the hole can be easily measured. Knowing this along with the length and the exact rotation of the drum, will result in reasonably accurate measurement of the particle velocity. Calculations show that the drag deceleration within the short drum would be negligible due to the low density at test section static pressure to which the drum would be vented.

Improvement of the dust spray-head would be highly desirable. Although the final design used during the subject test performed satisfactorily a better design may be able to distribute the debris more evenly throughout the stream core. This task would require a bench test tank so that the dust spray could be seen while operating against a back pressure of 1000 PSI. At present the system can only be tried by trial and error while the tunnel is operating - a costly procedure.

An improved method of measuring the specimen temperature is required. The flat horseshoe shaped foil thermocouples used in the subject test produced rather erratic traces during most of the run. This was due to a tendency for the material to delaminate in the vicinity of the thermocouple backing causing air pockets and sundry related problems. A possible solution to this problem might be the use of thermocouples buried in a very small diameter metal sheath.

VERIFICATION OF NEILSON-GILCHRIST

It is recommended that a future erosion test program should include test specimens specifically designed to verify the referenced erosion analysis method. These specimens should include a series with impingement angles ranging from 90° to as close to 0° as feasible. This would provide accurate data for the formulation of loss ratio curves, cutting resistance and impact resistance for any desired material.

LIMITATIONS

This document is controlled by Structures and Materials Technology, Orgn. 2-5563

All revisions to this document shall be approved by the above noted organization prior to release.

THE BOEING COMPANY

NUMBER D2-125929-1
REV LTR

ACTIVE SHEET RECORD

SHEET NUMBER	REV LTR	ADDED SHEETS				SHEET NUMBER	REV LTR	ADDED SHEETS			
		SHEET NUMBER	REV LTR	SHEET NUMBER	REV LTR			SHEET NUMBER	REV LTR	SHEET NUMBER	REV LTR

REVISIONS			
LTR	DESCRIPTION	DATE	APPROVAL

Unclassified
Security Classification

DOCUMENT CONTROL DATA - R&D

(Security classification of title, body of abstract and indexing annotation must be entered when the overall report is classified)

1. ORIGINATING ACTIVITY (Corporate author) THE BOEING COMPANY	2a. REPORT SECURITY CLASSIFICATION Unclassified 2b. GROUP

3. REPORT TITLE

Particle Erosion Testing in The Boeing Hypersonic Wind Tunnel

4. DESCRIPTIVE NOTES (Types of report and inclusive dates)

5. AUTHORS (First name, middle initial, last name)

George C. Lorenz

6. REPORT DATE	7a. TOTAL NO. OF PAGES	7b. NO. OF REFS
December 1968	87	19

8a. CONTRACT OR GRANT NO.	9a. ORIGINATOR'S REPORT NUMBERS
b.	D2-125929-1
c.	9b. OTHER REPORT NO(S) (Any other numbers that may be assigned this report)
d.	

10. DISTRIBUTION STATEMENT

This document is controlled by Structures and Materials Technology, Org. 2-5563.

11. SUPPLEMENTARY NOTES	12. SPONSORING MILITARY ACTIVITY

13. ABSTRACT

Missiles flying in the atmosphere could be subjected to passage through dust clouds formed by surface bursts of nuclear weapons. Such flight would result in the erosion of frontal surfaces, particularly the regions covered with ablative-insulative materials. The technique described in this paper was developed to provide data on the erosive effects of dust on cork, carborazole and silicone rubber (DC-93-072) in the Mach 3 to 6 flight regime.

The Erosion Test technique was developed utilizing the Boeing 12 inch Hypersonic Wind Tunnel. The wind tunnel was modified so that sand and glass beads could be introduced into the tunnel flow anytime during a test run. The material was injected up-stream of the nozzle throat and drag accelerated to high velocities prior to arrival at the test section. Drag computations based upon spherical particle drag, with the drag coefficient a function of Mach Number and Reynolds Number, indicate that the particles attained velocities, dependent upon size, of 2550 to 3250 feet-per-second. The tests were conducted at Mach Numbers of 6.05 and 6.50, P_t = 850, 1000 and 1150 PSI, T_t = 1000°F, with the test section gas velocity remaining constant at approximately 4000 ft/sec.

The conical test specimens introduced into the test stream were subjected to either an ablative or a combined ablative-erosive stream. The debris injection mechanism was capable of varying both the duration and the density of the particulate cloud. The cloud distribution throughout the tunnel test core was cali-

14. KEY WORDS	LINK A ROLE	LINK A WT	LINK B ROLE	LINK B WT	LINK C ROLE	LINK C WT
Ablation						
Ablation-Erosion						
Aerodynamic Heating						
Carborazole						
Collection Efficiency						
Contamination						
Cork						
Drag Coefficient						
Dust Cloud						
Dust Sampler						
Heat Transfer						
Hypersonic Flow						
Nuclear Cloud Debris						
Particle Velocity						
Radiant Heating						
Shear						
Silicone Rubber						
Wear						
Wind Tunnel						

INSTRUCTIONS TO FILL OUT DD FORM 1573 - DOCUMENT CONTROL DATA
(See ASPR 4 - 211)

1. ORIGINATING ACTIVITY: Enter the name and address of the contractor, subcontractor, grantee, Department of Defense activity or other organization (corporate author) issuing the report.

2a. REPORT SECURITY CLASSIFICATION: Enter the overall security classification of the report. Indicate whether "Restricted Data" is included. Marking is to be in accordance with appropriate security regulations.

2b. GROUP: Automatic downgrading is specified in DoD directive 5200.10 and Armed Forces Industrial Security Manual. Enter the group number. Also, when applicable, show that optional markings have been used for Group 3 and Group 4 as authorized.

3. REPORT TITLE: Enter the complete report title in all capital letters. Titles in all cases should be unclassified. If a meaningful title cannot be selected without classification, show title classification in all capitals in parenthesis immediately following the title.

4. DESCRIPTIVE NOTES: If appropriate, enter the type of report, e.g. interim, progress, summary, annual, or final. Give the inclusive dates when a specific reporting period is covered.

5. AUTHOR(S): Enter the name(s) of the author(s) in normal order, e.g. full first name, middle initial, last name. If military, show grade and branch of service. The name of the principal author is a minimum requirement.

6. REPORT DATE: Enter the date of the report as day, month, year, or month, year. If more than one date appears on the report, use date of publication.

7a. TOTAL NUMBER OF PAGES: The total page count should follow the normal pagination procedures, i.e. enter the number of pages containing information.

7b. NUMBER OF REFERENCES: Enter the total number of references cited in the report.

8a. CONTRACT OR GRANT NUMBER: If appropriate, enter the applicable number of the contract or grant under which the report was written.

8b, 8c, and 8d. PROJECT NUMBER: Enter the appropriate military department identification, such as project number, task area, systems numbers, work unit number, etc.

9a. ORIGINATOR'S REPORT NUMBER(S): Enter the official report number by which the document will be identified and controlled by the originating activity. This number must be unique to this report.

9b. OTHER REPORT NUMBER(S): If the report has been assigned any other report numbers (either by the originator or by the sponsor), also enter this number(s).

10. DISTRIBUTION STATEMENT: Enter the one distribution statement pertaining to the report.

Contractor-Imposed Distribution Statement

The Armed Services Procurement Regulations (ASPR), para 9-203 stipulates that each piece of data to which limited rights are to be asserted must be marked with the following legend:

"Furnished under United States Government Contract No. _____. Shall not be either released outside the Government, or used, duplicated, or disclosed in whole or in part for manufacture or procurement, without the written permission of _____, except for: (i) emergency repair or overhaul work by or for the Government, where the item or process concerned is not otherwise reasonably available to enable timely performance of the work; or (ii) release to a foreign government, as the interests of the United States may require, provided that in either case the release, use, duplication or disclosure hereof shall be subject to the foregoing limitations. This legend shall be marked on any reproduction hereof in whole or in part."

If the above statement is to be used on the form, enter the following abbreviated statement:

"Furnished under U. S. Government Contract No. _____. Shall not be either released outside the Government, or used, duplicated, or disclosed in whole or in part for manufacture or procurement, without the written permission of _____, per ASPR 9-203.

DoD Imposed Distribution Statements (reference DoD Directive 5200.20) "Distribution Statements (Other than Security) On Technical Documents," March 29, 1965

STATEMENT NO. 1. Distribution of this document is unlimited.

STATEMENT NO. 2 (UNCLASSIFIED document). This document is subject to special export controls and each transmittal to foreign government or foreign nationals may be made only with prior approval of (fill in controlling DoD office).

(CLASSIFIED document). In addition to security requirements which must be met, this document is subject to special export controls and each transmittal to foreign governments or foreign nationals may be made only with prior approval (fill in controlling DoD office).

STATEMENT NO. 3 (UNCLASSIFIED document). Each transmittal of this document outside the agencies of the U. S. Government must have prior approval of (fill in controlling DoD office).

(CLASSIFIED document). In addition to security requirements which apply to this document and must be met, each transmittal outside the agencies of the U. S. Government must have prior approval of (fill in controlling DoD office).

STATEMENT NO. 4 (UNCLASSIFIED document). Each transmittal of this document outside the Department of Defense must have prior approval of (fill in controlling DoD office).

(UNCLASSIFIED document). In addition to security requirements which apply to this document and must be met, each transmittal outside the Department of Defense must have prior approval of (fill in controlling DoD office).

STATEMENT NO. 5 (UNCLASSIFIED document). This document may be further distributed by any holder only with specific prior approval of (fill in controlling DoD office).

(UNCLASSIFIED document). In addition to security requirements which apply to this document and must be met, it may be further distributed by the holder ONLY with specific prior approval of (fill in controlling DoD office).

11. SUPPLEMENTARY NOTES: Use for additional explanatory notes.

12. SPONSORING MILITARY ACTIVITY: Enter the name of the departmental project office or laboratory sponsoring (paying for) the research and development. Include address.

13. ABSTRACT: Enter an abstract giving a brief and factual summary of the document indicative of the report, even though it may also appear elsewhere in the body of the technical report. If additional space is required, a continuation sheet shall be attached.

It is highly desirable that the abstract of classified reports be unclassified. Each paragraph of the abstract shall end with an indication of the military security classification of the information in the paragraph represented as (TS), (S), (C), or (U).

There is no limitation on the length of the abstract. However, the suggested length is from 150 to 225 words.

14. KEY WORDS: Key words are technically meaningful terms or short phrases that characterize a report and may be used as index entries for cataloging the report. Key words must be selected so that no security classification is required. Identifiers, such as equipment model designation, trade name, military project code name, geographic location, may be used as key words but will be followed by an indication of technical context. The assignment of links, roles, and weights is optional.

FORM DD 1 NOV 65 1473
U3 4802 1030 REV 7 66
PART 3 OF 3

THE BOEING COMPANY—AEROSPACE GROUP

MISSILE AND INFORMATION SYSTEMS DIVISION

SHIPPED TO:

DATE: March 4, 1969

DATA TRANSMITTAL NO.: MD 128301

Defense Documentation Center
Cameron Station
Alexandria, Virginia

1. The following data is transmitted:

One copy each of -

D2-114076-1, "Effects of Work Pacing and Teaming on Interpreter Performance"

D2-114077-1, "Illumination and Interpreter Performance"

One reproducible of -

D2-125929-1, "Particle Erosion Testing in The Boeing Hypersonic Wind Tunnel"

Four reproducibles of -

D2-125929-1, "50 Micron Glass Beads"

lt

FOR CLASSIFIED SHIPMENTS ONLY FACILITY SECURITY CLEARANCE VERIFIED BY

ACTION REQUIRED BY RECIPIENT

☐ APPROVAL OF DATA: IT IS REQUESTED THAT THE ABOVE DESCRIBED DATA BE REVIEWED AND APPROVED BY THE CONTRACTING OFFICER BY SEPARATE LETTER TO MISSILE DIVISION CONTRACT ADMINISTRATION WITHIN DAYS OF RECEIPT OF THE DATA AT ADDRESSEE'S FACILITY.

☒ ACKNOWLEDGMENT OF RECEIPT: IT IS REQUESTED THAT THE RECIPIENT OF THE DATA DESCRIBED ABOVE ACKNOWLEDGE RECEIPT BY SIGNING THE WHITE COPY OF THIS FORM IN THE SPACE PROVIDED AND RETURNING IT WITHIN 15 DAYS. MD-128301

RECEIPT IS ACKNOWLEDGED BY:

(PRINT OR TYPE FULL NAME)

(FULL SIGNATURE) DATE

RETURN TO: THE BOEING COMPANY
MISSILE AND INFORMATION SYSTEMS DIVISION
P. O. BOX 3985 MS 32-50
SEATTLE, WASHINGTON 98124

U3 4001 1012 REV. 4/67

THE BOEING COMPANY—AEROSPACE GROUP

MISSILE AND INFORMATION SYSTEMS DIVISION

SHIPPED TO:

DATE: March 4, 1969

DATA TRANSMITTAL NO.: MD 128301

Defense Documentation Center
Cameron Station
Alexandria, Virginia

1. The following data is transmitted:

One copy each of -

D2-114076-1, "Effects of Work Facing and Texture on Interpreter Performance"

D2-114077-1, "Illumination and Interpreter Performance"

One reproducible of -

D2-125969-1, "Particle Erosion Testing in The Boeing Hypersonic Wind Tunnel"

Four reproducibles of -

D2-125969-1, "50 Micron Glass Beads"

AD848524-L

16

FOR CLASSIFIED SHIPMENTS ONLY FACILITY SECURITY CLEARANCE VERIFIED BY

ACTION REQUIRED BY RECIPIENT

☐ APPROVAL OF DATA: IT IS REQUESTED THAT THE ABOVE DESCRIBED DATA BE REVIEWED AND APPROVED BY THE CONTRACTING OFFICER BY SEPARATE LETTER TO MISSILE DIVISION CONTRACT ADMINISTRATION WITHIN DAYS OF RECEIPT OF THE DATA AT ADDRESSEE'S FACILITY.

☒ ACKNOWLEDGMENT OF RECEIPT: IT IS REQUESTED THAT THE RECIPIENT OF THE DATA DESCRIBED ABOVE ACKNOWLEDGE RECEIPT BY SIGNING THE WHITE COPY OF THIS FORM IN THE SPACE PROVIDED AND RETURNING IT WITHIN 15 DAYS. MD-128301

RECEIPT IS ACKNOWLEDGED BY:

(PRINT OR TYPE FULL NAME)

(FULL SIGNATURE) DATE

RETURN TO: THE BOEING COMPANY
MISSILE AND INFORMATION SYSTEMS DIVISION
P. O. BOX 3985 MS 38-50
SEATTLE, WASHINGTON 98124

U3 4001 1012 REV. 4/67 Ps

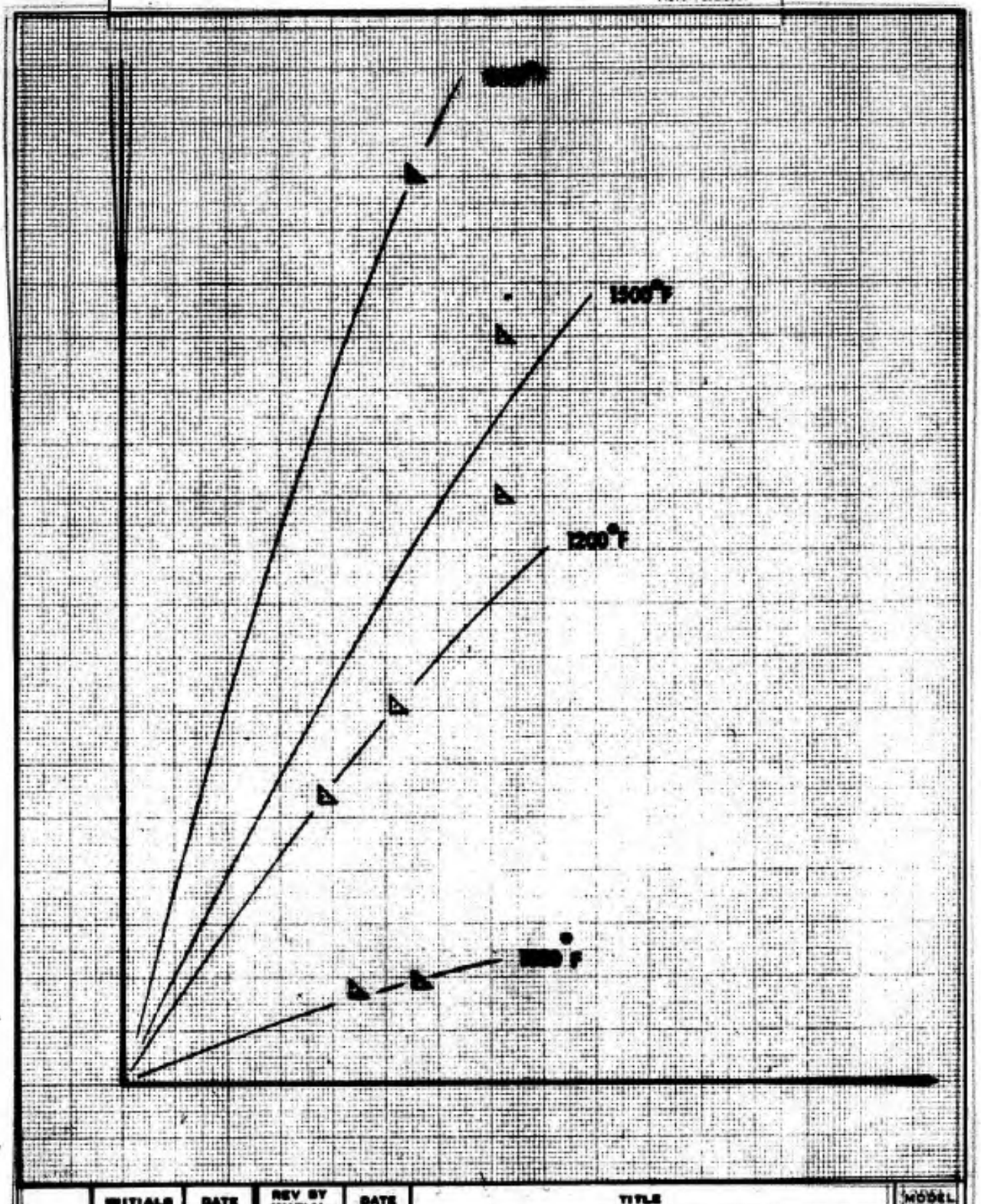

	INITIALS	DATE	REV BY INITIAL	DATE	TITLE	MODEL
DWG.					30 MICRON GLASS BEADS	Fig. 16A
CHECK						
APPD.						
APPD.						

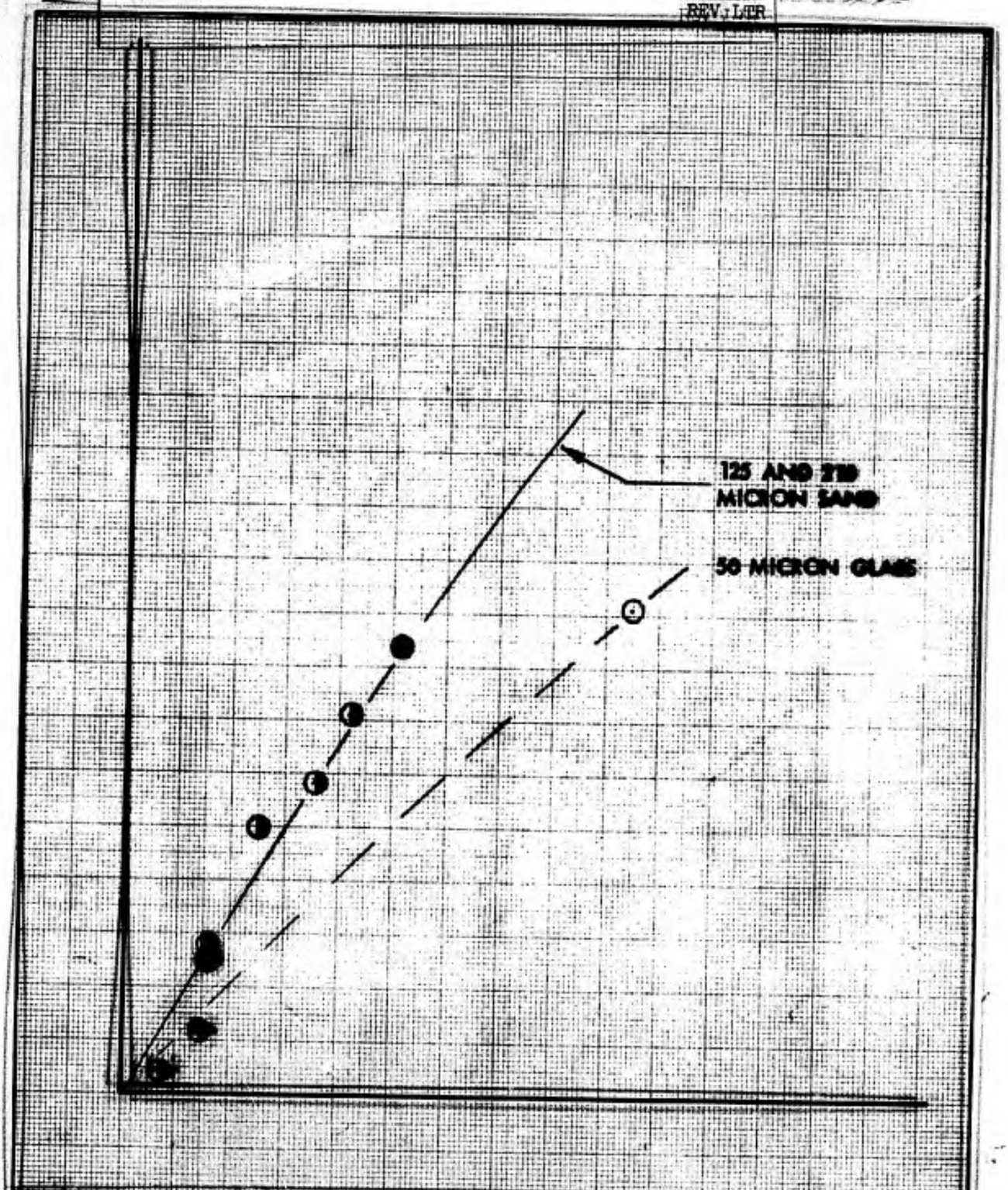

	INITIALS	DATE	REV. BY INITIAL	DATE	TITLE	MODEL
CHKD.					CARBORAZOLE	Fig. 18A
APPD.						
APPD.						

US 4013 6080 REV. 1/66

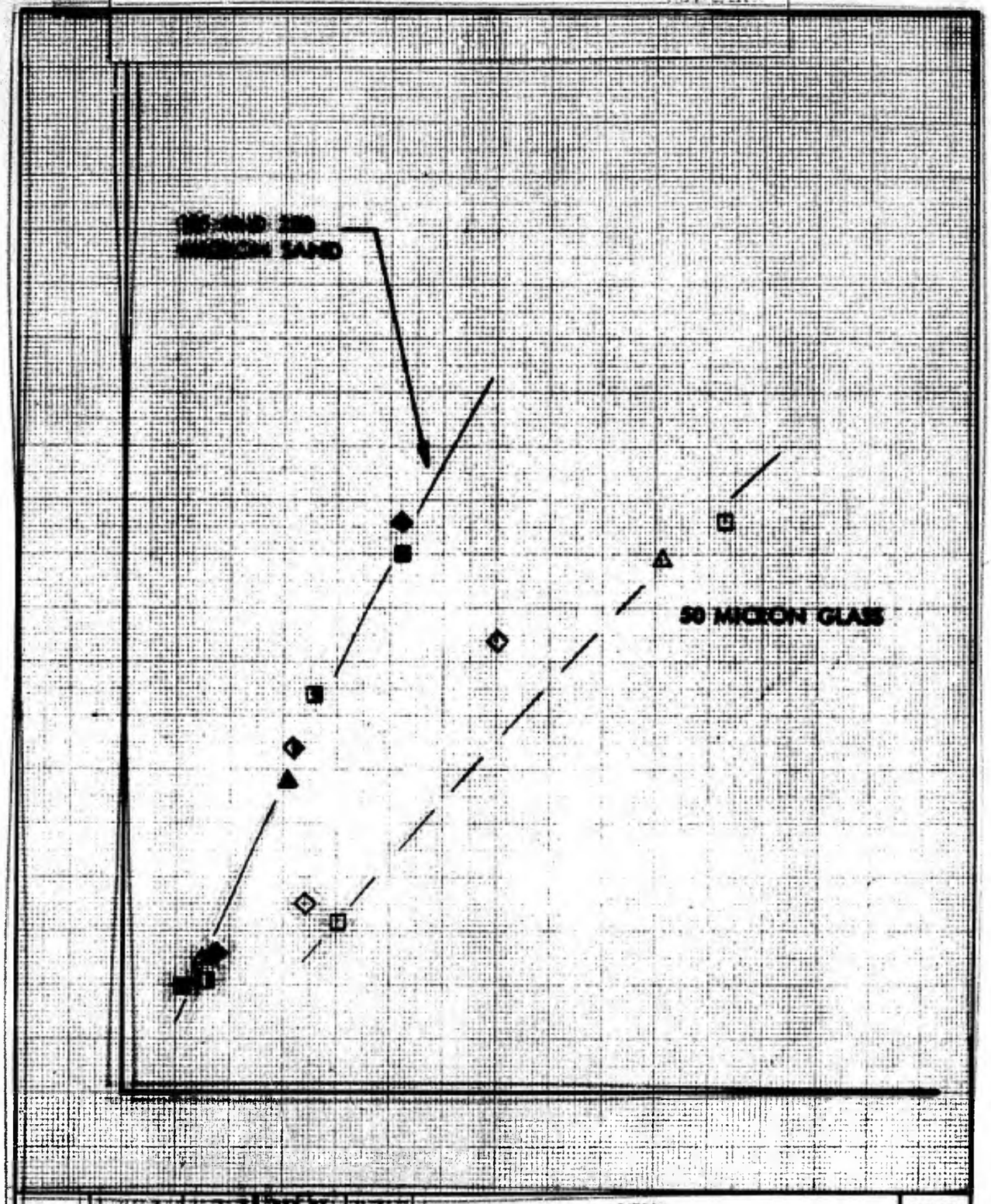

	INITIALS	DATE	INITIALS	DATE	TITLE	MODEL
CALC					CARBORAZOLE	Fig. 19A
CHK						
APPD						
APPD						

U31-013 P000 REV 1766

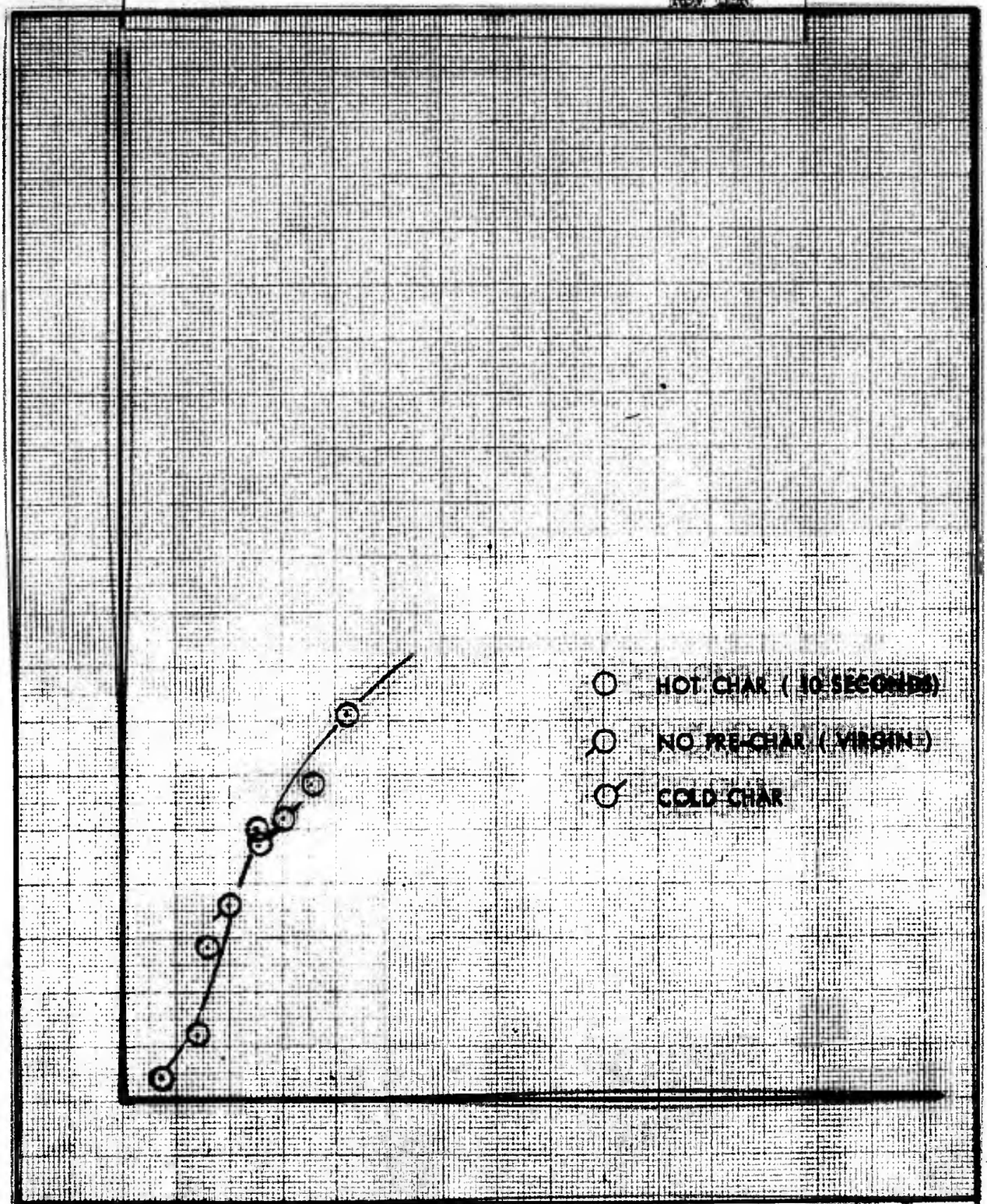

	INITIALS	DATE	REV BY INITIAL	DATE	TITLE	MODEL
CHKD					CARBORAZOLE NOMOGRAPHS FOR ALL CHAR SURFACE CONDITIONS	Fig. 28A
CHKD						
APPD						
APPD						